EXPERIMENTAL AND NUMERICAL STUDY OF COASTAL CLAYS OF BANGLADESH

by

A.K.M. Anisur Rahman Siddiquee

A thesis submitted in partial fulfillment of the requirements for the degree of Master of Science

Department of Civil Engineering

BANGLADESH UNIVERSITY OF ENGINEERING AND TECHNOLOGY

DHAKA

The thesis titled "Experimental and Numerical Study of Coastal Clays of Bangladesh" submitted by A.K.M. Anisur Rahman Siddiquee, Roll No. 040304206F, session April, 2003 has been accepted as satisfactory in partial fulfillment of the requirement for the degree of Master of Science on 10-10-2006

Board of Examiners

Dr. Mohammed Kabirul Islam
Associate Professor,
Department of Civil Engineering
BUET, Dhaka

Chairman
(Supervisor)

Dr. Md. Mazharul Hoque
Professor and Head,
Department of Civil Engineering
BUET, Dhaka

Member

Dr. Abdul Muqtadir
Professor, Department of Civil Engineering
BUET, Dhaka

Member

Dr. Abu Siddique
Professor, Department of Civil Engineering
BUET, Dhaka

Member

Dr. Muhammed Ali Bhuiyan
Professor, Department of Water Resources Engineering
BUET, Dhaka

Member
(External)

CANDIDATE'S DECLARATION

It is hereby declared that this thesis any part of it has not been submitted elsewhere for the award of any degree or diploma.

Anisur Rahman
03-10-06

A.K.M. Anisur Rahman Siddiquee

TABLE OF CONTENT

LIST OF FIGURES

LIST OF TABLES

NOTATIONS

A	pore pressure parameter
c	soil cohesion
CD	consolidated drained
CIU	isotropically consolidated undrained
CSL	critical state line
CU	consolidated undrained
c_u, s_u	undrained shear strength
E_i	initial modulus of elasticity
E_{50}	secant modulus of elasticity
e	void ratio
G	elastic shear modulus
I_1	the first invariant of the effective stress tensor
J_2	the second invariant of the deviatoric stress tensor
K	bulk modulus
LL, w_L	liquid limit
M	critical stress ratio
MC	Mohr-Coulomb model
MCC	Modified Cam Clay model
N	void ratio on normal consolidation line at unit pressure
NC	normally consolidated
NCL	normal consolidation line
OC	overconsolidated
OCR	overconsolidation ratio
PI, I_P	plasticity index
PL, w_P	plastic limit
p'	mean effective pressure=$(\sigma'_a + 2\sigma'_r)/3$
p'_0	preconsolidation pressure
q	deviator stress
$\bar{q}$	uniform pressure on the soil surface
u	pore pressure

UU	unconsolidated undrained test
v	specific volume
w	water content
γ	unit weight of the soil
σ'_v	effective vertical pressure
σ'_1	major principal effective stress
σ'_2, σ'_3	minor principal effective stresses
$\Delta\sigma_v$	change of vertical total stress
θ	Lode angle
λ	slope of the normal consolidation line
κ	slope of the elastic rebound line
τ_{ff}	peak or ultimate shear resistance
μ	Poisson's ratio
ϕ'	angle of internal friction (peak or ultimate)
ψ'	dilation angle
ε_p	axial strain at peak deviator stress
ε_a	axial strain
ε_v	volumetric strain
$d\varepsilon_q^p$	incremental plastic deviator strain
$d\varepsilon_v^p$	incremental plastic volumetric strain
η	stress ratio

ACKNOWLEDGEMENT

The author wishes to express his profound gratefulness and indebtedness to his supervisor Dr. Mohammed Kabirul Islam for his unfailing guidance, constant supervision, helpful criticisms and encouragement offered throughout the course of this research work. The author recognises and acknowledges, his unstinted help in both academic and personal concerns, throughout the years of the author's graduate studies at the Bangladesh University of Engineering and Technology, Dhaka.

The author expresses his profound gratitude to Dr. Md. Mazharul Hoque, Professor and Head of the Department of Civil Engineering, Bangladesh University of Engineering and Technology, Dhaka for providing laboratory facilities and necessary co-operation during the period of the research. The financial support provided by the authority of BUET, Dhaka is also gratefully acknowledged.

The author expresses his sincere thanks to all of the research colleagues of the Department of Civil Engineering, namely, Md. Arifuzzaman, Md. Sajjad Hossain and Ibrahim Khalil Ullah for their assistance and friendship during his study at BUET, Dhaka.

Thanks are also due to the staff of Geotechnical Engineering Laboratory, especially Mr. Habibur Rahman and Mr. Alimuddin for their help during the experimental works carried out as part of the research.

A very special debt of deep gratitude is offered to the author's parents for their unceasing prayer, love and encouragement.

ABSTRACT

Numerical and experimental investigations were undertaken in this research work to investigate how a critical state soil model (Modified Cam Clay model) and a frictional soil model (Mohr-Coulomb model) predict the stress-strain response of coastal clays of Bangladesh.

The Mohr-Coulomb model was first used to predict the drained and undrained triaxial shear behaviour of laboratory samples of coastal clays of Bangladesh. The ultimate behaviour is reasonably well predicted using this model. However this model could not predict the undrained stress paths of coastal clays.

The Modified Cam Clay (MCC) model using finite element method was used to predict the stress-strain, pore pressure and effective stress path of coastal clays under undrained triaxial condition. The MCC model was found to be a good qualitative predictor of the undrained response of coastal clays. It predicts the elasto-plastic strain hardening as observed experimentally. The Modified Cam Clay model predicts elastic response of highly overconsolidated clays before the onset of yield. The inability to predict elasto-plastic response before the onset of yield is a limitation of the model. However, the Modified Cam Clay model reallistically predicts the stress-strain and pore pressure response of coastal clays under undrained triaxial condition and various overconsolidation ratios.

The Modified Cam Clay model was also used to predict the stress-strain and volume change response of coastal clays under drained triaxial condition. The stress-strain and volume change response of coastal clays as predicted by the MCC model matches well with the drained response of the experimental stress-strain and volume change data for coastal clays as available in published literature.

An experimental program comprising of a series of model-scale footing and pile tests was carried out in order to investigate the footing and pile response to axial loads in coastal clays. The results obtained from these tests were compared to the footing and pile response predicted using the Mohr-Coulomb and Modified Cam Clay

models. The Modified Cam Clay model predictions for the model footing test at consolidation pressure of 50 kPa and 150 kPa was observed to be nonlinear with a gradually decreasing slope which closely approximated the experimental data. Similar nonlinear predictions were observed for the model-scale pile test at consolidation pressure of 150 kPa.

CHAPTER 1

INTRODUCTION

1.1 Introduction

The coastal region of Bangladesh comprise of the Chittagong coastal zone and the deltaic arcs of Khulna-Patuakhali-Noakhali. The clays found in this region are defined as coastal clays of Bangladesh. The geotechnical and engineering properties of coastal clays are described in detail in Bashar, 2002. Considerable development works are in progress in the Chittagong coastal zone. Flood protection embankments and cyclone shelters are needed to be built in large quantities in this region. It is important to safely design the foundations for structures to be built there. Hence it is essential to understand the stress-strain characteristics of the soil in this region.

Undrained triaxial shearing of coastal clays collected from Anwara, Banshkhali and Chandanaish in Chittagong was carried out in the laboratory (Bashar, 2002). Simplified equations were established to predict undrained shear strength. Some numerical simulations of the stress-strain response of coastal clays were also carried out using the Cam Clay and Modified Cam Clay model. However, the numerical simulations of the stress-strain response of coastal clays carried out (Bashar, 2002) were limited both in scope and in detail. The Cam Clay and Modified Cam Clay models are described in detail in Chapters 2, 4 and 6. There has been no detailed numerical investigation of the stress-strain behaviour of coastal clays under triaxial conditions, using advanced constitutive models. This thesis attempts to use these models within a finite element program to simulate the stress-strain response of triaxial samples, both under drained and undrained conditions. This thesis also describes some experiments carried out to investigate the load-displacement response of model-scale footings and piles resting on coastal clays of Bangladesh. The load-displacement response of model scale footings and piles were numerically simulated using the finite element method and compared with the experimental data obtained in this study. The constitutive models used within the finite element programs are the Mohr-Coulomb model and Modified Cam Clay model.

In summary, in this research investigation attempts have been made to carry out detailed numerical analysis of coastal clays of Bangladesh under drained and undrained conditions. The predictions were compared with experimental data (Bashar, 2002). The strengths and weaknesses of the Mohr-Coulomb and Modified Cam Clay models for predicting the stress-strain response of coastal clays was evaluated. Experiments on model-scale footings and piles were performed. Elasto-plastic finite element analysis was carried out to predict the load-displacement response of model-scale footings and piles.

1.2 Aims and Objectives of Proposed Study

In this section, the aims and objectives of the proposed research are elaborated. The broad objective of the study is to investigate the strengths and weaknesses of critical state models such as the Modified Cam Clay and traditional frictional models such as the Mohr-Coulomb to predict the stress-strain response of coastal clays of Bangladesh under triaxial states of stress.

The specific aims of this research were:

- To review the characteristics of the Mohr-Coulomb and Modified Cam Clay model and make a preliminary assessment of suitability of these models to predict drained and undrained stress-strain response of coastal clays during triaxial shear.

- To predict the stress-strain response, excess pore pressure and effective stress path of coastal clays tested at various cell pressures during triaxial shear using the Mohr-Coulomb and Modified Cam Clay model and compare the predictions with available experimental data.

- To predict the stress-strain and volume strain response of coastal clays during triaxial shear under drained conditions using the Mohr-Coulomb and Modified Cam Clay model.

- To undertake experimental investigations of the load-displacement response of model-scale footings and piles resting on coastal clay under undrained conditions.

- To predict the load-displacement response of model-scale footings and piles on coastal clay using the Mohr-Coulomb and Modified Cam Clay model and elasto-plastic finite element analysis.

- Finally, to compare the load-displacement predictions of elasto-plastic finite element analysis with experimental data of model scale footing and pile.

1.3 Limitations of the Proposed Study

Limitations that were necessarily applicable to the scope of the present study are described below:

- Experimental data of coastal clays in triaxial shearing under drained conditions was not available. Hence drained predictions of the triaxial shearing of coastal clays could not be compared with experimental data. In this case, the qualitative nature of the drained stress-strain curves were observed to see whether the trends were similar to the experimental data as recorded in the published literature for coastal clays.

- The load-displacement response of model-scale footings and piles resting on coastal clays was simulated for undrained conditions and axial loading only. It is not known whether these specific situations are truly representative of field conditions. In this case, numerical analysis was performed to simulate the laboratory condition and the results of the numerical analysis were matched with the model experiment.

1.4 Outline of the Thesis

The research work has been described in detail in the following Chapters of this thesis as follows:

In Chapter 1, the aims, objectives and limitations of the current research work have been described.

In Chapter 2, a literature review of clay and coastal clay behaviour, constitutive modelling of soils and elasto-plastic finite element analysis is presented. This chapter also outlines the rational for carrying out the present research study.

In Chapter 3, the Mohr-Coulomb model is described. It is then used to make predictions of the stress-strain response of coastal clays during triaxial shearing under undrained conditions. The predictions are compared with experimental data. The strengths, weaknesses and limitations of the model to predict the stress-strain response of coastal clays during undraned triaxial shear is discussed.

In Chapter 4, the Modified Cam model is described. It is used to make predictions of the stress-strain response, excess pore pressure and effective stress path of coastal clays during triaxial shearing under undrained conditions. The predictions are compared with experimental data. The strengths and limitations of the Modified Cam Clay model to predict the stress-strain response, excess pore pressure and effective stress path of coastal clays during undrained triaxial shear is discussed.

In Chapter 5, the Mohr-Coulomb model is used to make drained predictions of triaxial shearing of coastal clays. The approach necessary to use the Mohr-Coulomb model for drained prediction is discussed. The methods of obtaining drained Mohr-Coulomb parameter values for coastal clays from undrained parameters are described. Several different approaches each consisting of different sets of parameters are used to make drained predictions of coastal clays using the Mohr-Coulomb model. These methods are discussed, compared and evaluated. Finally, the drained predictions of the Mohr-Coulomb model are compared with undrained predictions.

In Chapter 6, the Modified Cam Clay model is used to predict the stress- strain and volume change behavior of coastal clays during drained triaxial shear. In the absence of experimental data, the drained Modified Cam Clay predictions cannot be compared with actual data and validated. Instead, the predictions of the Modified Cam Clay

model under drained conditions are compared with those of the Mohr Coulomb model. Finally the strengths, weaknesses and limitations of the Modified Cam Clay model to predict the stress-strain and volume strain response of coastal clays are discussed.

In Chapter 7, details of the experimental investigation of the load-displacement response of a model-scale footing and pile resting on coastal clay under undrained conditions is discussed. The method used to numerically predict the load-displacement response of model-scale footing and pile resting on coastal clay using elasto-plastic finite element analysis is then discussed. The predictions are compared with experimental data obtained. The strength and weaknesses of the Mohr-Coulomb and Modified Clay model to simulate boundary value problems in geotechnical engineering is discussed.

Chapter 8 summarises the main findings of this study and presents recommendations for further research.

CHAPTER 2

LITERATURE REVIEW

2.1 Introduction

The objective of this research investigation is the numerical modelling of the stress-strain response of coastal clays during triaxial shear. For this purpose, first a review of the stress-strain behaviour of clays during triaxial shear is undertaken. The different aspects of general clay behaviour is then evaluated. The second phase of the literature review looks at different aspects of coastal clay behaviour in particular. The similarities, differences and peculiarities of the stress-strain behaviour of coastal clays is evaluated. Subsequently, the stress-strain or constitutive modelling aspects of soil behaviour is studied. Constitutive models that are generally used to model the stress-strain response of clays during triaxial shear are particularly investigated. This is expected to result in the choice of a suitable constitutive model or models for numerical simulation of the stress-strain response of coastal clays during triaxial shear. Finally, a review of elasto-plastic finite element analysis is made. The applicability and use of single element modelling to predict triaxial shear behaviour of clays under both drained and undrained condition using non-linear finite element analysis and soil constitutive models is studied. Finally, the use and applicability of finite element modelling to simulate the pressure-displacement response of model scale footings and piles in clay soils is looked into. This may help to determine whether results of model scale footing and pile test in coastal clays may be verified using elasto-plastic finite element analysis.

2.2 Stress-Strain Behaviour of Clays

Clay layers are prevalent almost everywhere around the world. The behaviour of structures built over clay are significantly determined by the mechanical, stress-strain or constitutive properties of clay. The finest fractions of soils with particle sizes smaller than 0.002 mm are generally termed as clays. Interparticle forces play a major role in determining many of the physical and mechanical characteristics of finer soil particles. These effects have been investigated by various authors (Bowles et al, 1969,

Kenney et al, 1967, Loiselle et al, 1971, Mitchell et al, 1969, 1960, Morgernstern et al, 1967, Pusch, 1966, 1973a, 1973b, Rowe, 1962 and Sangrey, 1972a). These micro level characteristics in turn determine the macro-mechanical properties of clay such as cohesion, plasticity and permeability. The macro characteristics in turn determine the macro-mechanical or stress-strain response of clays. Various researchers have studied the effect of micro properties of clays on its macroscopic behaviour (Mitchell, 1976 and Mitchell et al, 1969, Penner, 1964, Yong et al, 1973). The macroscopic stress-strain behaviour of clays is characterised primarily by two significant aspects of clay behaviour. Firstly, consolidation, compressibility and settlement and secondly the shear strength and stiffness of clay.

The consolidation and compressibility behaviour of various types of inorganic clays, viz, normally consolidated clays, overconsolidated clays, stiff clays, soft clays, natural or undisturbed clays, remolded clays, fissured clays, sensitive clays, structured clays, marine or coastal clays etc have been thoroughly investigated by many researchers (Ameen et al, 1986, Barden, 1969, Bjerrum, 1967, Burland, 1990, Kamaluddin, 1990, 1999, Leonards et al, 1964, Mesri et al, 1974,1975, Olson, 1977 and Rendulic, 1936).

Figure 2.1 shows typical stress-displacement response, the failure line and water content or volume change vs. displacement curve of soils at peak and residual or ultimate stress conditions. Figure 2.2 shows typical ultimate or critical state condition of soil in specific volume vs. effective pressure plane and deviator stress vs. effective pressure plane. Figures 2.3 to 2.5 show typical consolidation behaviour of stiff clays, soft clays and remolded clays. In all cases, the consolidation curves or void ratio by log of effective mean pressure curves show an initial stiff and elastic response followed by a relatively softer and plastic response once a certain mean pressure is exceeded. This pressure is termed as the preconsolidation pressure or stress in the standard literature. The preconsolidation pressure thus divides the clay response in primarily two distinct zones: a stiff and primarily elastic zone and a softer and primarily plastic zone. An unloading results in a flatter elastic rebound or load-reload curve approximately parallel to the initial elastic and stiff curve. However, when the soil is loaded beyond the preconsolidation pressure, it again starts to show plastic response and yield. If the isotropic pressure is increased, the preconsolidation pressure increases to the new value of the isotropic pressure. This increase of preconsolidation

pressure, which divides the elastic from the plastic zone, is termed as hardening in constitutive modelling literature. More specifically, this is termed as the density hardening aspect of the plastic consolidation response of clays.

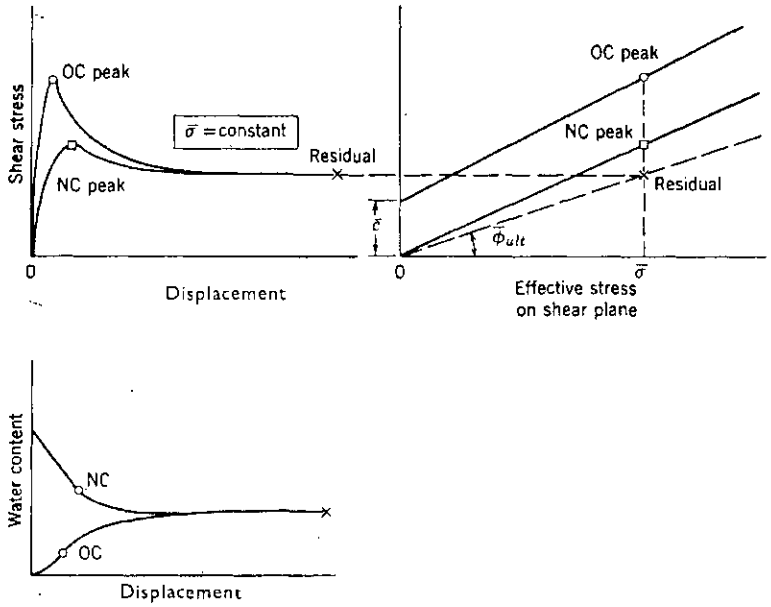

Figure 2.1 Relation between peak and ultimate conditions (Lambe and Whitman, 1979)

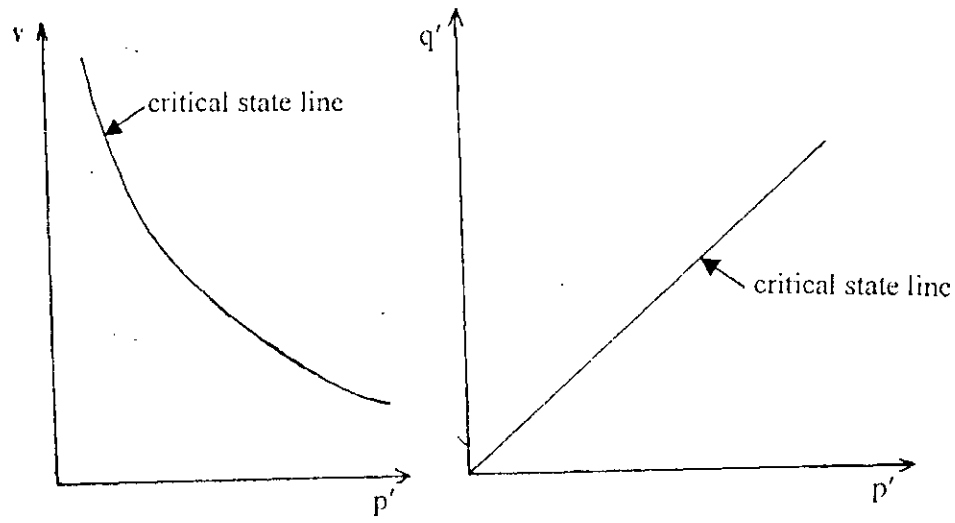

Figure 2.2 Critical State line in specific volume vs. effective pressure plane and deviator stress vs. effective pressure plane (Bashar, 2002)

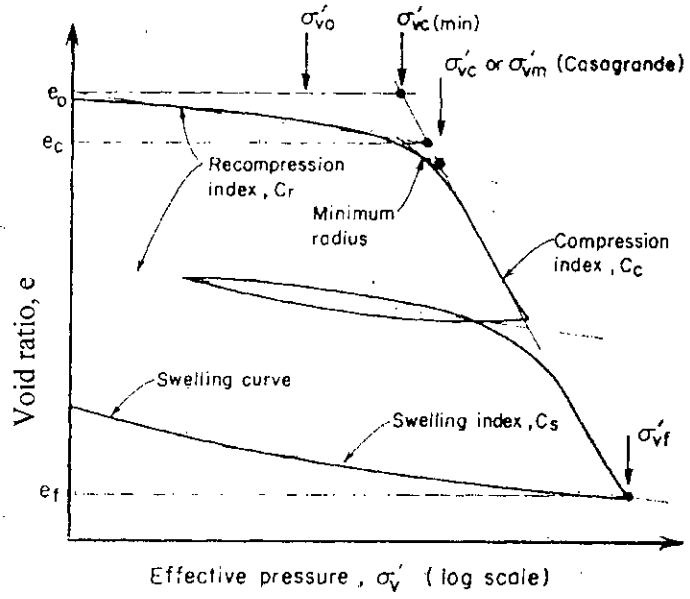

Figure 2.3 Consolidation behaviour of stiff clays (Brand and Brenner, 1981)

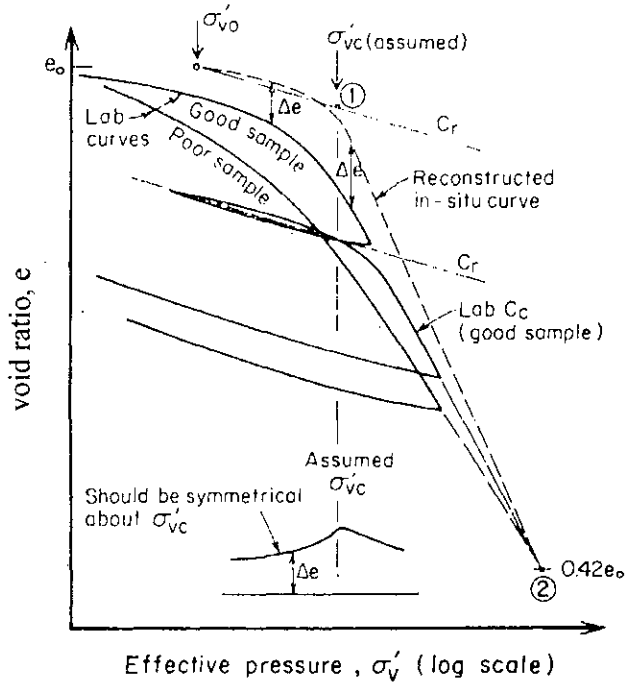

Figure 2.4 Consolidation behaviour of soft clays (Brand and Brenner, 1981)

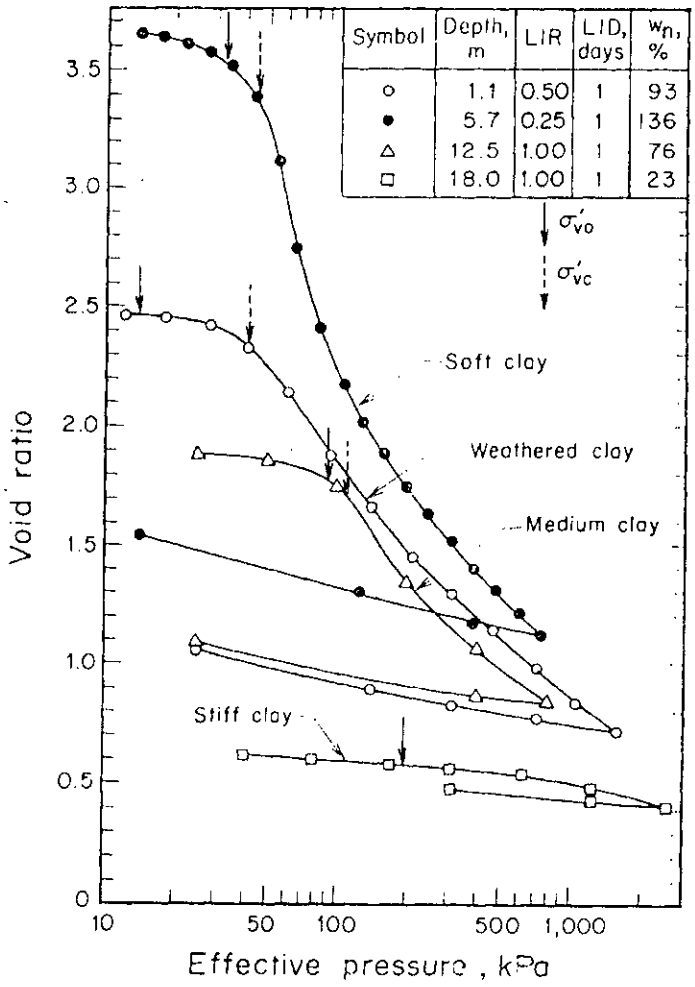

Figure 2.5 Consolidation behaviour of remolded clays (Brand and Brenner, 1981)

Various authors (Berre et al, 1973, Balasubramaniam, et al, 1978, Ladd, 1977 and Ladd et al, 1975) have studied the stress-strain behaviour of clays. Figures 2.6 to 2.10 show the typical stress-strain response in undrained triaxial shear for a typical stiff overconsolidated clay, normally consolidated clay and coastal clay. In each case, it is observed that the stress-strain behaviour is highly non-linear form the onset of the shearing process.

Figures 2.10 to 2.12 show undrained stress-paths, while Figures 2.13 and 2.14 show pore pressure responses for a typical stiff overconsolidated clay, normally consolidated clay and coastal clay. It is observed that while the stiff overconsolidated clay shows a peak shear strength followed by continuous shearing at a lower strength (generally termed as the ultimate or residual shear). No peaks are observed for normally consolidated and soft marine or coastal clays. These clays gradually reach a maximum value of shear strength generally termed as the ultimate shear. At this stage the soil undergoes continuous shear deformation at constant shear stress. The pore-pressure response of stiff clays during undrained triaxial shear shows the development of negative excess pore pressures or suction pressures, while the stress path shows increase of the mean effective stress. On the contrary, normally consolidated clays show development of positive excess pore pressures and gradual decrease of the mean effective stress.

Figure 2.15 show the stress-strain response of overconsolidated clays respectively during drained shearing. Qualiatively, the shear behaviour is similar to the undrained case. However, overconsolidated clay samples show expansive volume change, while the normally consolidated clays show compressive volume change during the shearing process. Figure 2.16 shows the stress paths during drained triaxial shear of normally consolidated clays.

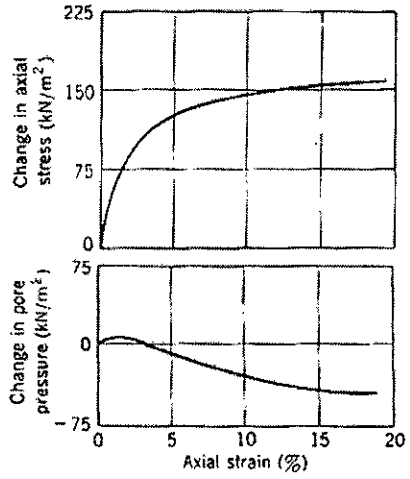

Figure 2.6 Stress-strain response in undrained triaxial shear for overconsolidated clays (Lambe and Whitman, 1979)

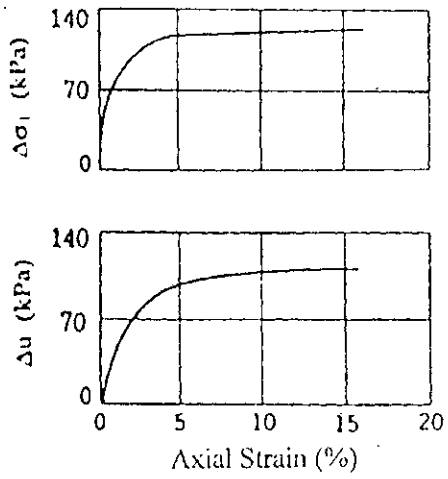

Figure 2.7 Stress-strain response in undrained triaxial shear for normally consolidated clays (Lambe and Whitman, 1979)

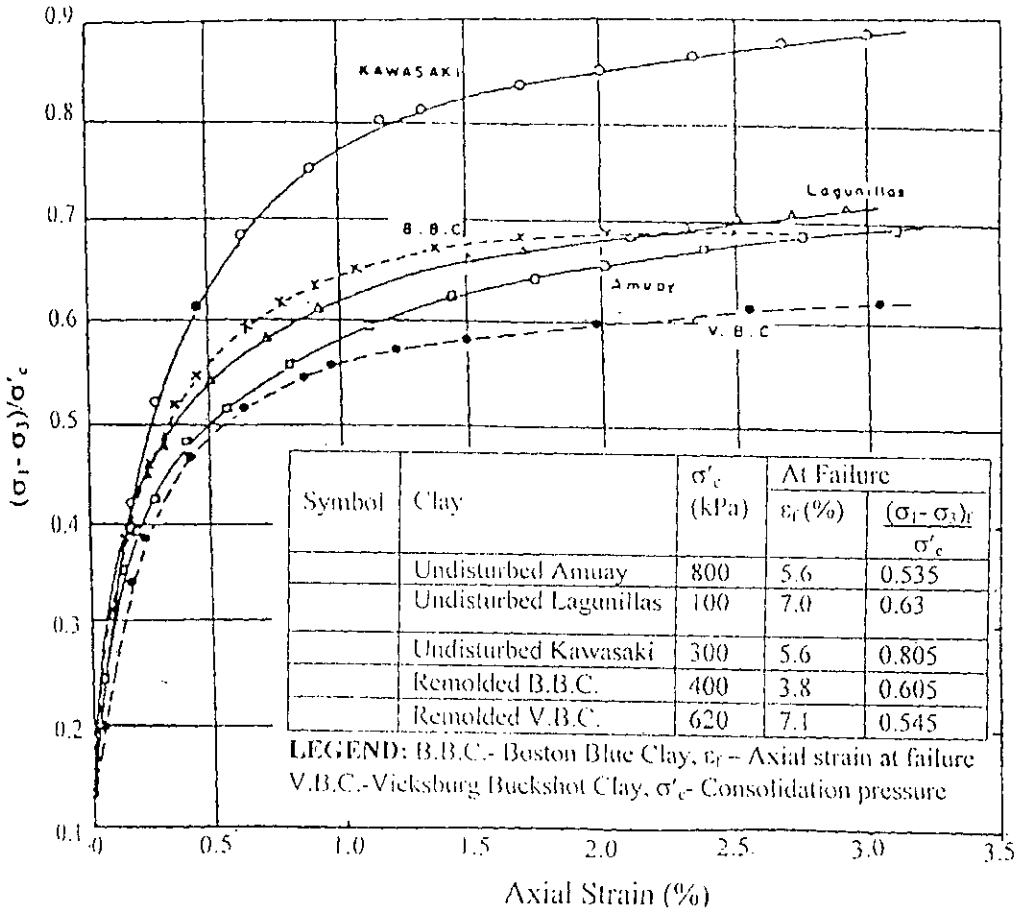

Symbol	Clay	σ'_c (kPa)	At Failure	
			ε_f (%)	$\frac{(\sigma_1-\sigma_3)_f}{\sigma'_c}$
	Undisturbed Amuay	800	5.6	0.535
	Undisturbed Lagunillas	100	7.0	0.63
	Undisturbed Kawasaki	300	5.6	0.805
	Remolded B.B.C.	400	3.8	0.605
	Remolded V.B.C.	620	7.1	0.545

LEGEND: B.B.C.- Boston Blue Clay, ε_f – Axial strain at failure
V.B.C.-Vicksburg Buckshot Clay, σ'_c- Consolidation pressure

Figure 2.8 Stress-strain response in undrained triaxial shear for normally consolidated clays (Ladd, 1964, Bashar, 2002)

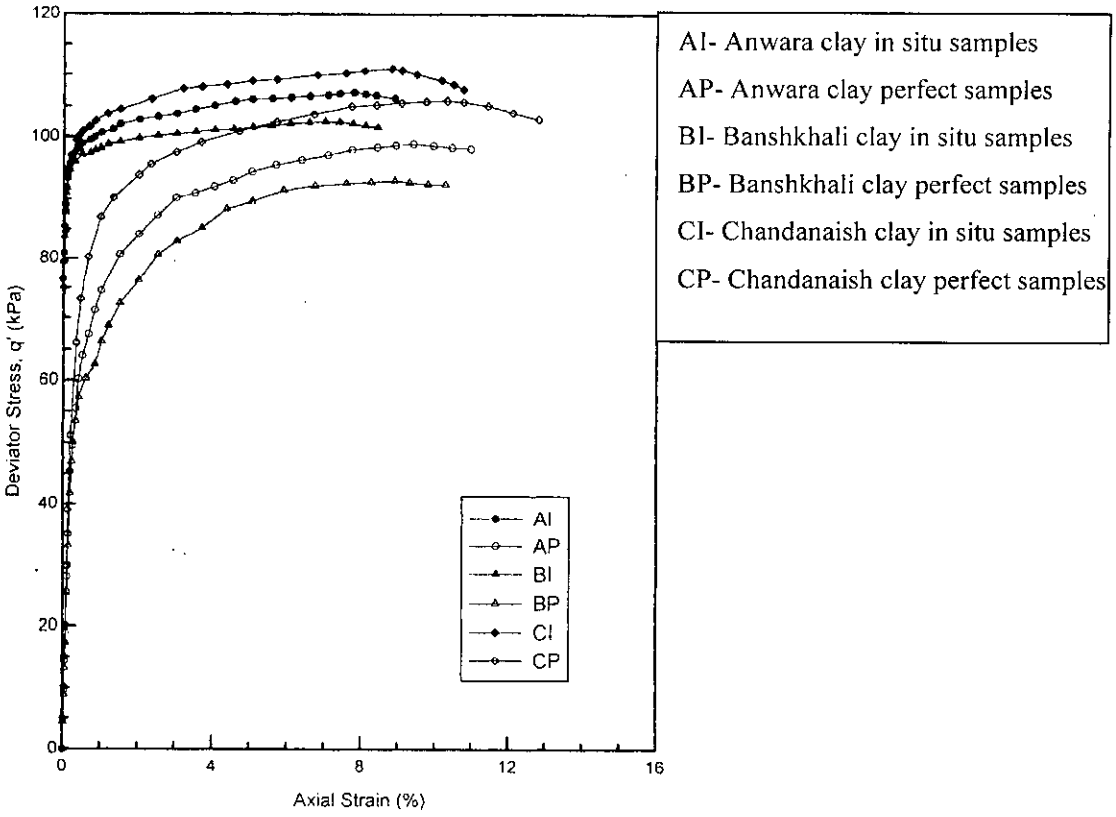

Figure 2.9 Stress-strain response in undrained triaxial shear for marine or coastal clays (Bashar, 2002)

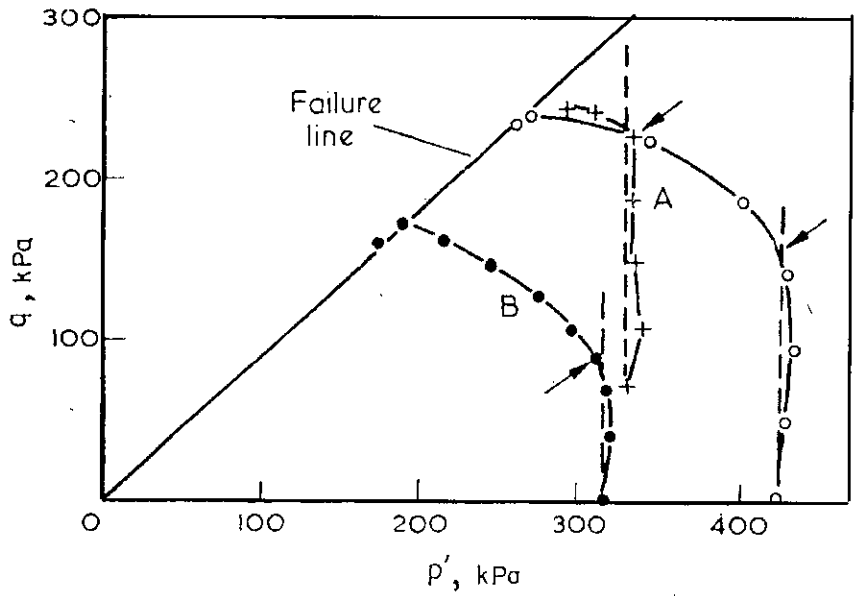

Figure 2.10 Undrained stress paths for normally consolidated clays (Brand and Brenner, 1981)

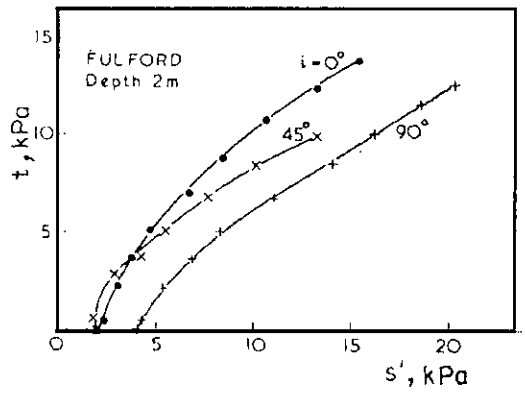

Figure 2.11 Undrained stress paths for overconsolidated clays (Brand and Brenner, 1981)

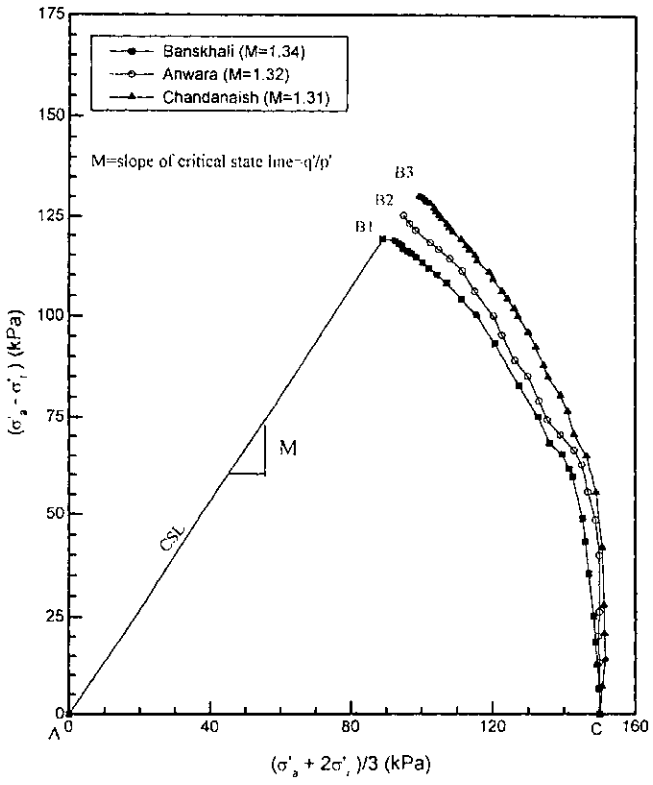

Figure 2.12 Undrained stress paths for marine or coastal clays (Bashar, 2002)

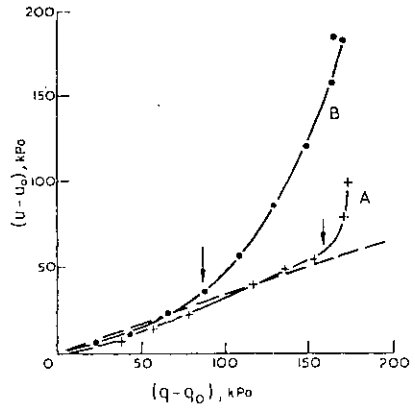

Figure 2.13 Pore pressure responses for normally consolidated clays
(Brand & Brenner, 1981)

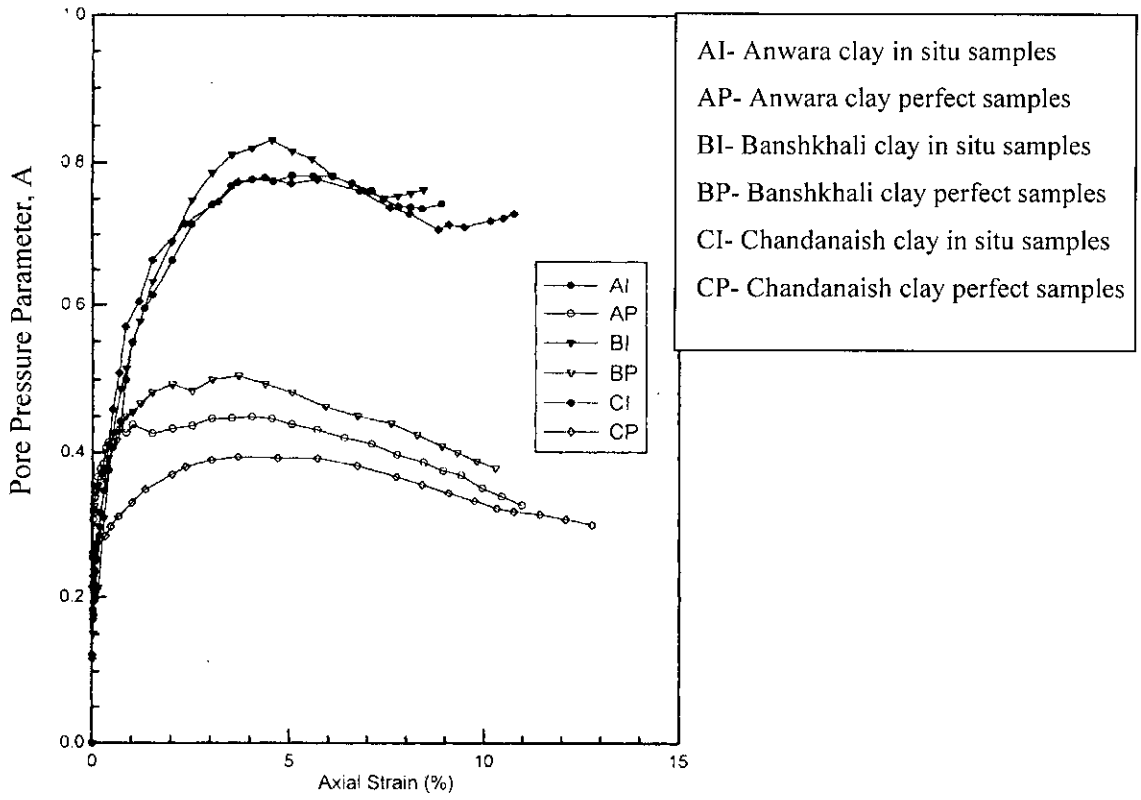

Figure 2.14 Pore pressure parameter vs. axial strain plot for marine or coastal clays
(Bashar, 2002)

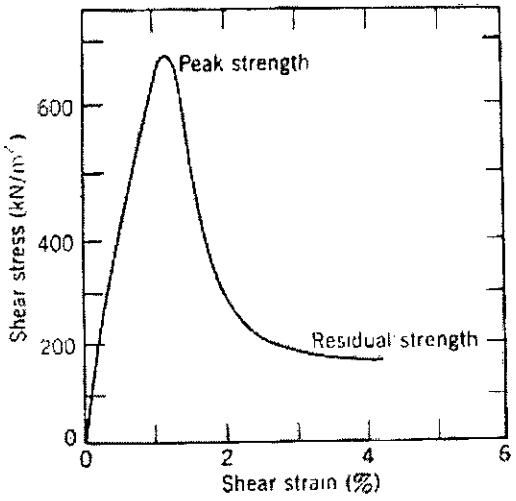

Figure 2.15 Stress-strain response in drained direct shear test of highly overconsolidated clays (Lambe and Whitman, 1979)

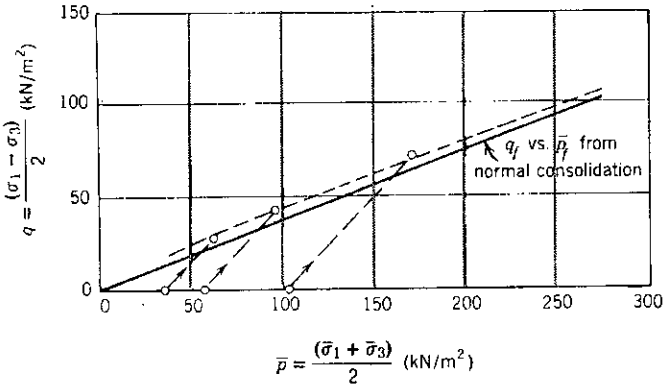

Figure 2.16 Drained stress paths for overconsolidated clays (Lambe and Whitman, 1979)

2.3 Stress-Strain Behaviour of Coastal Clays

Experimental investigation of coastal clays of Bangladesh during isotropic consolidation and shearing, both under drained and undrained conditions, have been carried out by many researchers (Amin et al, 1987, Ansary, 1993, Ansary et al, 1999, Bashar, 2002, Bjerrum, 1954, Hanzawa, 1979, Koutsoftas, 1981 and Siddique et al, 1997). The observed behaviour of typical clays as published in the literature, both under drained and undrained conditions, are very similar in a qualitative sense to the consolidation and triaxial shear response of the coastal of clays of Bangladesh.

A literature review of coastal or marine clays around the world show some characteristic behaviour also observed in coastal clays of Bangladesh. Coastal clays are generally deposited in a marine environment. The pore water thus contains salts or electrolytes which interact with charges on the clay particles. This generally results in increased compressive or shear strength of coastal clays. This behaviour has been observed in coastal clays of Bangladesh. The basic geotechnical properties of coastal clays of Bangladesh may be correlated with the development of higher compressive or shear strength of the clay.

Researchers found that coastal clays of Bangladesh generally exhibit higher plastic compressibility relative to non-coastal clays. This is also similar to findings in coastal clays around the world. From the point of view of double layer theory coastal clays should generally show a higher compressibility relative to other clays. This is what has been actually observed.

The consolidation and shear properties of coastal clays of Anwara, Banshkhali and Chandanaish clays are given in Tables 1.1 to 1.5 of Appendix I. The Mohr-Coulomb and Modified Cam Clay model parameters of coastal clays of Anwara, Banshkhali and Chandanaish clays as determined from experimental data of Bashar, 2002 are tabulated in Tables 2.1 to 2.7 of Appendix II.

2.4 Constitutive Modelling of Coastal Clays

The modelling of the stress-strain response of soils is complex and difficult. Some of the postulates of modern plasticity theory were formulated by several authors (Drucker et al., 1952 and Hill, 1950). Elastic theories applicable to soils were studied (Poulos, and Davis, 1974). Various frictional constitutive models for soils were proposed (Dimaggio et al, 1971, Drucker et al, 1952, Duncan et al, 1970, Gens et al 1988, Lade, 1977 and Lade et al, 1975 and Pastor et al, 1990).

Figures 2.17 to 2.20 show respectively the Drucker-Prager model, Lade-Duncan model, the Mohr-Coulomb model and the Modified Cam Clay model. The stress-strain behaviour of clays was also extensively studied (Balasubramaniam et al, 1980, Mitchell, 1970, Nakase et al, 1988, Parry et al, 1973, Roscoe et al, 1968, 1963, 1958 and Schofield et al 1968). Standard texts were published dealing with constitutive modelling of soils (Atkinson et al, 1978, Schofield et al 1968 and Chen et al, 1990).

Constitutive models imply a series or system of mathematical equations which determine the relationship between stresses and strains for a soil for a given set of soil parameters under generalised conditions of stresses and strains. The first widely used soil model was the traditional Mohr-Coulomb model. The Mohr-Coulomb model states that soil is fundamentally a frictional material. This implies that the shear strength that can be resisted by a soil at a given plane is directly proportional to the normal stresses acting on that plane. The ratio between the shear stress and normal stress at incipient failure is a measure of the mobilised frictional angle of the soil. This was observed to be true both for sands as well as clays. For clays under undrained condition, the undrained shear strength was observed to be independent of mean normal stress acting on any plane. Thus clay soils in undrained shear could be modelled using the Von Mises or Tresca criterion. Von Mises and Tresca models assume that the ultimate or failure shear stress acting on any plane is constant and independent of the normal stresses acting on the plane. Limit state and closed from solutions for various boundary value problems of undrained shearing of clays are still based on the Von Mises, Tresca or Mohr-Coulomb model with zero friction angle and constant cohesion or undrained shear strength.

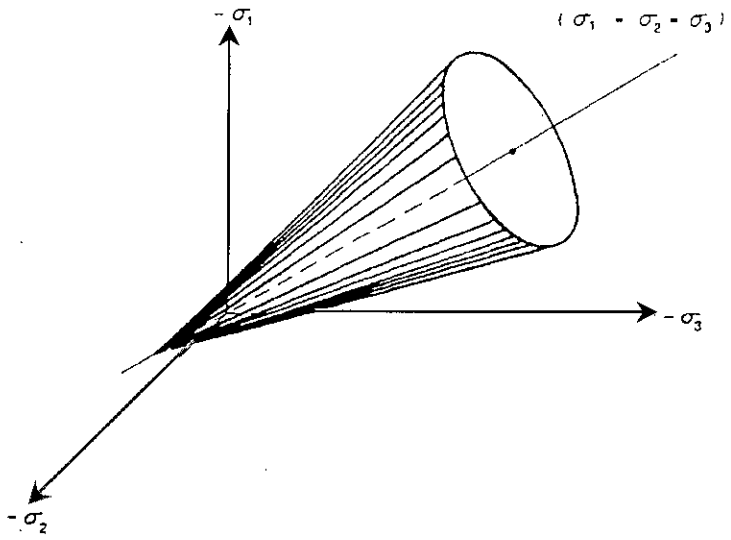

Figure 2.17 Drucker-Prager Model in principal stress space (Chen and Mizuno, 1990)

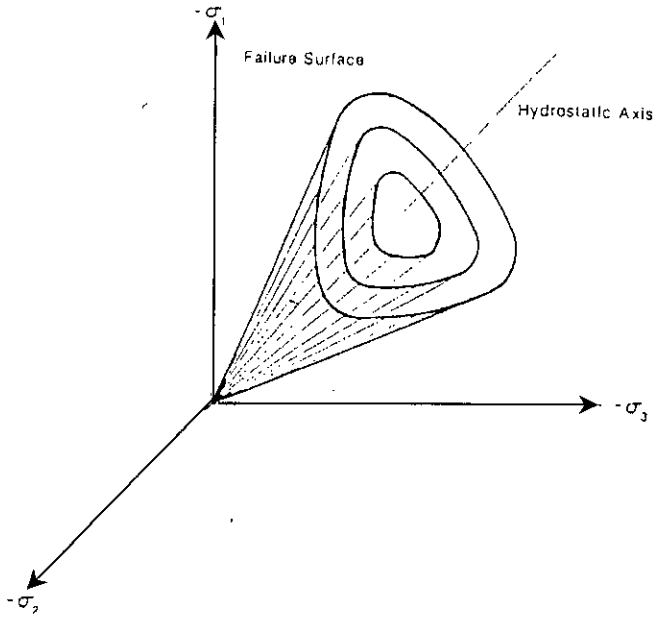

Figure 2.18 Lade-Duncan Model in principal stress space (Lade and Duncan, 1975)

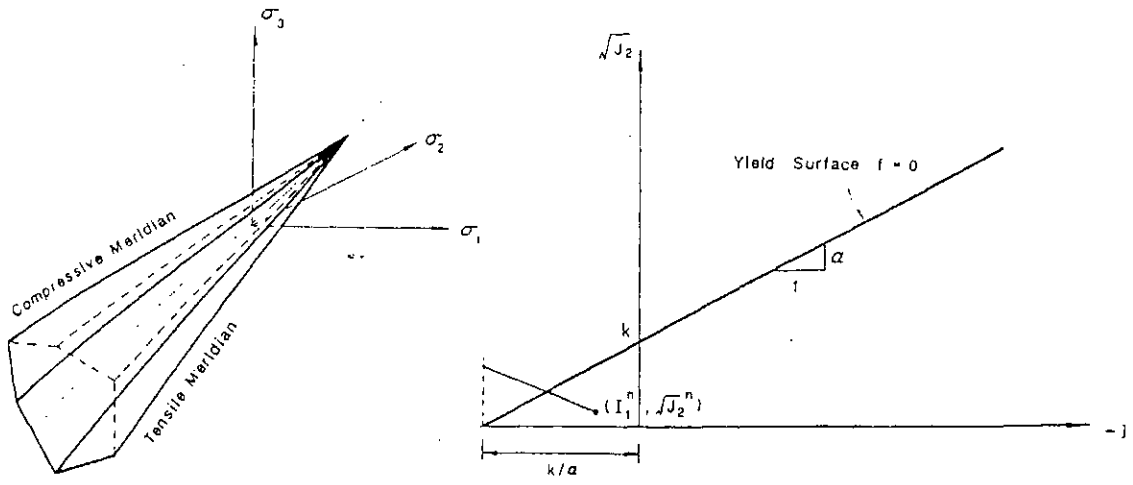

Figure 2.19 Mohr Coulomb Model (Chen and Mizuno, 1990)

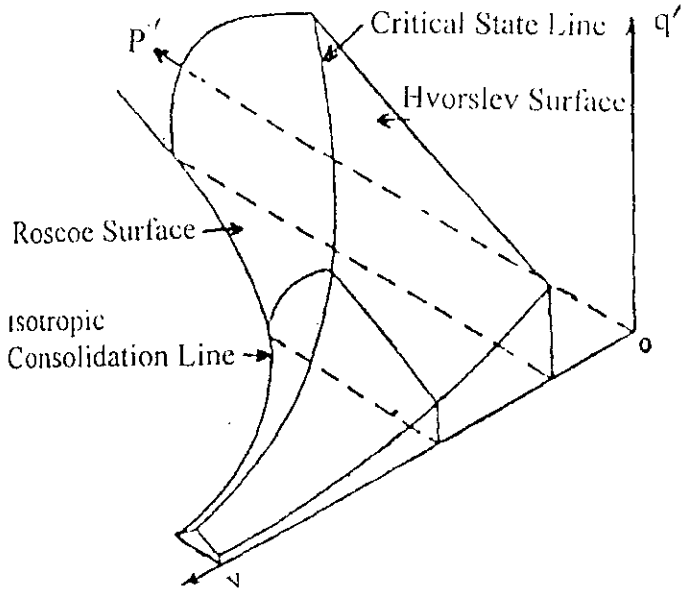

Figure 2.20 Modified Cam Clay Model (Bashar, 2002)

For numerical analysis, the generalised Mohr-Coulomb as well as the Tresca model suffers from the mathematical limitation of having sharp corners at certain transition points in generalised stress space. This makes the gradients of the Mohr-Coulomb yield function indeterminate at these points. This causes numerical problems of instability when the stress conditions are close to this region. The Drucker-Prager model (Drucker, 1959, 1956, and Drucker et al, 1952) solved this problem by formulating a smooth function at generalised stress space. All these models suffered from the severe limitation of being elastic, perfectly plastic type of model. All these models would predict either expansive (Mohr-Coulomb and Drucker-Prager) volume change or zero volume change (Von Mises or Tresca), assuming the associated flow rule. The associated flow rule defines that the yield function is identical to the plastic potential function. The associated flow rule was postulated from considerations of stability enunciated by Drucker (1959, 1956).

Normally consolidated and soft clays show strain-hardening elasto-plastic behaviour from the onset of loading to the utlimate mobilised shear strength of the soil. Clays were observed to harden and undergo plastic strain at the same time. The Mohr-Coulomb, Drucker-Prager, Von-Mises and Tresca models were unable to predict non-linearity with associated strain hardening response. The density hardening Cam-Clay model (Roscoe et al, 1963, 1958 and Schofield et al 1968) predicted non-linear strain hardening stress-strain behaviour with perfectly plastic response at the ultimate state. This model would predict compressive volume change for normally consolidated clays and clays of low overconsolidation ratios and loose sands. Expansive volume change would be predicted for highly overconsolidated clays along with peak strength, loss of shear stiffness and perfectly plastic response at the ultimate state. At the ultimate state the full shear strength of the soil is mobilised. The Cam Clay model follows an associated flow rule. Density hardening was assumed. Density hardening was defined by the plastic part of the standard consolidation equation for clays. It was observed that the Cam Clay yield locus does not coincide with experimentally observed yield locus for clays. In the generalised stress space at the point of the isotropic preconsolidation stress, the Cam Clay yield locus was observed to exhibit sharp corners. This gives rise to indeterminate gradients at these points. This may cause problems when using this model in numerical analysis with finite element methods.

To overcome these problems, the Modified Cam Clay model was proposed (Roscoe and Burland, 1968). This model assumes an elliptic yield locus at $p' - q$ or mean stress by deviator stress space. The Modified Cam Clay model has been successfully used to analyse laboratory behaviour of normally consolidated and lightly overconsolidated clays. It has also been successfully used to predict the boundary value problems of loading in clay layers using elasto-plastic finite element analysis. Till now, the Mohr-Coulomb model and the Modified Cam Clay model are two of the most widely used models for solving stress-strain and boundary value problems involving loading of clay deposits. Thus it is quite appropriate to attempt to model the stress-strain response of coastal clays of Bangladesh, both under drained and undrained conditions, using the Mohr-Coulomb and Modified Cam Clay model. However, it may be necessary to make relevant assumptions and approximations when solving boundary value problems using these models.

2.5 Elasto-Plastic Finite Element Analysis

Solving boundary problems in clays using non-linear soil models has been the subject of intensive research in recent times. Such problems have been studied extensively by various authors (de Borst and Vermeer, 1984, Smith, 1982, Zienkiewicz and Naylor, 1971 and Britto and Gunn, 1987). Satisfactory and realistic solutions could be obtained by many authors for problems involving footings, piles, embankments and excavations in clays. In elasto-plastic finite element analysis, the issue of non-linearity is addressed by dividing the problem into a series of incrementally linear steps. As the problem is solved step by step for each increment, the solution for each step is incrementally added to the next successive one. In this way, the final solution for the boundary value problem using a non-linear soil model may be obtained. Mesh discretisation, numerical integration, definition of boundary conditions such as boundary restraint or loading, predictor-corrector methods for solving non-linear constitutive models, defining nodal connectivity to map local to global degrees of freedom etc. involved in traditional finite element analysis are all defined. Once the problem is defined, it is solved iteratively in steps using a given constitutive model. Good qualitative agreement has been obtained between numerically predicted and experimentally observed values in many cases. Whether good qualitative agreement between experimentally observed and predicted values are obtained depends to a large

extent on choice of the material parameters for the constitutive model and proper and realistic discretisation as well as definition of boundary restraints and loading.

The most common numerical integration scheme employed in finite element analysis is Gaussian integration and the integration points are referred to as Gauss points. For Gaussian integration the optimum integration order depends on the type of element being used and on its shape. Experience has shown that for the 8-noded isoparametric element either a 2x2 or a 3x3 order should be used. Fig. 2.21 illustrates the location of the Gauss points in the parent element and an example of their positions in a global element for the 2x2 and 3x3 integration orders. 2x2 and 3x3 integration orders are often referred to as reduced and full integration respectively. (Potts, 1999)

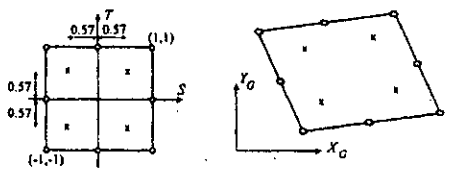

Parent Element Global Element

a) 2x2 order

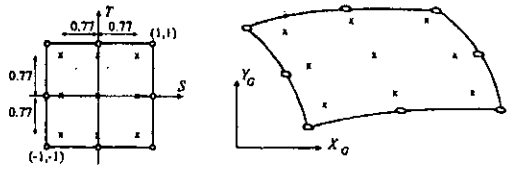

Parent Element Global Element

b) 3x3 order

Fig. 2.21 Location of Gauss Points (Potts, 1999)

No elasto-plastic constitutive analysis of boundary value problems in coastal clays of Bangladesh has been carried out till now. Such an analysis may demonstrate the usefulness of such methods for analysing and designing structures on coastal clays of Bangladesh.

2.6 Conclusion

A literature review of the geotechnical properties and stress-strain behaviour of clay in general and coastal and marine clays in particular was carried out. The stress-strain behaviour of the coastal clays of Bangladesh was specifically studied. It was observed that although coastal clays show some specific behaviour, in general the geotechnical and stress-strain properties of coastal clays are similar to clays as a whole. The literature review also show that the Mohr-Coulomb and Modified Cam Clay model are two widely used model for numerical modelling and elasto-plastic finite element analysis of geotechnical and boundary value problems in clays. Almost no or very limited numerical analysis has been carried out of coastal clays of Bangladesh using either the Mohr-Coulomb model or strain hardening constitutive models such as the Modified Cam Clay model. There exists a need to carry out a detailed numerical analysis and study of coastal clays using the Mohr-Coulomb and the Modified Cam Clay models. Such a study will help in understanding the strengths and weaknesses of these models to predict the stress-strain response of coastal clays of Bangladesh. No experimental studies of model scale footings and piles on coastal clays of Bangladesh have been carried out till date. Finite element analysis and validation of experimental data of such model scale footings and piles may help to establish the validity of constitutive models such as the Mohr-Coulomb and Modified Cam Clay to solve boundary value problems in coastal clays. Thus numerical and experimental investigation of coastal clays of Bangladesh could be a subject of a serious and detailed investigation.

CHAPTER 3

PREDICTION OF UNDRAINED STRESS-STRAIN RESPONSE: THE MOHR-COULOMB MODEL

3.1 Introduction

The Mohr-Coulomb Model is commonly and widely used to investigate and analyse many geotechnical problems. In case of elastic-perfectly plastic behaviour assumption, these analyses are known in the geotechnical literature as limit state analysis. This chapter gives an overview of the Mohr-Coulomb model. It is then used to predict the triaxial stress-strain behaviour of three coastal clays of Bangladesh. The numerical predictions of the model are compared with experimental data. Inferences are then made regarding the strengths, weaknesses and limitations of the Mohr-Coulomb Model in predicting the triaxial stress-strain behaviour of coastal clays.

3.2 Mohr-Coulomb Model

The different aspects of the Mohr-Coulomb model, both in its general and particular form, are discussed in detail in the following subsections given below.

3.2.1 Mohr-Coulomb Equation

The Mohr-Coulomb equation is a failure line or a failure criterion for pressure dependent or frictional material. It plots as a line on shear by effective normal stress or $\tau - \sigma'$ plane. Its equation is given as follows:

$$\tau_{ff} = c + \sigma_{ff} \tan\phi' \qquad (3.1)$$

In equation 3.1, τ_{ff} may be the peak or ultimate shear resistance, c the soil cohesion and ϕ' the drained angle of internal friction of the soil (peak or ultimate). Fundamentally, equation 3.1 states that a soil element fails by shearing when the shear

and normal stress on any plane satisfies equation 3.1. A constant shear resistance c is added to the right hand side of the equation 3.1 to express the shear resistance occurring as a result of intrinsic forces of attraction within the soil. Fig. 3.1 shows the Mohr-Coulomb line in $\tau - \sigma'$ space.

3.2.2 Generalized Mohr-Coulomb Failure Envelope

The generalized Mohr-Coulomb failure envelope in terms of stress invariants I_1, J_2 and lode angle θ is given as follows:

$$I_1 \sin\phi' + \frac{1}{2}\left[3(1-\sin\phi')\sin\theta + \sqrt{3}(3+\sin\phi')\cos\theta\right]\sqrt{J_2} - 3c\cos\phi' = 0 \quad (3.2)$$

In equation 3.2, I_1 is the first invariant of the effective stress tensor and it is proportional to the effective mean pressure. J_2 is the second invariant of the deviatoric stress tensor and it is proportional to the shear stress acting on the octahedral plane. Fig 3.2 shows the Mohr-Coulomb failure envelope given by equation 3.2 plotted in the I_1 -J_2 invariant stress space.

The Mohr-Coulomb model assumes that once stress state reaches the failure envelope, continuous shearing or plastic flow occurs at constant stress. Stress states outside the failure envelope are not possible.

3.2.3 Elastic Behaviour

Within the Mohr-Coulomb failure envelope or stress space, the stress-strain behaviour of the soil is assumed to be elastic. The elasticity may be linear. In that case, it is defined by a constant Young's modulus E and Poisson's ratio μ. The elasticity may be non-linear. In that case, a pressure-dependent Young's modulus $E(p')$ of the form given as below is assumed.

$$E(p') = k(p')^n \quad (3.3)$$

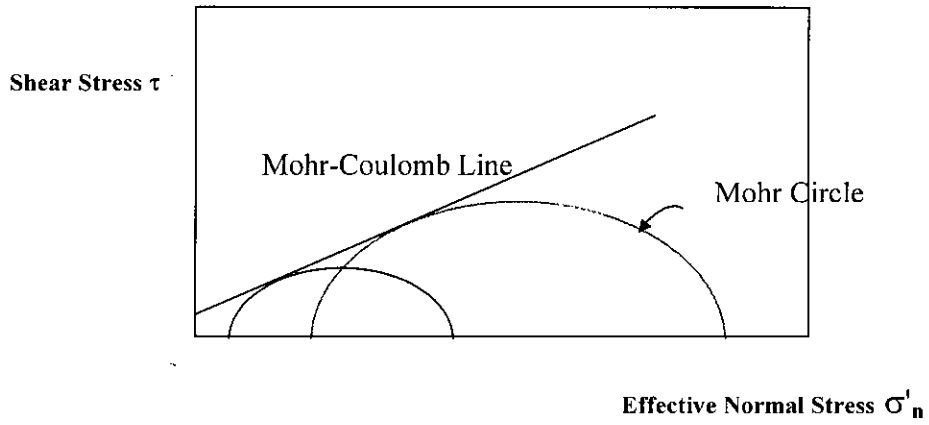

Figure 3.1 Mohr-Coulomb model (Peck et al., 1974)

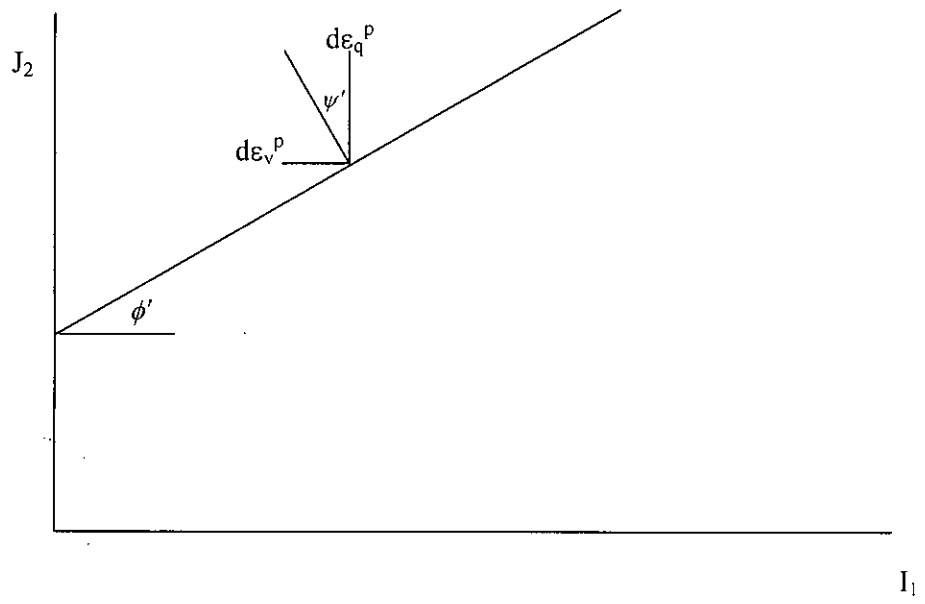

Figure 3.2 Mohr-Coulomb model representation in stress invariant space
(Chen and Mizuno,1990)

In equation 3.3, the constant term k and the exponent n are considered as material parameters of the model. In this thesis, non-linear elastic behaviour has not been considered.

3.2.4 Plastic Flow

When the stress state of a soil reaches the Mohr-Coulomb failure envelope, continuous shearing or plastic flow occurs at constant stress. Thus the Mohr-Coulomb model predicts elastic, perfectly plastic soil behaviour. Stress states outside the failure envelope are unattainable by the soil, as the soil fails by shear before reaching such stress states.

3.2.5 Plastic Flow Rule

The plastic flow rule gives the direction of the incremental plastic strains. In the typical case, the flow direction is normal to the Mohr-Coulomb failure envelope. This is termed as the associated flow rule. In this case, significant expansive volumetric strains are predicted by the Mohr-Coulomb model (Fig. 3.2). For special cases, the flow direction is assumed not to be normal to the yield envelope. This is termed as the non-associated flow rule. In that case, the flow direction is given as an angular measurement from J_2 direction. This angle is generally termed as the dilation angle ψ' (Fig. 3.2). For $\phi' = \psi'$, i.e., when the dilation angle is equal to the effective friction angle, the flow rule is associated. For $\psi' < \phi'$, i.e., when the dilation angle is less than the effective friction angle, the flow rule is non-associated.

3.3 Mohr-Coulomb Model for Clays

The Mohr-Coulomb model is widely used to predict undrained or fast loading behaviour of clays. In that case, c is taken equal to the undrained shear strength s_u and the effective friction angle ϕ' is taken to be zero (Figures 3.3 and 3.4). If appropriate values for elastic modulus E and Poisson's ratio μ are chosen for a given problem, the Mohr-Coulomb model can be used to give a reasonable approximation of the undrained stress-strain response of clays.

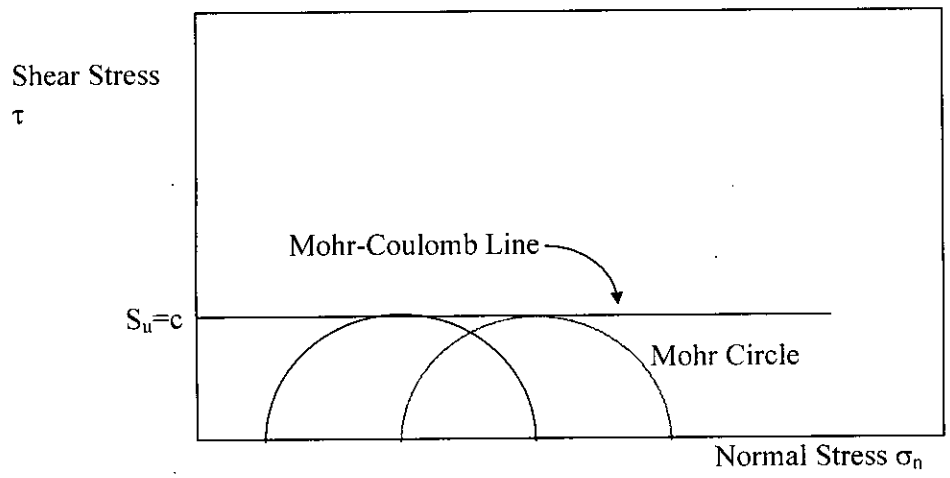

Figure 3.3 Mohr-Coulomb model under undrained conditions (Peck et al., 1974)

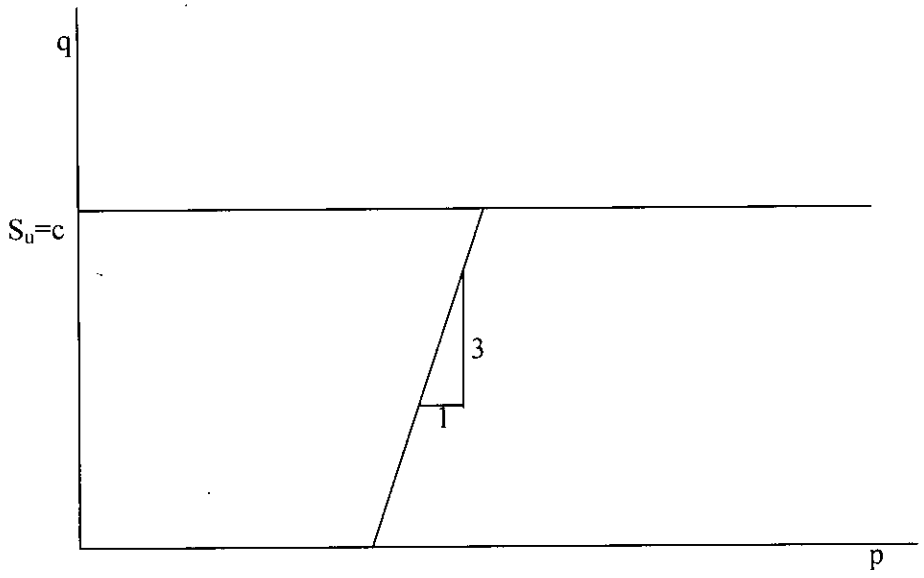

Figure 3.4 Total stress path followed during undrained triaxial shear (Atkinson and Bransby, 1978)

The Poisson's ratio μ is assumed to be close to 0.5 to simulate elastic incompressibility condition. Plastic incompressibility is simulated by assuming the dilation angle $\psi' = 0$. For undrained tests, the Mohr-Coulomb model predicts total stress paths and not the effective stress paths. This is because the model cannot predict pore pressures.

In case of drained or slow tests, the stress-strain response of clays are predicted by assuming $c = 0$ and ϕ' equal to the effective friction angle of the soil. Apparent drained elastic modulus and drained Poisson's ratio μ (generally between 0.1-0.3) need to be assumed. For a partially saturated soil, a $c - \phi'$ construct is generally used.

3.4 Mohr-Coulomb Model Parameters for Clays

The Mohr-Coulomb model parameters for a soil are the soil cohesion c, effective friction angle ϕ', elastic Young's modulus E and elastic Poisson's ratio μ. A value of the dilation angle ψ' controlling prediction of expansive volume strains also needs to be assumed. In this chapter, the Mohr-Coulomb model is used to predict the undrained triaxial stress-strain response for coastal clays of Anwara, Banshkhali and Chandanaish. The method of determination of the Mohr-Coulomb model parameters for coastal clays are discussed below.

3.4.1 Cohesion c

Cohesion c is defined as intercept at the shear stress axis of the Mohr-Coulomb line. Thus it is the shear strength of the soil at zero normal stress. This shear strength is the result of inter-particle forces of attraction that exists between the soil grains. Cohesion c is generally a measure of the undrained shear strength of the soil. In an unconfined compression test, it is equal to half of the unconfined compression strength or half of the deviator stress in an UU test. The cohesion or c values for coastal clays of Anwara, Banshkhali and Chandanaish are shown in Appendix II.

3.4.2 Effective Friction Angle ϕ'

The angle of slope of the plot of the Mohr-Coulomb line in shear stress by effective normal stress or $\tau - \sigma'$ plane is termed as the effective friction angle ϕ' of the soil. For overconsolidated clays, when the peak shear stress of the soil is plotted with respect to the normal stresses, the slope of the Mohr-Coulomb line gives the peak effective friction angle of the soil. When the ultimate shear stress of the soil is plotted with respect to normal stress, the ultimate effective friction angle is obtained. The peak effective friction angle varies with the overconsolidation ratio (OCR) of the soil. The effective friction angle is however approximately constant and independent of the OCR. The effective friction angle of soils for undrained triaxial shearing of clays is generally assumed to be zero.

3.4.3 Poisson's Ratio μ

The ratio of elastic radial or lateral strain to axial strain is termed as the Poisson's ratio μ. For undrained triaxial tests, there is zero volume change and the soil sample is incompressible. Incompressibility is simulated by an undrained Poisson's ratio μ equal to a value very close to 0.5. An exact value of Poisson's ratio 0.5 is not assumed as this gives rise to numerical problems. For drained shearing of clays, the elastic Poisson's ratio varies generally between 0.1 to 0.3.

3.4.4 Undrained Stress-Strain Modulus E_s

The tangential stress-strain modulus at any given stress is the slope of the tangent to the stress-strain curve of the soil at that stress, where stress is the deviator stress q and the strain is the axial strain ε_a of the soil sample. The tangential stress-strain modulus generally varies non-linearly with the state of stress. The initial tangent modulus E_i is the slope of the deviator stress q versus axial strain ε_a plot of the stress-strain curve, at the start of the test. The secant modulus equals the slope of the line joining the origin and a point at a specified level of stress or strain on the plot of deviator stress q versus axial strain ε_a of the stress-strain curve of the soil. Among a number of specified levels of stress or strain that are used to measure the secant modulus from the stress-

strain curve of the soil are axial strain ε_a = 2%, ε_a = 5%, etc. The secant modulus is also frequently measured at a level of deviator stress q or $\sigma_1' - \sigma_3'$ equal to half of the value of the deviator stress at failure or $(\sigma_1' - \sigma_3')_f$. The secant modulus at this stress level is termed as E_{50}. This is also called secant modulus at a factor of safety level equal to two. The values of E_i and E_{50} obtained for coastal clays of Anwara, Banshkhali and Chandanaish (Bashar, 2002) are tabulated in Appendix II.

3.5 Review of Triaxial Shear Experiments

Bashar (2002) conducted undrained triaxial shearing on block soil samples prepared and consolidated in K_0 condition. Triaxial samples were prepared from the block samples, which were isotropically consolidated to a cell pressure of 150 kPa. Some of the soil samples were sheared at a cell or consolidation pressure of 150 kPa. For others, the cell pressure was reduced to 100, 75, 30, 15, 7.5 and 5 kPa respectively before shearing. Thus the overconsolidation ratios (OCR) of the sheared soil samples were 1, 1.5, 2, 5, 10, 20 and 30 respectively with respect to the isotropic preconsolidation pressure. The experimental stress-strain curve for each overconsolidation ratio was plotted by Bashar (2002) for the coastal clays of Anwara, Banshkhali and Chandanaish. The plots were made in terms of the deviator stress $\sigma_1' - \sigma_3'$ versus axial strain ε_a of the triaxial soil samples. The experimentally measured excess pore pressure u versus axial strain ε_a of each of the coastal clay triaxial soil samples at various OCR's were also plotted.

3.6 Modeling Triaxial Shear

The triaxial shearing of the coastal clays was numerically simulated by a single element finite element model using a finite element program called AFENA (Carter & Balaam, 1995). An 8-noded axisymmetric quadrilateral and isoparametric element with reduced integration was used (Fig.3.5). Constant all round pressure equal to the cell pressure was generated in the radial and vertical direction. The bottom boundary of the element was prevented from movement in the vertical direction. The single element was loaded by displacement control by allowing the nodes of the top

boundary of the single element to move in the vertically downward direction. An incremental elasto-plastic analysis with drift correction was employed. The Mohr-Coulomb model was used to simulate the stress-strain or constitutive behaviour of the clay both for drained and undrained analysis.

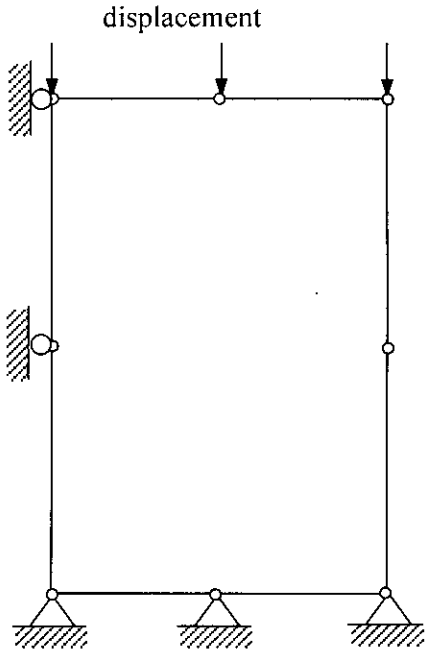

Fig. 3.5 An 8-noded axisymmetric quadrilateral and isoparametric element with reduced integration for simulating triaxial test

3.7 Undrained Analysis (ϕ'=0 approach)

For simulating undrained analysis of soil using the Mohr-Coulomb model, the effective friction angle of the soil $\phi' = 0$ was assumed. The cohesion component of the soil was assumed to be equal to the undrained shear strength of the soil. An elastic Poisson's ratio very close to 0.5 was assumed to generate elastic volume incompressibility. A dilation angle equal to zero was used to simulate incompressible behaviour in the plastic state. Thus incompressible behaviour as expected under undrained conditions, during both elastic and plastic stress state respectively, was simulated using the Mohr-Coulomb model within the finite element program AFENA (Carter & Balaam, 1995). The Mohr-Coulomb model numerical analysis generates the total stress path only during undrained tests. This is because pore pressures cannot be predicted using the conventional Mohr-Coulomb model.

3.8 Prediction of CIU Response

The undrained shear behaviour of coastal clays was generated for elastic initial tangent modulus E_i and secant modulus E_{50} defined in the previous sections. The values of the Mohr-Coulomb model parameters used for generating the undrained triaxial shear stress-strain response of coastal clays of Anwara, Banshkhali and Chandanaish are shown in Appendix B. The comparison of the undrained predictions of triaxial shearing response of coastal clays using the Mohr-Coulomb model with the experimental data are discussed in the following subsections.

3.8.1 Stress-Strain

Figures 3.6 and 3.7 compare the experimental stress-strain curves of undrained triaxial shearing of Anwara clay with the predicted curves using the Mohr-Coulomb Model for initial elastic modulus E_i. Figures 3.8 and 3.9 compare the experimental stress-strain curves of undrained triaxial shearing of Anwara clay with the predicted curves using the Mohr-Coulomb Model for secant elastic modulus E_{50}. It is observed that using secant modulus E_{50} gives a better fit of the overall stress-strain path with experimental data.

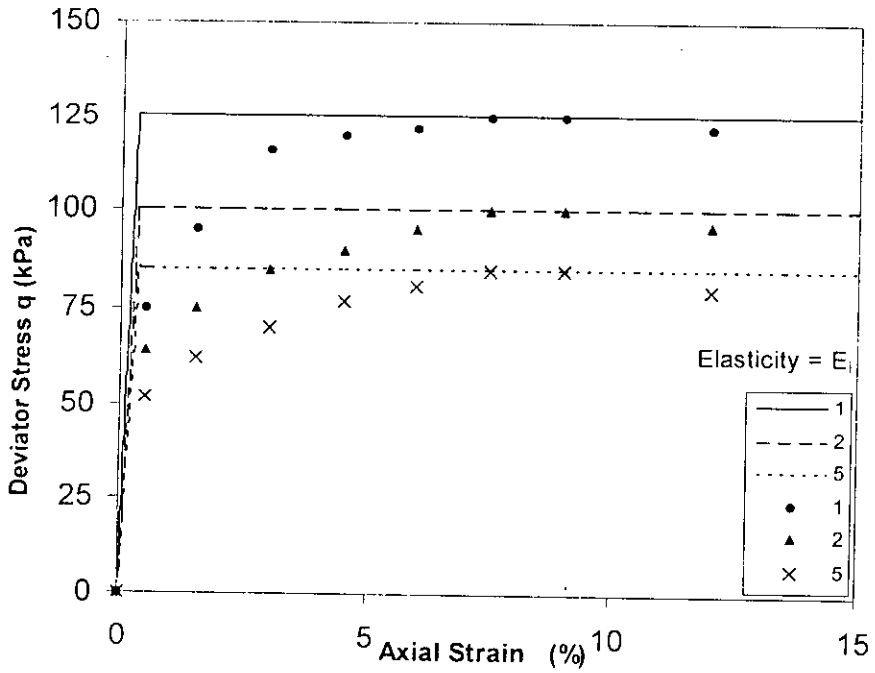

Figure 3.6 Mohr-Coulomb prediction of undrained stress-strain response, Anwara soil (OCR=1, 2, 5 and $E = E_i$)

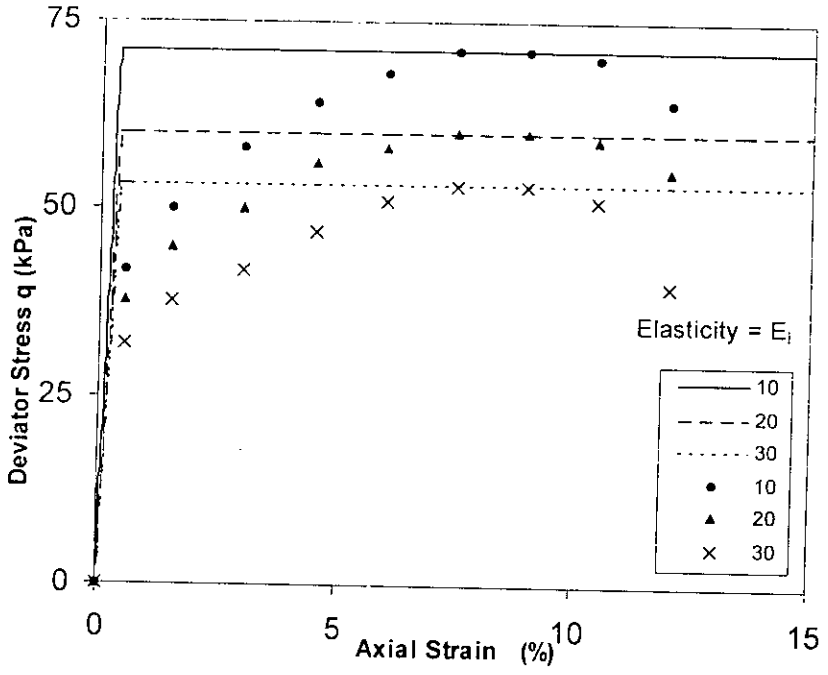

Figure 3.7 Mohr-Coulomb prediction of undrained stress-strain response, Anwara soil (OCR=10, 20, 30 and $E = E_i$)

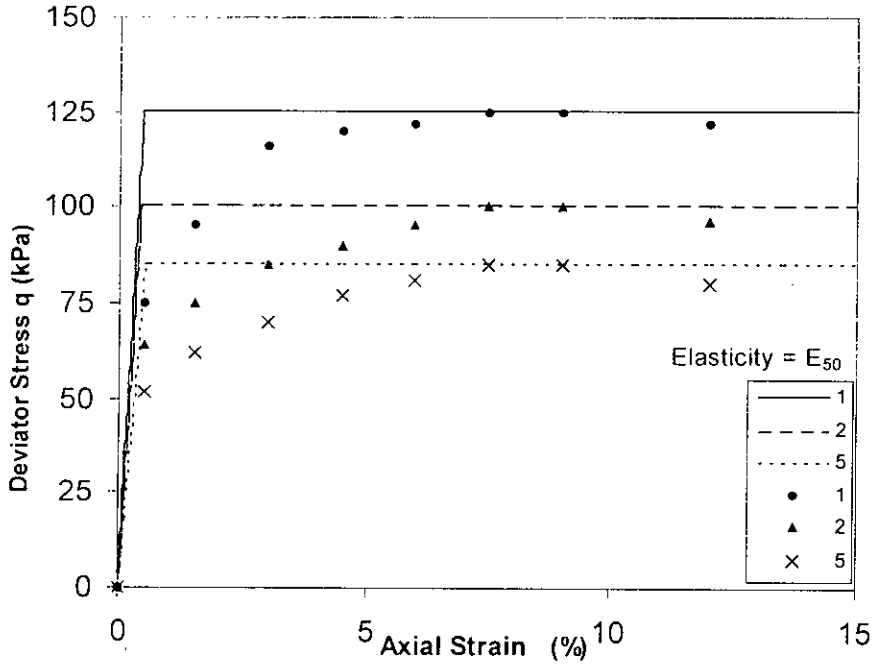

Figure 3.8 Mohr-Coulomb prediction of undrained stress-strain response, Anwara soil (OCR=1, 2, 5 and $E = E_{50}$)

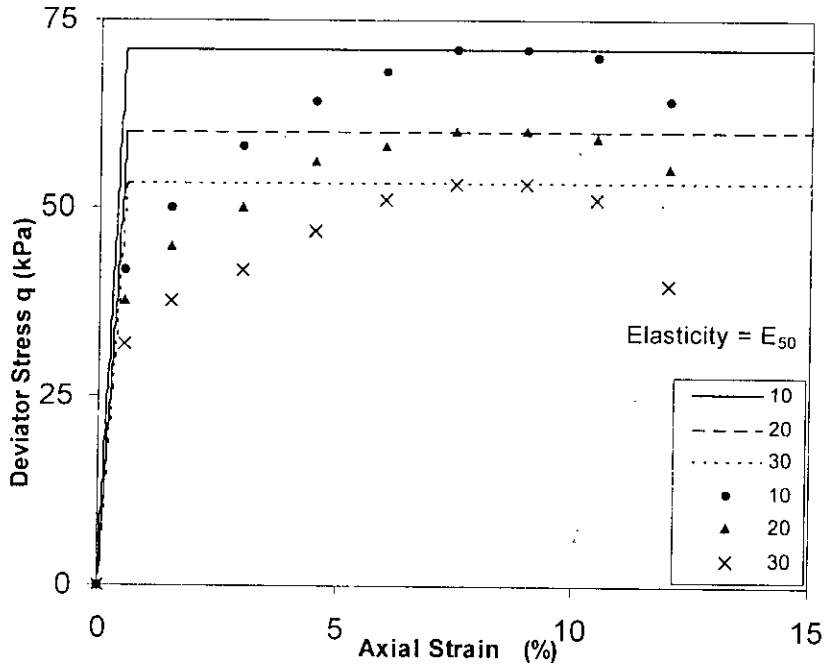

Figure 3.9 Mohr-Coulomb prediction of undrained stress-strain response, Anwara soil (OCR=10, 20, 30 and $E = E_{50}$)

Similar results were observed for Banshkhali (Figures 3.10, 3.11, 3.12 and 3.13) and Chandanaish (Figures 3.14, 3.15, 3.16 and 3.17). The ultimate stress is well predicted if the ultimate failure stress is used to compute undrained shear strength and cohesion. However, the peak stress can be properly predicted if the peak undrained shear strength is used to compute cohesion. The choice of whether to use the peak or ultimate shear strength to compute cohesion in numerical analysis using the Mohr-Coulomb model is dependent on the problem at hand. It may be based on the analyst's judgment of whether the peak or the ultimate cohesion may be mobilised at failure strain for the problem concerned.

3.8.2 Stress Path and Excess Pore Pressure

The Mohr-Coulomb model always gives the total stress path when simulating undrained shearing in a conventional triaxial shear test. It cannot predict the effective stress path during undrained shearing. This is because the Mohr-Coulomb model cannot predict any excess pore water pressure u that may be generated within the soil sample during undrained shearing. This is a shortcoming of the model.

3.9 Evaluation of the Mohr-Coulomb Model

The Mohr-Coulomb model was used to predict the experimentally obtained stress-strain curves of undrained triaxial shearing of coastal clays of Anwara, Banshkhali and Chandanaish. Undrained predictions of Anwara clay, Banshkhali clay and Chandanaish clay using the Mohr-Coulomb model are shown in Tables 3.1, 3.2 and 3.3.

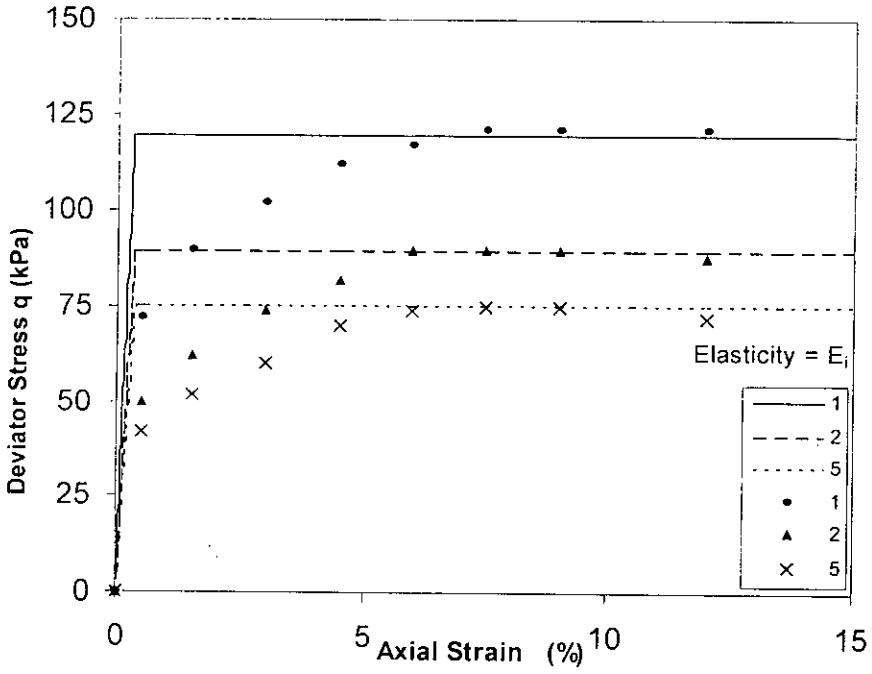

Figure 3.10 Mohr-Coulomb prediction of undrained stress-strain response, Banshkhali soil (OCR=1, 2, 5 and E = E_i)

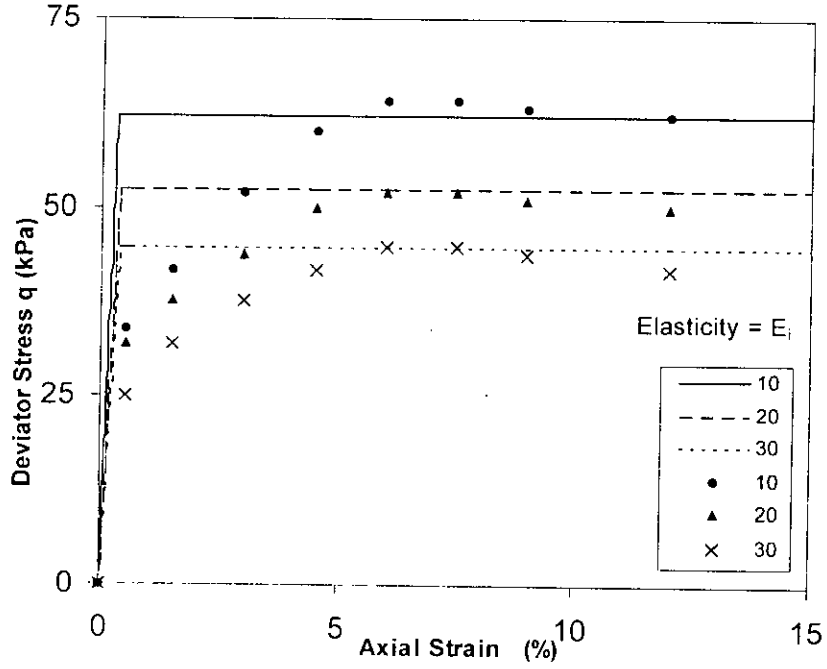

Figure 3.11 Mohr-Coulomb prediction of undrained stress-strain response, Banshkhali soil (OCR=10, 20, 30 and E = E_i)

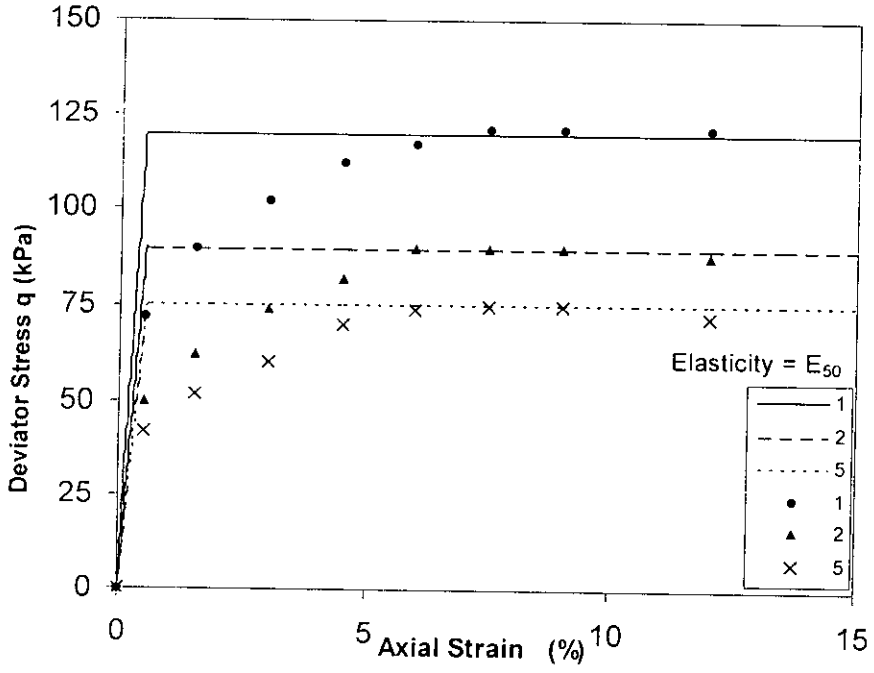

Figure 3.12 Mohr-Coulomb prediction of undrained stress-strain response, Banshkhali soil (OCR=1, 2, 5 and $E = E_{50}$)

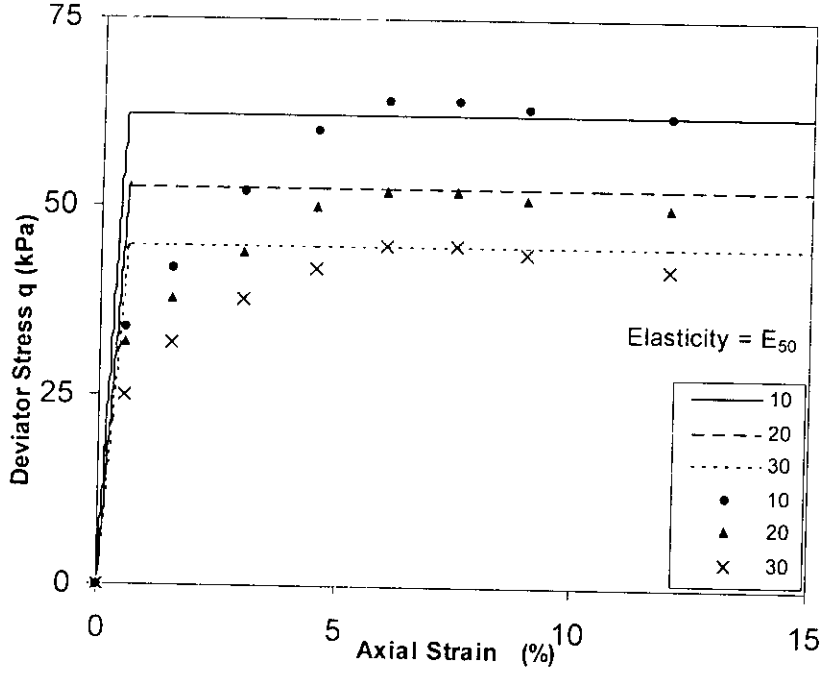

Figure 3.13 Mohr-Coulomb prediction of undrained stress-strain response, Banshkhali soil (OCR=10, 20, 30 and $E = E_{50}$)

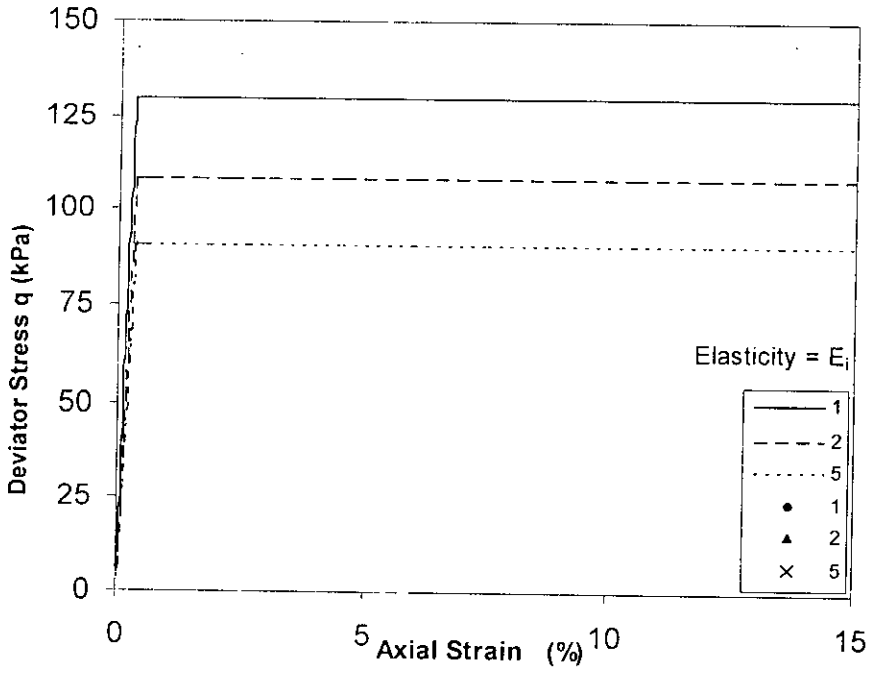

Figure 3.14 Mohr-Coulomb prediction of undrained stress-strain response, Chandanaish soil (OCR=1, 2, 5 and $E = E_i$)

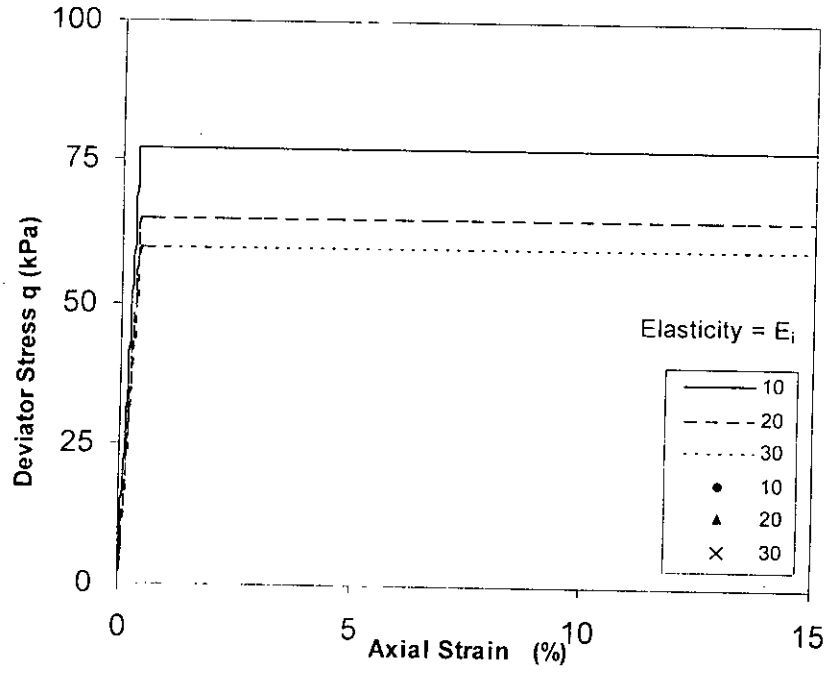

Figure 3.15 Mohr-Coulomb prediction of undrained stress-strain response, Chandanaish soil (OCR=10, 20, 30 and $E = E_i$)

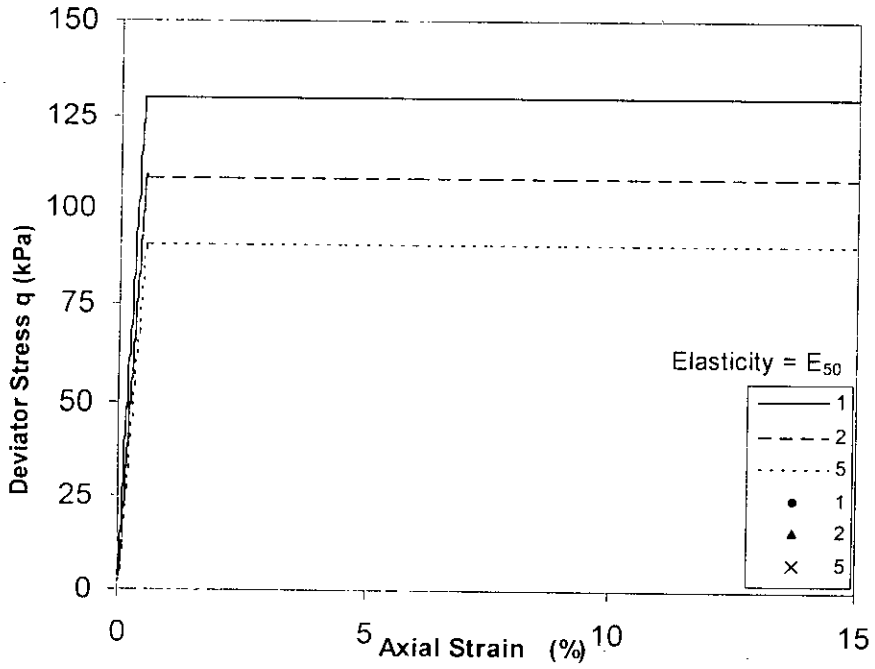

Figure 3.16 Mohr-Coulomb prediction of undrained stress-strain response, Chandanaish soil (OCR=1, 2, 5 and $E = E_{50}$)

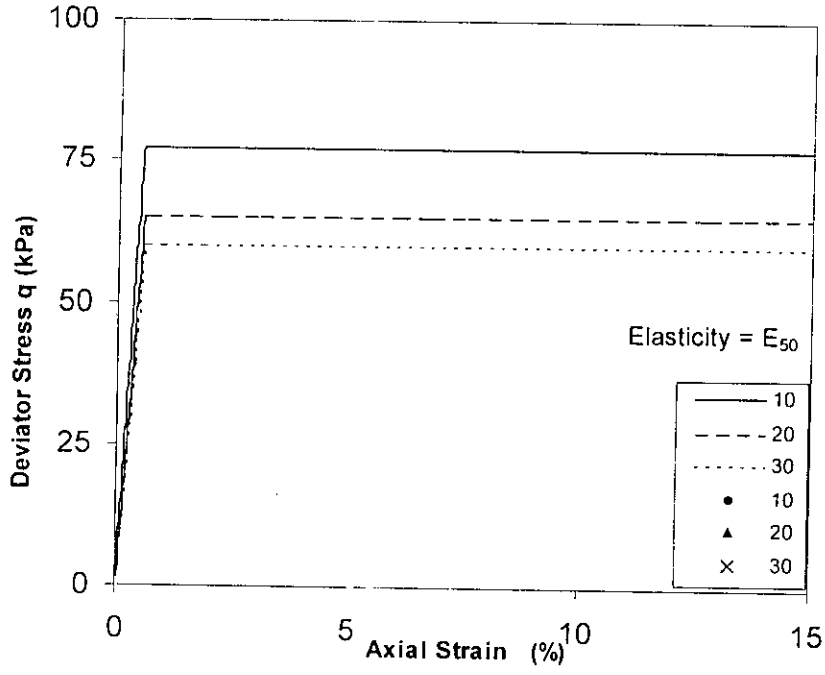

Figure 3.17 Mohr-Coulomb prediction of undrained stress-strain response, Chandanaish soil (OCR=10, 20, 30 and $E = E_{50}$)

Table 3.1 Undrained predictions using the Mohr-Coulomb model: Anwara clay

Cell pressure (kPa)	OCR	Initial			Secant		
		Deviator Stress at failure (kPa)	Strain at failure (%)	Pore pressure at failure (kPa)	Deviator Stress at failure (kPa)	Strain at failure (%)	pore pressure at failure (kPa)
150	1	125.4	0.33	N.A.	125.4	0.48	N.A.
75	2	100.5	0.33	N.A.	100.5	0.42	N.A.
30	5	85.5	0.345	N.A.	85.5	0.525	N.A.
15	10	71.1	0.36	N.A.	71.1	0.54	N.A.
7.5	20	60.0	0.375	N.A.	60.0	0.555	N.A.
5	30	53.2	0.375	N.A.	53.2	0.555	N.A.

Table 3.2 Undrained predictions using the Mohr-Coulomb model: Banshkhali clay

Cell pressure (kPa)	OCR	Initial			Secant		
		Deviator Stress at failure (kPa)	Strain at failure (%)	Pore pressure at failure (kPa)	Deviator Stress at failure (kPa)	Strain at failure (%)	Pore pressure at failure (kPa)
150	1	119.2	0.33	N.A.	119.2	0.495	N.A.
75	2	90.0	0.33	N.A.	90.0	0.51	N.A.
30	5	75.6	0.36	N.A.	75.6	0.525	N.A.
15	10	62.0	0.33	N.A.	62.0	0.51	N.A.
7.5	20	52.4	0.375	N.A.	52.4	0.555	N.A.
5	30	45.0	0.375	N.A.	45.0	0.555	N.A.

Table 3.3 Undrained predictions using the Mohr-Coulomb model: Chandanaish clay

Cell pressure kPa	OCR	Initial			Secant		
		Deviator Stress at failure (kPa)	Strain at failure (%)	Pore pressure at failure (kPa)	Deviator Stress at failure (kPa)	Strain at failure (%)	pore pressure at failure (kPa)
150	1	130.0	0.315	N.A.	130.0	0.48	N.A.
75	2	108.6	0.33	N.A.	108.6	0.495	N.A.
30	5	91.0	0.345	N.A.	91.0	0.51	N.A.
15	10	76.8	0.36	N.A.	76.8	0.525	N.A.
7.5	20	65.0	0.36	N.A.	65.0	0.54	N.A.
5	30	59.8	0.375	N.A.	59.8	0.555	N.A.

The strengths, weaknesses and limitations of the Mohr-Coulomb model are discussed below:

3.9.1 Strengths

The Mohr-Coulomb model was used to predict the undrained shearing response of laboratory samples of coastal clays of Bangladesh under triaxial stress conditions. The predictions were then compared with the available triaxial laboratory data for the coastal soils. Based on the comparisons of the Mohr-Coulomb model predictions with available experimental data, the strengths and weaknesses of the Mohr-Coulomb model for predicting undrained triaxial shear response of coastal clays of Bangladesh are enumerated below:

- The Mohr-Coulomb model is a simple model, is easy to use, and familiar to most soil mechanics practitioners.

- The Mohr-Coulomb model has only two plastic model parameters (c and ϕ') and two elastic model parameters (E and μ).

- The Mohr-Coulomb model parameters may be easily determined from simple laboratory tests.

- The Mohr-Coulomb model can be used for drained (c = 0 approach) and undrained analysis (ϕ' = 0 approach) and it may be used to predict the limit state behaviour of both clays and sands.

- The Mohr-Coulomb model can be used for partially drained or partially saturated soils using the so-called c-ϕ' approach.

- Analytical solutions, also called limit state solutions in geotechnical literature, may be obtained for many practical soil mechanics problems using the Mohr-Coulomb model.

3.9.2 Weaknesses

- The Mohr-Coulomb model cannot predict pore pressures in undrained analysis.

- The Mohr-Coulomb model cannot predict hardening. Thus it is unable to predict stress-strain behaviour of elasto-plastic strain-hardening materials such as clays correctly.

- The Mohr-Coulomb model is unable to predict undrained stress paths of clays where pore pressures are generated.

3.10 Summary and Conclusion

The Mohr-Coulomb model was used to predict the drained and undrained triaxial shear behaviour of laboratory samples of coastal clays of Bangladesh. It was observed

that although the peak or ultimate behaviour can be well predicted using this model, the stress path generated during undrained triaxial shear of coastal clays cannot be predicted. This is a result or consequence of the inability of the model to simulate strain-hardening plasticity. The Mohr-Coulomb model can simulate initially elastic and finally perfectly plastic behaviour. The model is simple and may be used for the analysis of a wide range of practical geotechnical problems. Understanding the context in which the model can be used allows one to obtain realistic predictions for many practical problems.

CHAPTER 4

PREDICTION OF UNDRAINED STRESS-STRAIN RESPONSE: THE MODIFIED CAM CLAY MODEL

4.1 Introduction

A unified framework of modelling the stress-strain response of strain hardening materials such as normally consolidated and overconsolidated clays was formulated in Cambridge, UK in the late 1950's. Different aspects of the widely used version of the Cambridge soil model, the "Modified Cam Clay Model" (MCC) is described in this chapter. The MCC model is then used to predict the undrained stress-strain response of some coastal clays of Bangladesh. The model parameter relevant for undrained analysis of coastal clays using the MCC model is then discussed. Next, the capability of the MCC model to predict the undrained response of coastal clays is investigated. The predicted undrained stress-strain response, effective stress paths and pore pressures are compared with available experimental data. Finally the strengths, weaknesses and limitations of the MCC model to predict the undrained response of coastal clays is evaluated.

4.2 Modified Cam Clay (MCC) Model

The Modified Cam Clay Model (MCC) is a volumetric strain hardening model within the critical state framework. The model is generally used to predict the stress-strain response of normally consolidated and lightly overconsolidated clays. The model may be described in terms of the following components.

4.2.1 Critical or Ultimate State

The critical state framework states that as an element of soil undergoes shearing, it ultimately reaches a state termed as the critical or ultimate state. At this state soil undergoes continuous shearing strain at constant volume. For any soil, there exists a locus of stress states defined by the mean effective stress p' and deviator stress q, at which it reaches the critical state. This locus is generally a straight line in (p', q)

space and it is termed as the critical state line. The slope of this line is termed as the critical state ratio M. The mean pressure p' and the deviator stress q may be obtained in terms of the effective principal stresses $\sigma_1', \sigma_2', \sigma_3'$ as follows:

$$p' = (\sigma_1' + \sigma_2' + \sigma_3')/3$$

$$q = \frac{1}{\sqrt{2}}\sqrt{\{(\sigma_1' - \sigma_2')^2 + (\sigma_2' - \sigma_3')^2 + (\sigma_3' - \sigma_1')^2\}}$$

$$M = \frac{q_f'}{p_f'}$$

In the above equations σ_1' may be considered as the major principal effective stress and σ_2', σ_3' are the minor principal effective stresses. M is the stress ratio at the ultimate or critical state of the soil. The critical state ratio M is considered as a fundamental soil parameter in critical state soil mechanics. This is because all soils when sheared, ultimately reach the critical state.

4.2.2 Yield Function

When a soil undergoes shear, the strains are recoverable or elastic up to a certain level of the effective stress (p' , q). Beyond this stress state, irrecoverable or plastic straining of soil occurs. This stress state is termed as the yield stress. The locus of stress states (p' , q) at which the strain becomes plastic or yielding occurs is a convex function in (p' , q) space. This function is generally given as follows:

$$f(p', q, p_o') = 0$$

The above function is termed as the yield function. p_o' is the preconsolidation pressure of the soil. As the soil compresses plastically, its void ratio decreases and its preconsolidation pressure p_o' increases. The current preconsolidation pressure p_o' of the soil defines a new enlarged yield function. If the soil is now unloaded, the new yield function with an increased value of the preconsolidation pressure p_o' determines

the limit of the locus of effective stresses (p' , q) up to which the soil will respond elastically. Beyond this locus, the soil behaviour will become elasto-plastic. p'_o is defined as the hardening parameter in the Modified Cam Clay model. All stress states within the region of yield function are assumed to be elastic. Hence loading in any direction from a stress state within the yield locus and remaining completely within this locus will lead to elastic or recoverable strains only. When a stress state is on the yield function and an increment of applied stress is directed in the outward region of yield function, incremental plastic strains are assumed to occur.

4.2.3 Hardening

An applied increment of stress directed in the outward region of the yield function results both in incremental plastic strains and incremental elastic strains. This results in hardening or increase in the value of the hardening parameter p'_o with consequent expansion of the yield function such that the current stress state lies on the new expanded yield surface. The stress zone of elastic response is thus permanently expanded, which is termed as soil hardening. The parameter p'_o termed as the hardening parameter and assumes a new and increased value. If the current stress state is $(\overline{p}', \overline{q})$ and the current value of the hardening parameter is $\overline{p}'_o$, then these parameters will satisfy the yield function as follows:

$$f(\overline{p}', \overline{q}, \overline{p}'_o) = 0$$

The elastic region is enlarged permanently and the old yield function ceases to exist. The hardening parameter p'_o is thus a monotonically increasing function of plastic volumetric strain. This function may be derived from the $e - \log p'$ curve of a soil and is given as follows:

$$\frac{dp'_o}{d\varepsilon_v^p} = \frac{p'_o(1+e)}{(\lambda - \kappa)}$$

In the above equation, p_o' is the preconsolidation pressure, dp_o' is the increase of the preconsolidation pressure due to hardening, e is the current void ratio of the soil, λ and κ are respectively the slope of the normal consolidation line and elastic rebound line of the $e - \log p'$ curve of the soil. Stress states can lie only within or on the yield function. Stress states outside the yield function are impossible as such stress states immediately results in expansion and hardening of the yield function. Thus the new stress states are again on the yield function defined by an increased value of the hardening parameter p_o'. The increase of the value of p_o' and consequent expansion of the yield locus in the stress space resulting in an expansion of the zone of elastic response of the soil is generally termed as hardening.

4.2.4 Stress Dilatancy and Plastic Potential Function

During shearing, the relative direction of incremental plastic strains is directly related to the dilatancy ratio. Dilatancy ratio is defined as the ratio of incremental plastic deviator strain $d\varepsilon_q^p$ to incremental plastic volumetric strain $d\varepsilon_v^p$. Elasto-plastic models such as the Modified Cam Clay model assumes the dilatancy ratio to be a function of the stress state of the soil when it is in plastic or yield condition. At the yield state, the Modified Cam Clay model assumes the dilatancy ratio to be a function of the stress ratio $\eta = \frac{q}{p'}$ as follows:

$$\frac{d\varepsilon_q^p}{d\varepsilon_v^p} = \frac{M^2 - \eta^2}{2\eta}$$

In the above equation, the stress ratio $\eta = M$ is the stress ratio at the critical or ultimate stress state of the material. At this stress state, the material undergoes continuous plastic shear at zero incremental plastic volume strain i.e. at constant volume. At stress ratios $\eta > M$, the soil undergoes expansive volume strain and soften. This results in a decrease of the hardening parameter p_o' of the soil and consequent contraction of the yield surface. The shear or deviator stresses continue to decrease. This is an unstable state. At stress ratios $\eta < M$, the soil undergoes compressive plastic volume strain. Consequently, the value of the hardening

parameter p'_o increases and there is strain hardening of the soil. In elasto-plasticity, the plastic potential function is defined as a function of stresses in (p' , q) space. At any stress state, the normal to the plastic potential function gives the direction of incremental plastic strains. In the Modified Cam Clay model, the associated flow rule is assumed i.e. the yield function is assumed to be identical to the plastic potential function. The given stress-dilatancy function is incorporated in the differential form of the yield equation which is then integrated. This give the yield and the plastic potential function for the Modified Cam Clay model as below:

$$\left(\frac{q}{Mp'}\right)^2 = \frac{p'}{p'_o} - 1$$

The assumption of associated flow rule ensures that Drucker's stability postulates and basic thermodynamic relations are satisfied by the soil. The Modified Cam Clay model satisfies the relations. Figures 4.1 and 4.2 illustrate the different aspects of the Modified Cam Clay model.

4.2.5 Elastic Behaviour

The stress strain response of the soil is assumed to be recoverable or elastic inside the yield locus. The stress-strain responses of the soil are generally assumed to be described by two elastic parameters: the elastic bulk modulus and elastic shear modulus. The elastic bulk modulus of soil may be obtained from the unload-reload or elastic rebound portion of the $e - \log p'$ curve as follows:

$$\frac{dp'}{d\varepsilon_v^e} = \frac{p'(1+e)}{\kappa} = K$$

Thus in Modified Cam Clay model, the elastic modulus is directly proportional to the mean effective stress p'. The Modified Cam Clay framework assumes a constant value of the Poisson's ratio μ.

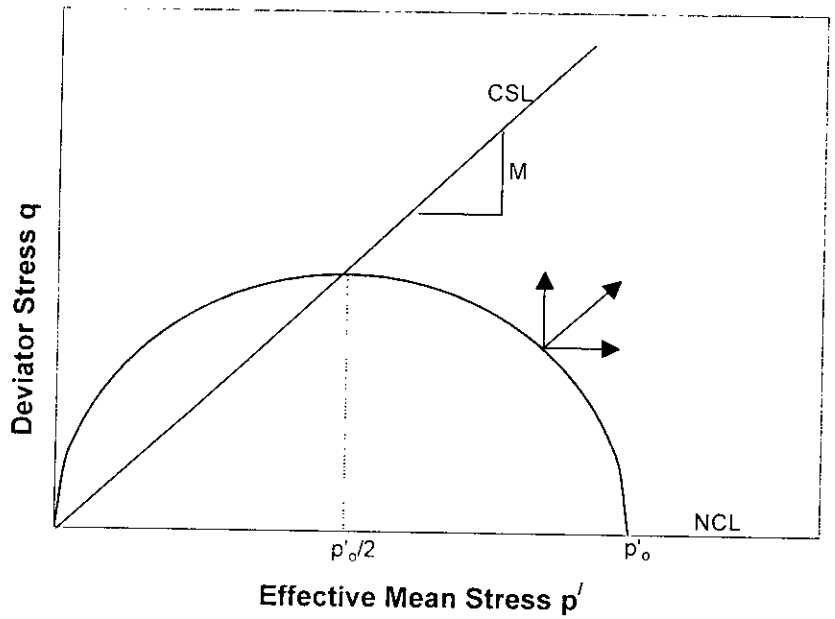

Figure 4.1 Modified Cam Clay (MCC) model elliptical yield locus and plastic potential function (Schofield and Wroth, 1968)

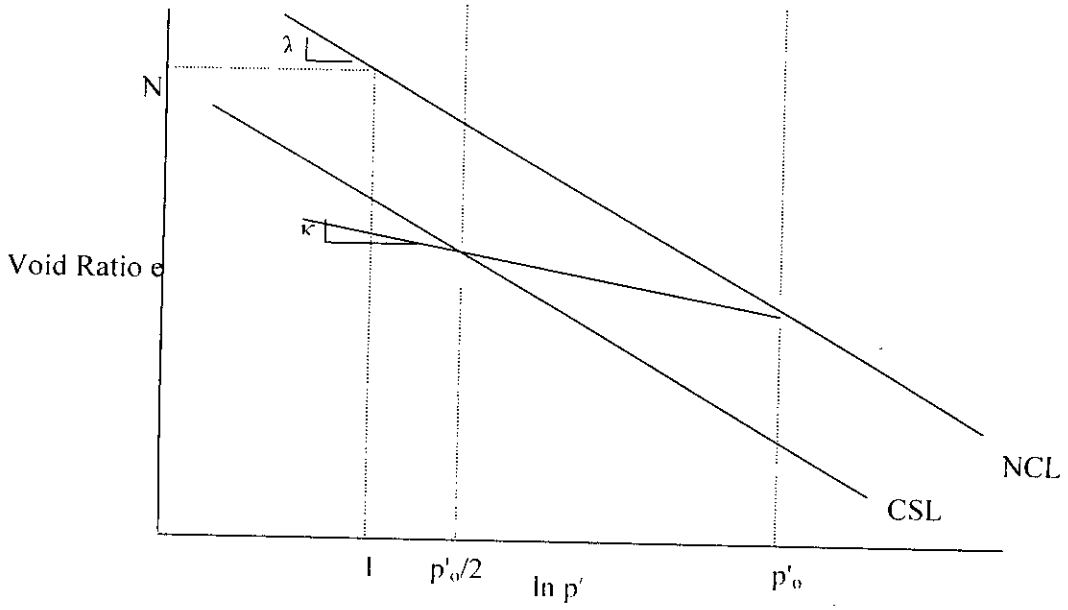

Figure 4.2 Modified Cam Clay (MCC) model Critical State Line (CSL) and Normal Consolidation Line (NCL) in e-ln p' space(Schofield and Wroth, 1968)

The elastic shear modulus G may be computed from the elastic bulk modulus and elastic Poisson's ratio as follows:

$$G = \frac{3K(1-2\mu)}{2(1+\mu)}$$

Thus in the Modified Cam Clay model both the elastic shear modulus G and bulk modulus K are nonlinear and vary directly with the mean effective stress p' and current void ratio e.

4.3 Suitability of Modified Cam Clay Model for Predicting Coastal Clay Behaviour

Despite its limitations, the Modified Cam Clay model has been generally found to be quite suitable for predicting the shear response of clays in triaxial stress states both in drained and undrained conditions. Coastal clays of Bangladesh exhibit consolidation or time dependent stress-strain response. For such clays, a well-defined void ratio by effective stress ($e - \log p'$) curve or consolidation curve may be obtained in the laboratory by simple consolidation tests. The elastic rebound and plastic consolidation part of the $e - \log p'$ curve and their break at the initial preconsolidation pressure p'_o can thus be distinctly identified for coastal clays. The slope κ of the elastic rebound curve, the slope λ of the normal consolidation line and the preconsolidation pressure p'_o can be easily obtained from the consolidation curve of coastal clays. The three parameters λ, κ and p'_o are the most significant parameters of the Modified Cam Clay model. The other important parameters are the initial void ratio e, drained Poisson's ratio μ and critical state ratio M of the soil. All of these parameters may be easily obtained from simple laboratory tests. The Modified Cam clay yield locus generally shows good agreement with the experimental yield curve for clays. During triaxial shear, low OCR clays exhibit strain hardening with simultaneous development of positive pore pressures (undrained case) or compressive volume strain (drained case). At high OCR's, softening response associated with negative pore pressure (undrained case) or expansive volume strain (drained case) is exhibited. This type of response was also observed for coastal clays. The Modified

Cam Clay model can predict such soil behaviour. When sheared, clays exhibit constant pore pressure (undrained case) or constant volume strain (drained case) and constant stress at critical state. The Modified Cam Clay model predicts such constant pore pressure or constant volume strain behaviour at the ultimate state. The Modified Cam Clay model may thus be considered quite appropriate for predicting both the drained and undrained stress-strain response of coastal clays.

4.4 Modified Cam Clay Parameters for Coastal Clays

The Modified Cam Clay model has 2 elastic parameters and 4 plastic parameters. The elastic parameters are respectively the slope κ of the elastic unload-reload line plotted in the $e - \log p'$ space and the elastic Poisson's ratio μ. The plastic parameters are plastic consolidation slope λ, preconsolidation pressure p'_o, the critical state ratio M and the void ratio on the normal consolidation line, at unit pressure N. The critical state ratio M is a function of the ultimate friction angle of the soil. It defines the ultimate state of the soil. All of the Modified Cam Clay model parameters may be obtained from simple and conventional laboratory tests of soil. The MCC model parameters have physical interpretation and they can be directly correlated with the stress-strain response of the soil. The major advantage of the Modified Cam Clay model is that it's model parameters are not numerical quantities designed to curve fit the observed stress-strain response of soils. The meaning of each of the model parameters and the method of computing them are described separately below.

4.4.1 Elastic Parameters

The elastic parameter κ of the Modified Cam Clay model is obtained as the slope of the unload-reload part of the consolidation curve plotted in $e - \log p'$ space. The consolidation curve of coastal clays may be obtained by conducting an isotropic or K_o consolidation test on a clay sample. The details of such test are described in the standard literature. κ along with current void ratio and mean effective pressure p' is used to obtain the elastic bulk modulus K of the soil. The average drained Poisson's ratio of a coastal clay sample may be computed from the volume strain and axial strain response of the soil. The drained elastic Poisson's ratio of clays generally vary

between 0.2 to 0.4. The undrained Poisson's ratio is taken to be close to 0.5. A value of 0.5 for elastic Poisson's ratio theoretically predicts volume incompressibility. Incompressibity or no volume change condition of clays is obtained in undrained tests.

4.4.2 Plastic Parameters

The plastic parameter λ is obtained as the slope of the virgin portion of the consolidation curve or normal consolidation line as drawn in $e - \log p'$ space. The consolidation curve of clays may be plotted by conducting isotropic or K_o consolidation tests on clay samples. The plastic parameter preconsolidation pressure p'_o is the pressure at which the slope of the consolidation line of the soil is observed to change from elastic (low) to plastic(high). Except for very stiff or structured soils, no distinct or abrupt change is generally observed. Rather the change is smooth and gradual. One of several empirical approaches may be used to make an estimate of the preconsolidation pressure p'_o from the consolidation curve. Such approaches are described in standard soil mechanics text. The parameter N is the void ratio on the normal consolidation line, at unit pressure. It is dependent on the unit of pressure used to plot the $e - \log p'$ curve. It defines the position of the virgin or normal consolidation line in $e - \log p'$ space. Once λ, p'_o and N are known, the void ratio at any other mean effective pressure p' may be computed.

4.4.3 Critical State Parameter

The critical state parameter M is the stress ratio $M = \frac{q_f}{p'_f}$ at the ultimate stress state.

At the ultimate stress state, the soil shears at constant stress and constant excess pore pressure (undrained case) or constant volume strain (drained case). The locus of ultimate stress states is generally a straight line in (p', q) space passing through the origin. This line is termed as the critical state line and the slope of this line is termed as the critical state ratio M. The critical state ratio M may be obtained by plotting the effective stress ratio at the ultimate state for a series of triaxial shear tests conducted at various cell pressures.

The Modified Cam Clay model parameters for coastal clays of Anwara, Banshkhali and Chandanaish as obtained by Bashar (2002) are described in Appendix II.

4.5 Consolidated Undrained Shearing of Coastal Clays

Block samples of Anwara, Banshkhali and Chandanaish clays were first isotropically consolidated to a cell pressure of 150 kPa and then subjected to undrained shearing in a triaxial apparatus (Bashar, 2002). A series of soil samples were sheared in this process. For other samples, after applying the consolidation pressure of 150 kPa, the cell pressure was reduced to 100, 75, 30, 15, 7.5 and 5 kPa respectively. Thus for these soil samples an isotropic overconsolidation ratio (OCR) of 1, 1.5, 2, 5, 10, 20 and 30 respectively was achieved. After reducing the cell pressure, the overconsolidated coastal clay samples were sheared. For each of the sheared samples and at various overconsolidation ratios (OCR's), the plots of deviator stress q by axial strain ε_a, the deviator stress q by mean effective pressure p' and excess pore pressure u by axial strain ε_a were drawn (Bashar, 2002).

4.6 Numerical Modelling of Triaxial Shear

The consolidated undrained triaxial shearing of coastal clays at various OCR's were numerically simulated by a single element finite element model using the finite element program AFENA (Carter and Balaam, 1995). The Modified Cam Clay model was used as the elasto-plastic constitutive model to simulate the stress strain response of the element. The Modified Cam Clay parameters for the coastal clays and the cell pressures applied in triaxial tests was input in the finite element program. An 8-noded axisymmetric, quadrilateral and isoparametric element with reduced Gaussian integration was used. A constant all round cell pressure was generated in the element model and the response of the soil element to isotropic load was first computed. Vertically downward displacement was applied at the top boundary nodes of the element. The bottom boundary was fixed in the vertical direction. The lateral boundaries were free to move both vertically and radially. An incremental iterative analysis with stress scaling and drift correction was employed.

4.7 Numerical Predictions of Consolidated Undrained Tests

A numerical simulation of consolidated undrained shearing of coastal clays under triaxial states of stress was carried out. An axisymmetric single element elasto-plastic finite element analysis was conducted using the Modified Cam Clay model. For simulating incompressibility, a no or zero volume change condition i.e. zero volume strain condition need to be simulated. This condition is generated by adding the elastic bulk modulus of water to each of the diagonal terms of the elasto-plastic stress-strain matrix of the elasto-plastic constitutive element. Adding a value of elastic bulk modulus for water as any value that is several orders of magnitude higher than the elastic bulk modulus of the soil element will generally suffice. This results in the sum of the diagonal term of the computed incremental strain matrix to be zero. The sum of the diagonal terms of the incremental strain matrix represents the incremental volume strain of the soil. This being zero, volume incompressibility condition, or essentially an undrained shearing response of the soil, under triaxial states of stress is simulated.

4.8 Prediction of CIU Response of Coastal Clays

The stress-strain response of coastal clays of Anwara, Banshkhali and Chandanaish during undrained triaxial shear was generated using the MCC model parameters given in Appendix B. Predictions were generated for overconsolidation ratios of 1, 2, 5, 10, 20 and 30 respectively. The observed and predicted responses for coastal clays are discussed below.

4.8.1 Stress-Strain

Figures 4.3 and 4.4, Figures 4.5 and 4.6 and Figures 4.7 and 4.8 show the predicted and observed behaviour regarding undrained stress-strain response of Anwara, Banshkhali and Chandanaish in triaxial shear. It is observed that unlike the Mohr-Coulomb model, the Modified Cam Clay model predicts non-linear strain hardening response before the ultimate stress state is reached. Thus the qualitative nature of the stress-strain response of clays is more correctly represented by the Modified Cam Clay model in comparison to the Mohr-Coulomb model.

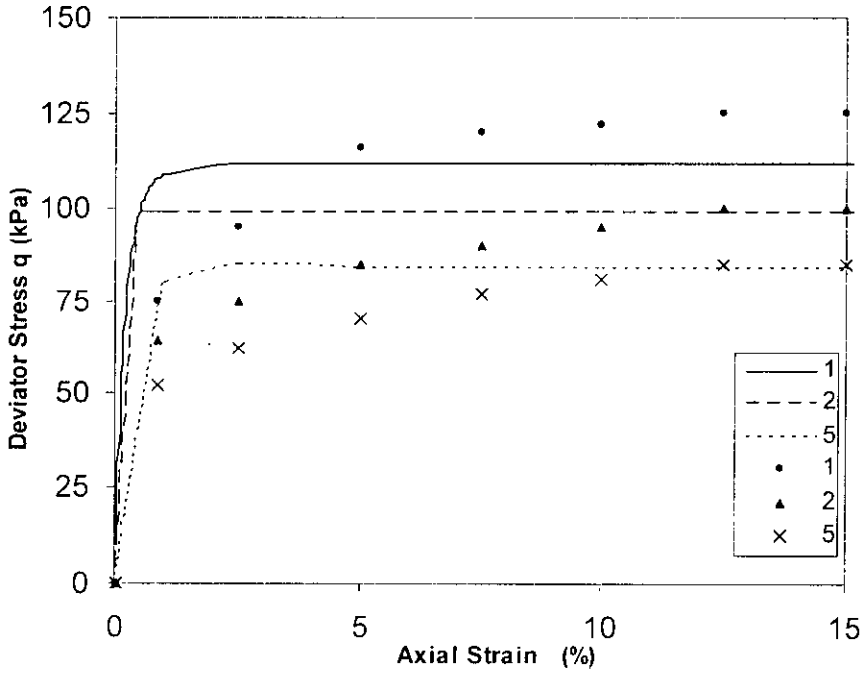

Figure 4.3 MCC prediction of undrained triaxial stress-strain response of Anwara clay (OCR=1, 2, 5)

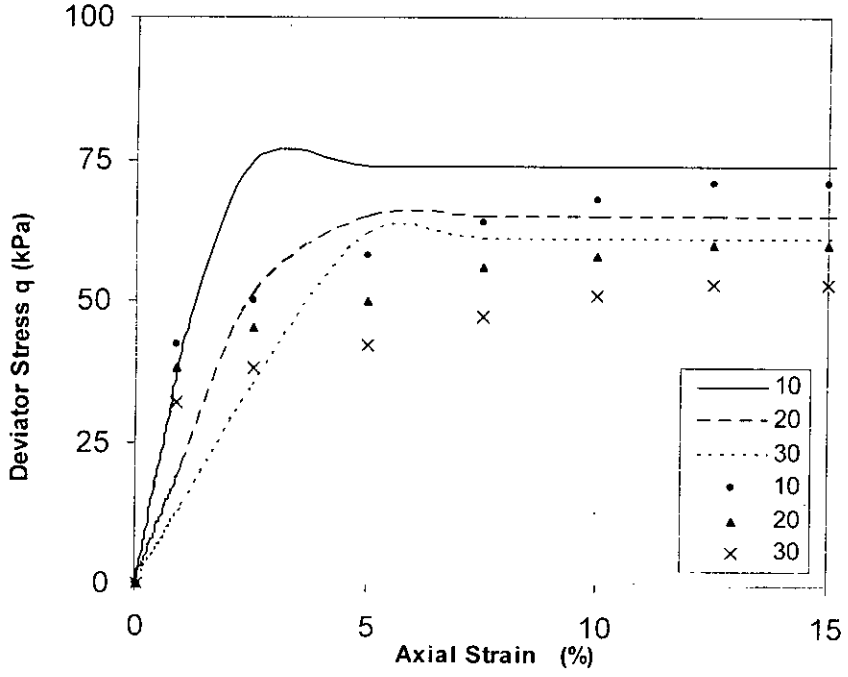

Figure 4.4 MCC prediction of undrained triaxial stress-strain response of Anwara clay (OCR=10, 20, 30)

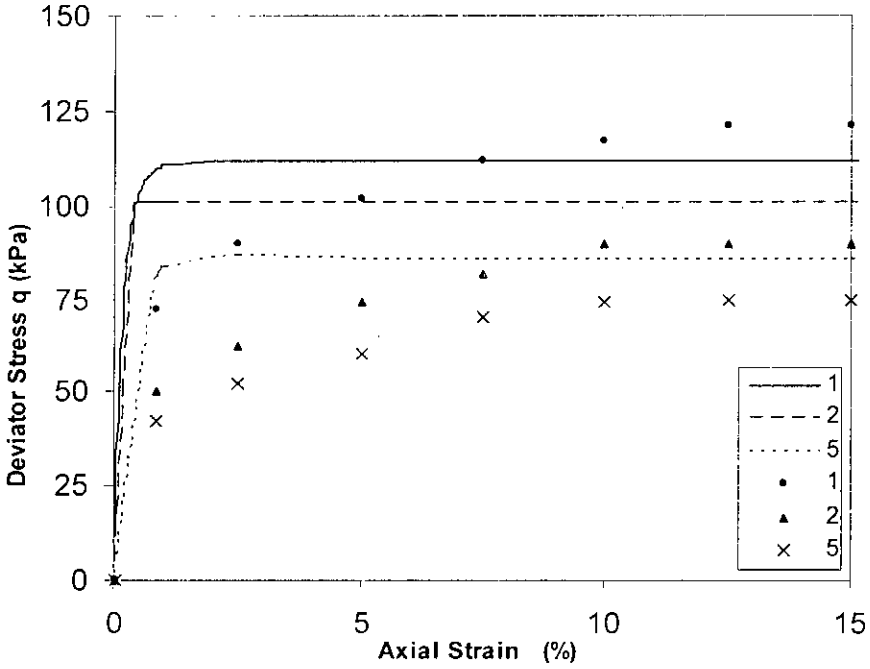

Figure 4.5 MCC prediction of undrained triaxial stress-strain response of Banshkhali clay (OCR=1, 2, 5)

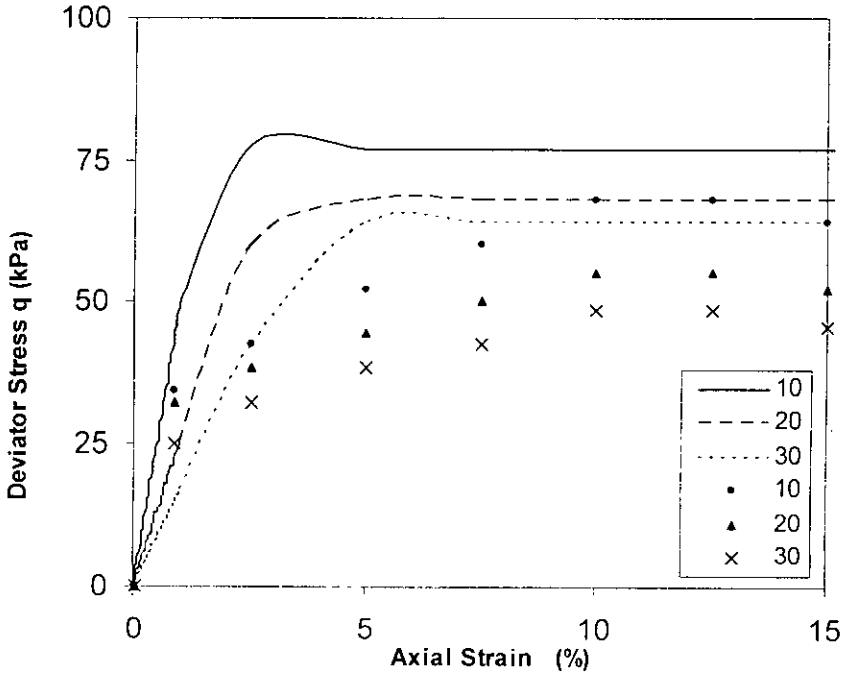

Figure 4.6 MCC prediction of undrained triaxial stress-strain response of Banshkhali clay (OCR=10, 20, 30)

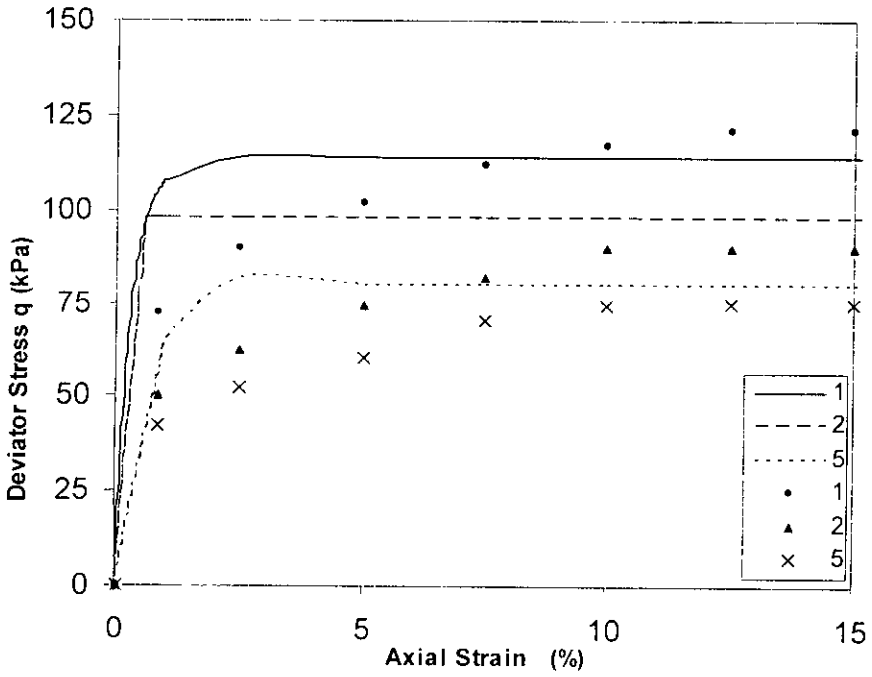

Figure 4.7 MCC prediction of undrained triaxial stress-strain response of Chandanaish clay (OCR=1, 2, 5)

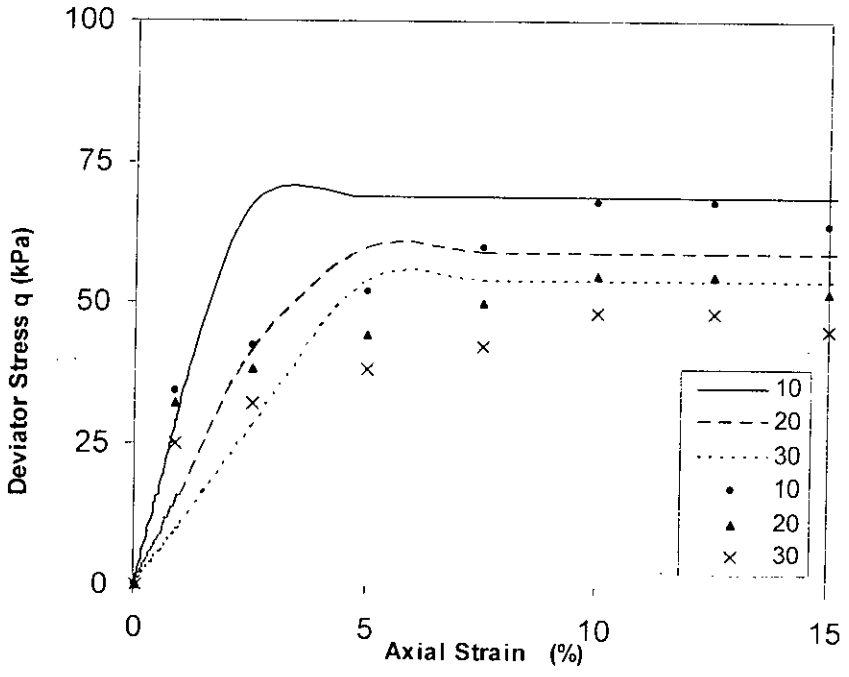

Figure 4.8 MCC prediction of undrained triaxial stress-strain response of Chandanaish clay (OCR=10, 20, 30)

4.8.2 Stress Path

Figures 4.9 and 4.10, Figures 4.11 and 4.12 and Figures 4.13 and 4.14 show the predicted and observed undrained stress paths for Anwara, Banshkhali and Chandanaish clays during undrained triaxial shear. It is observed that stress paths for normally consolidated clays are qualitatively well predicted. However, the observed stress paths for high OCR clays are significantly non-linear even initially. The Modified Cam Clay predicts stress paths for overconsolidated clays that are straight lines initially. This happens as the Modified Cam Clay model simulates elastic behaviour prior to yielding in case of high OCR clays.

4.8.3 Pore Pressure

Figures 4.15 and 4.16 and Figures 4.17 and 4.18 and Figures 4.19 and 4.20 show excess pore pressure response during undrained triaxial shear at various OCR's for Anwara, Banshkhali and Chandanaish clays. At higher OCR's, Modified Cam Clay model predicts negative pore pressures as observed experimentally. Thus the Modified cam Clay model is a rational predictor of excess pore pressure response of coastal clays, at least qualitatively.

4.9 Comparison of Modified Cam Clay with Mohr-Coulomb Model Predictions

In this section, the undrained stress-strain prediction of coastal clay using the Mohr Coulomb model are compared. Tables 4.1, 4.2 and 4.3 compare the predictions of the two models considering $E=E_i$ for Mohr Coulomb model. Tables 4.4, 4.5 and 4.6 compare the predictions of the two models considering $E=E_{50}$ for Mohr Coulomb model. The Modified Cam Clay model predicts non-linear, elasto-plastic and strain hardening stress-strain response until the ultimate failure state is reached. At the ultimate state the soil is predicted to undergo continuous plastic shear at constant state of stress. The Modified Cam Clay model gives a qualitatively correct approximation of the undrained shearing response of coastal clays. The Mohr-Coulomb model predicts elastic and perfectly plastic behaviour. It cannot generate plastic response of the soil before the ultimate state is reached. The Mohr-Coulomb model thus gives only an average elastic-perfectly plastic idealization of the undrained shear response of coastal clays.

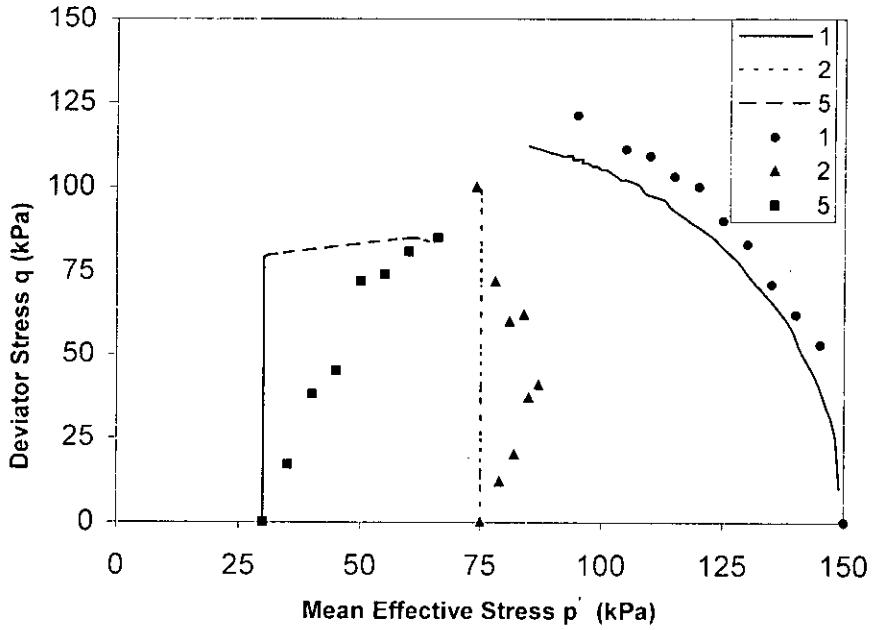

Figure 4.9 MCC prediction of undrained triaxial stress path of Anwara clay (OCR=1, 2, 5)

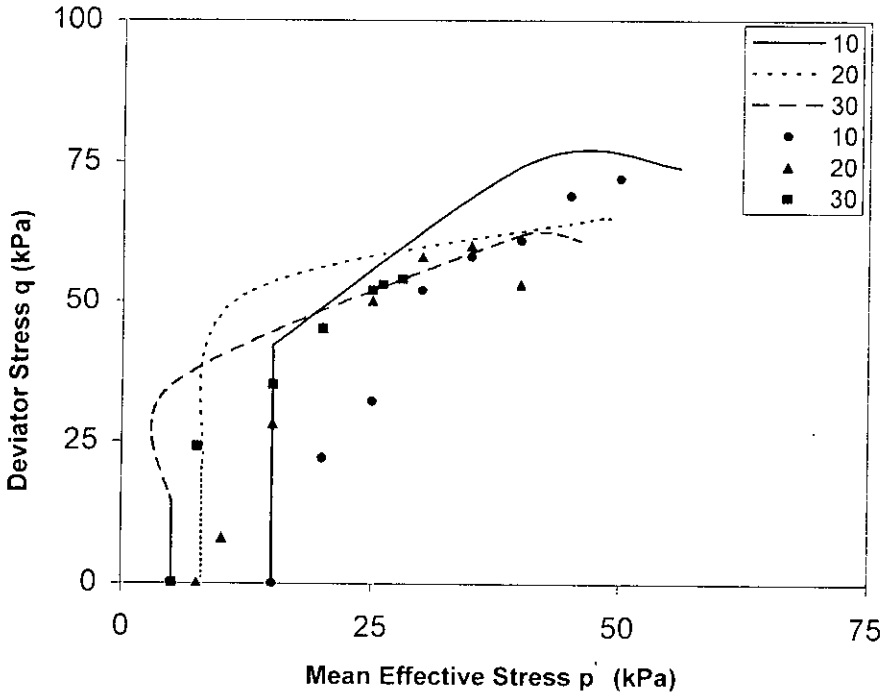

Figure 4.10 MCC prediction of undrained triaxial stress path of Anwara clay (OCR=10, 20, 30)

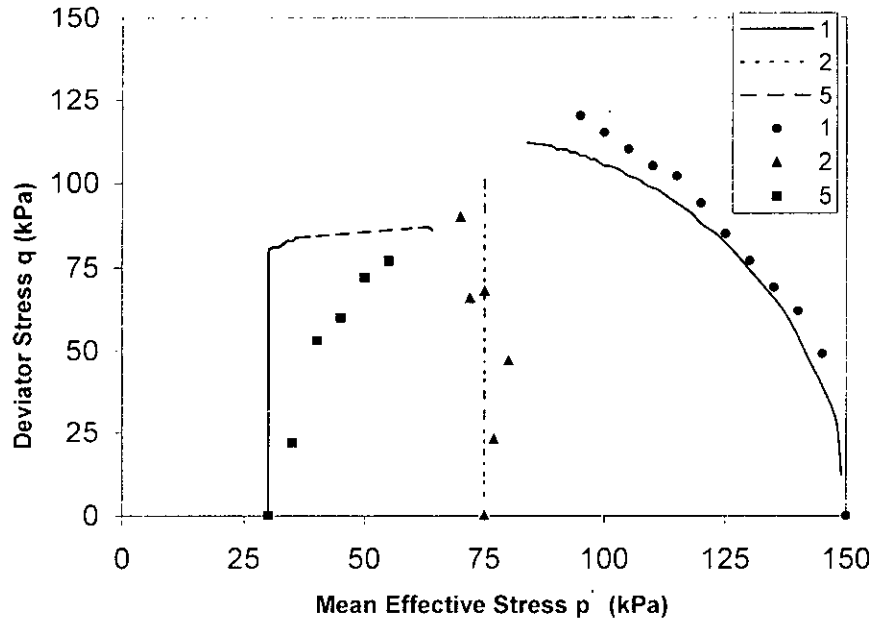

Figure 4.11 MCC prediction of undrained triaxial stress path of Banshkhali clay (OCR=1, 2, 5)

103112

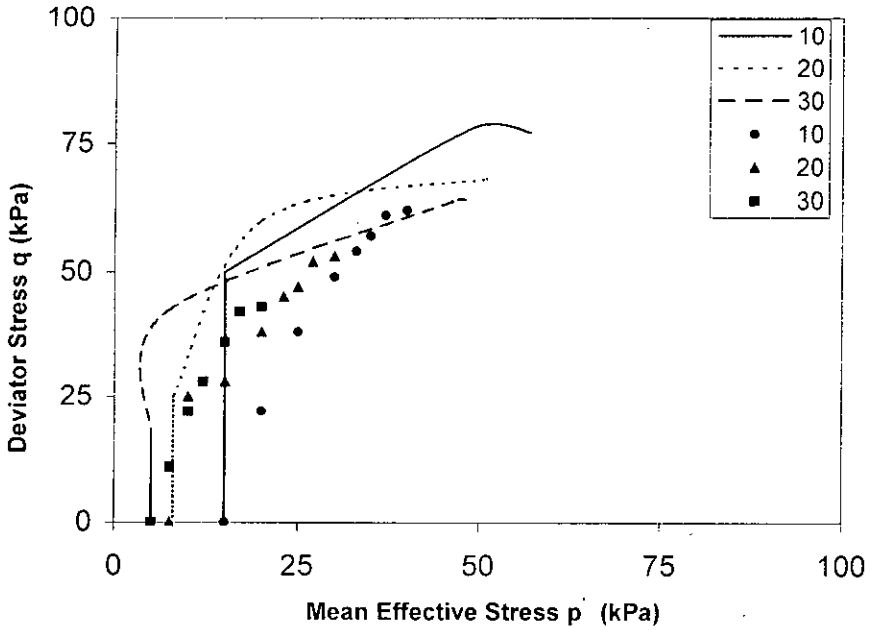

Figure 4.12 MCC prediction of undrained triaxial stress path of Banshkhali clay (OCR=10, 20, 30)

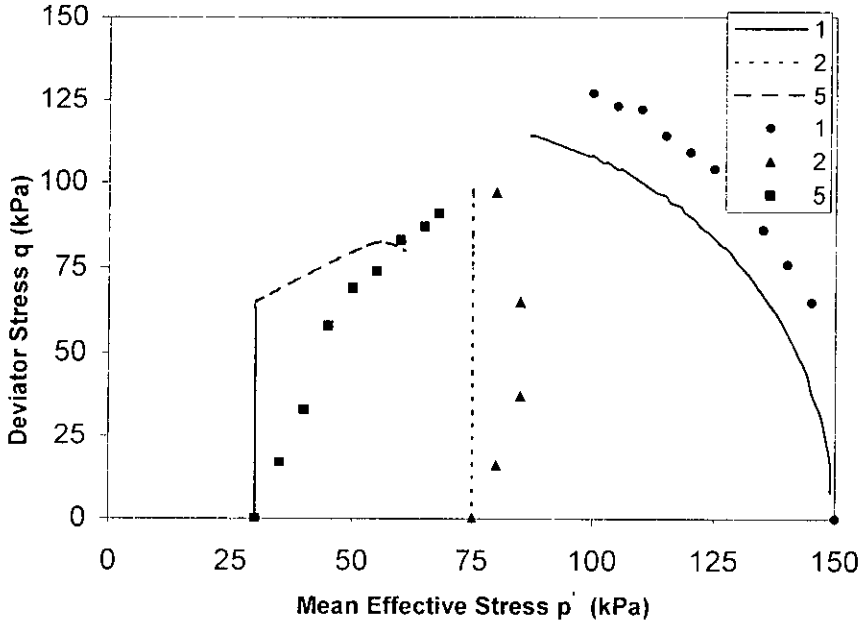

Figure 4.13 MCC prediction of undrained triaxial stress path of Chandanaish clay (OCR=1, 2, 5)

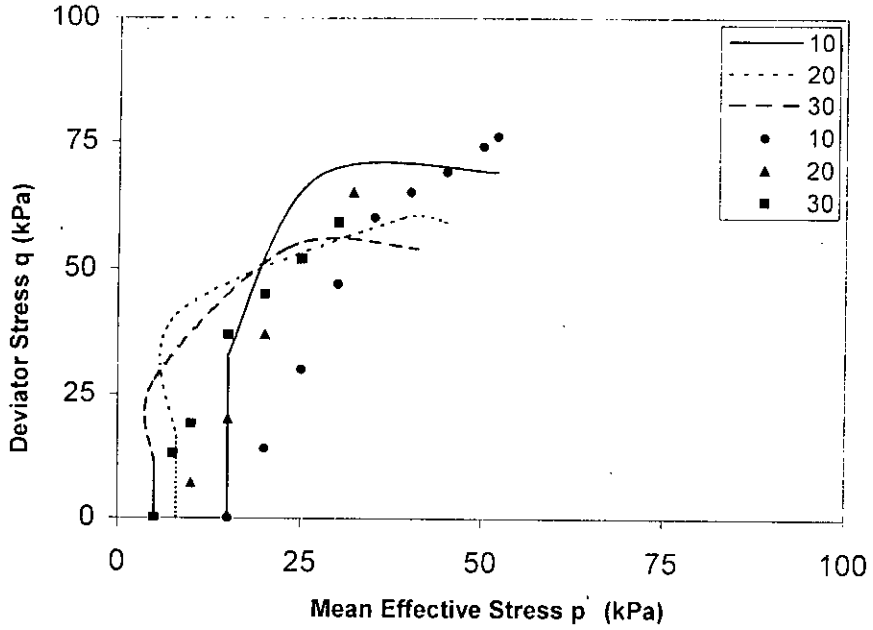

Figure 4.14 MCC prediction of undrained triaxial stress path of Chandanaish clay (OCR=10, 20, 30)

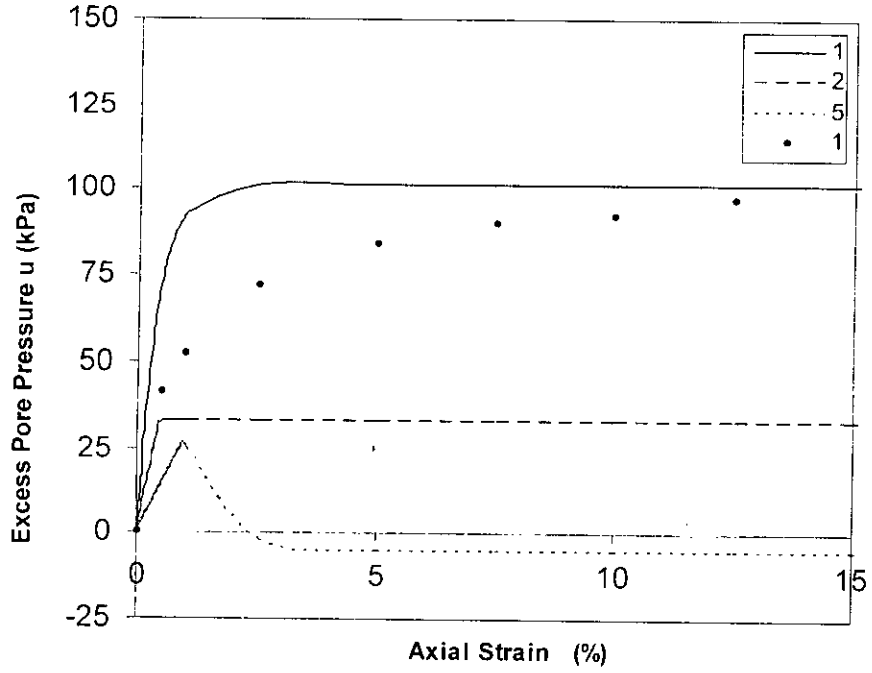

Figure 4.15 MCC prediction of excess pore pressure response of Anwara clay (OCR=1, 2, 5)

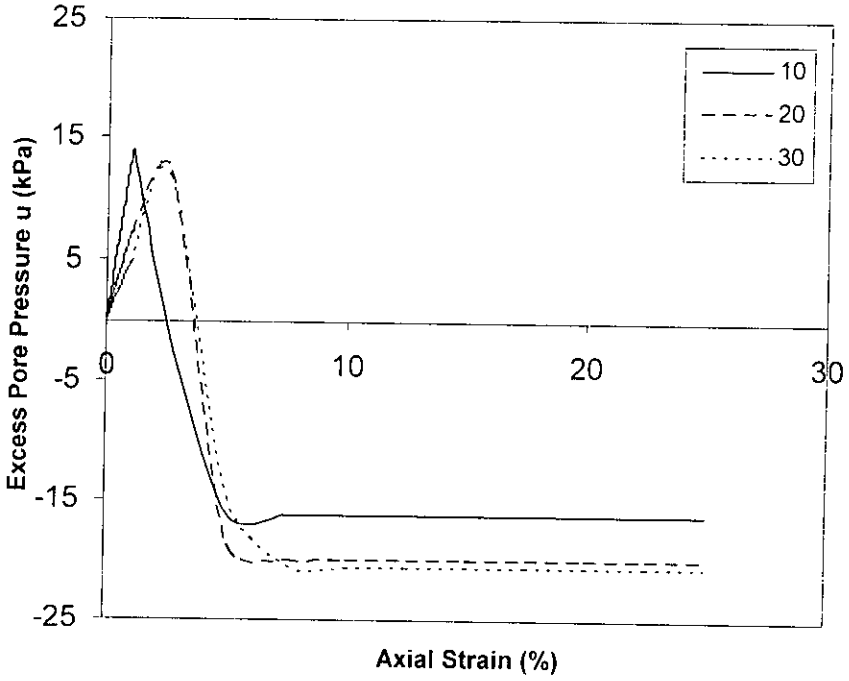

Figure 4.16 MCC prediction of excess pore pressure response of Anwara clay (OCR=10, 20, 30)

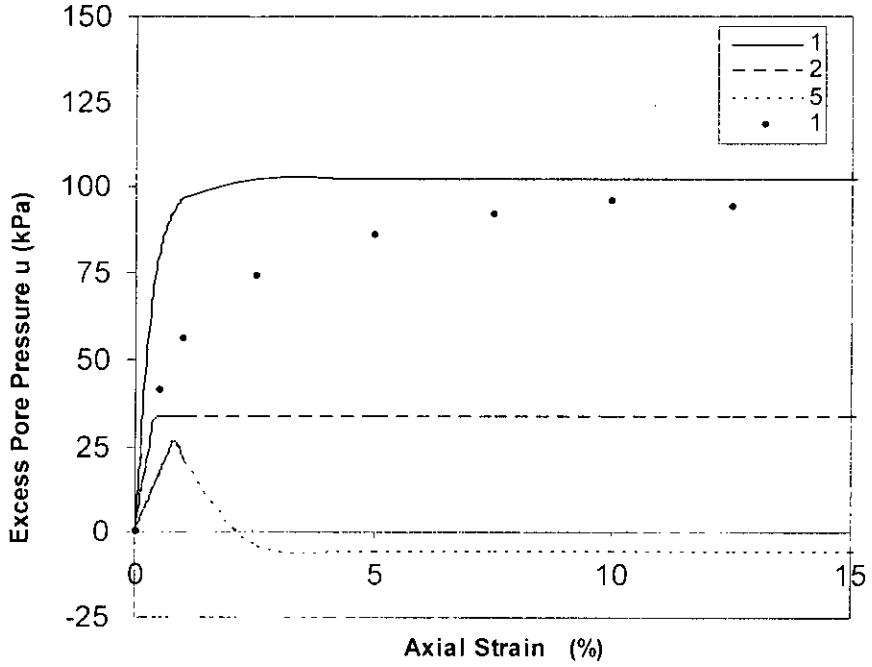

Figure 4.17 MCC prediction of excess pore pressure response of Banshkhali clay (OCR=1, 2, 5)

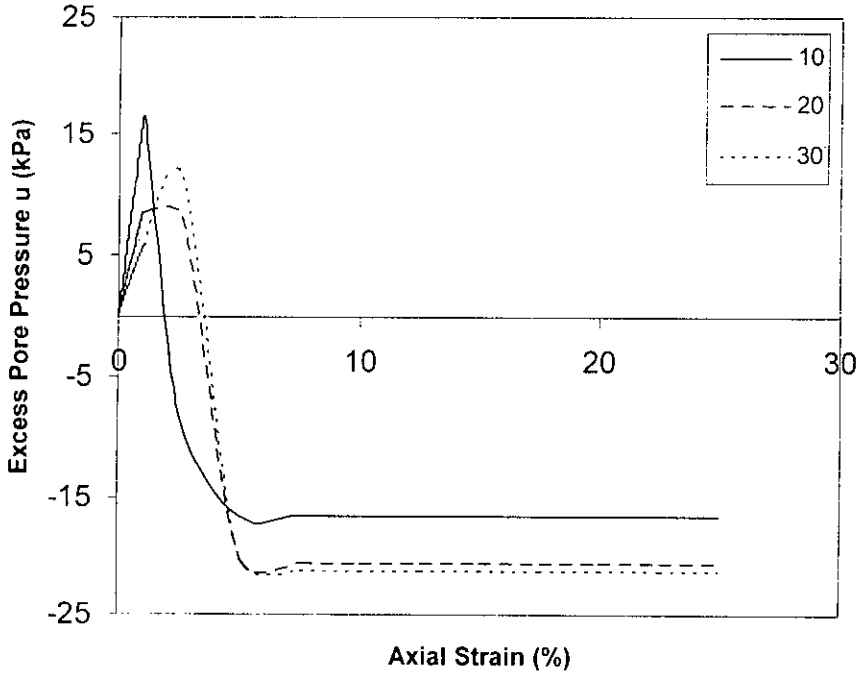

Figure 4.18 MCC prediction of excess pore pressure response of Banshkhali clay (OCR=10, 20, 30)

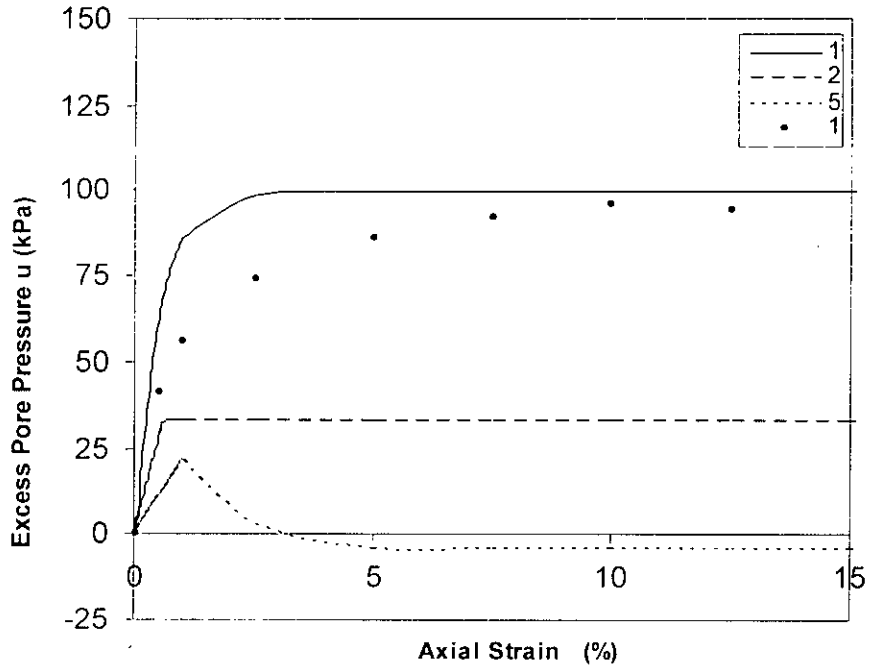

Figure 4.19 MCC prediction of excess pore pressure response of Chandanaish clay (OCR=1, 2, 5)

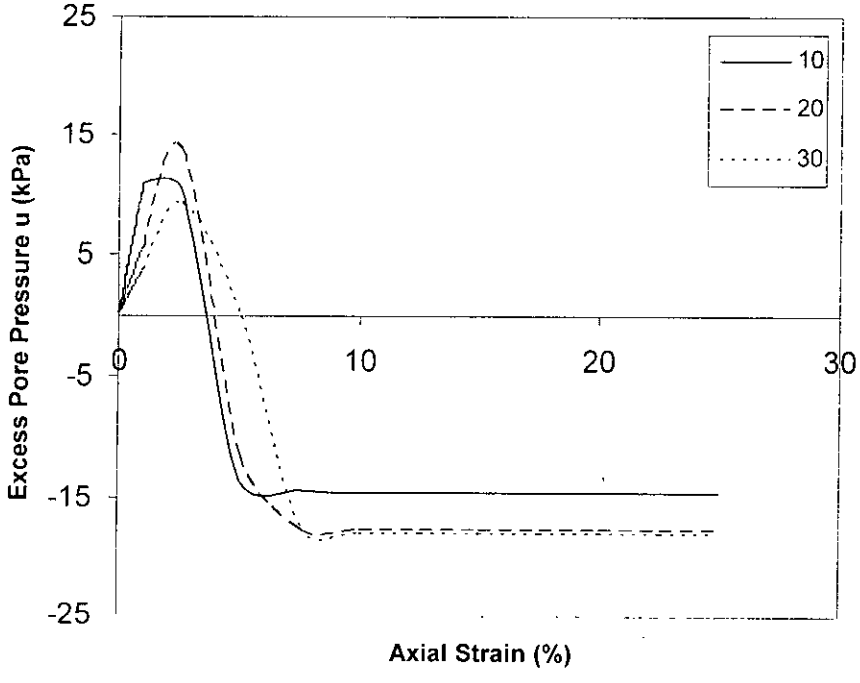

Figure 4.20 MCC prediction of excess pore pressure response of Chandanaish clay (OCR=10, 20, 30)

Table 4.1 Comparison of undrained predictions: Anwara clay (considering $E = E_i$ for Mohr-Coulomb model)

Cell pressure (kPa)	OCR	Deviator Stress at failure (kPa)		Strain at failure (%)		Pore pressure at failure (kPa)	
		MCC	MC (Initial)	MCC	MC (Initial)	MCC	MC (Initial)
150	1	112	125.4	2.5	0.33	101.17	N.A.
75	2	99	100.5	0.5	0.33	32.69	N.A.
30	5	84	85.5	5.0	0.345	-5.55	N.A.
15	10	74	71.1	5.0	0.36	-16.2	N.A.
7.5	20	65	60.0	5.0	0.375	-18.86	N.A.
5	30	61	53.2	7.5	0.375	20.64	N.A.

Table 4.2 Comparison of undrained predictions: Banshkhali clay (considering $E = E_i$ for Mohr-Coulomb model)

Cell pressure (kPa)	OCR	Deviator Stress at failure (kPa)		Strain at failure (%)		Pore pressure(kPa) at failure	
		MCC	MC (Initial)	MCC	MC (Initial)	MCC	MC (Initial)
150	1	112	119.2	2.5	0.33	102.45	N.A.
75	2	101	90.0	0.425	0.33	33.05	N.A.
30	5	86	75.6	5.0	0.36	-5.61	N.A.
15	10	77	62.0	5.0	0.33	-16.66	N.A.
7.5	20	68	52.4	5.0	0.375	-20.49	N.A.
5	30	64	45.0	5.0	0.375	-20.23	N.A.

Table 4.3 Comparison of undrained predictions: Chandanaish clay (considering E = E_i for Mohr-Coulomb model)

Cell pressure (kPa)	OCR	Deviator Stress at failure (kPa)		Strain at failure (%)		Pore pressure at failure (kPa)	
		MCC	MC (Initial)	MCC	MC (Initial)	MCC	MC (Initial)
150	1	114	130.0	2.5	0.315	98.84	N.A.
75	2	98	108.6	0.625	0.33	32.17	N.A.
30	5	80	91.0	5.0	0.345	-4.33	N.A.
15	10	69	76.8	5.0	0.36	-13.67	N.A.
7.5	20	59	65.0	7.5	0.36	-17.69	N.A.
5	30	54	59.8	5.0	0.375	-0.09	N.A.

Table 4.4 Comparison of undrained predictions: Anwara clay (considering E = E_{50} for Mohr-Coulomb model)

Cell pressure (kPa)	OCR	Deviator Stress at failure (kPa)		Strain at failure (%)		Pore pressure at failure (kPa)	
		MCC	MC (Secant)	MCC	MC (Secant)	MCC	MC (Secant)
150	1	112	125.4	2.5	0.48	101.17	N.A.
75	2	99	100.5	0.5	0.42	32.69	N.A.
30	5	84	85.5	5.0	0.525	-5.55	N.A.
15	10	74	71.1	5.0	0.54	-16.2	N.A.
7.5	20	65	60.0	5.0	0.555	-18.86	N.A.
5	30	61	53.2	7.5	0.555	20.64	N.A.

Table 4.5 Comparison of undrained predictions: Banshkhali clay (considering E = E_{50} for Mohr-Coulomb model)

Cell pressure (kPa)	OCR	Deviator Stress at failure (kPa)		Strain at failure (%)		Pore pressure at failure (kPa)	
		MCC	MC (Secant)	MCC	MC (Secant)	MCC	MC (Secant)
150	1	112	119.2	2.5	0.495	102.45	N.A.
75	2	101	90.0	0.425	0.51	33.05	N.A.
30	5	86	75.6	5.0	0.525	-5.61	N.A.
15	10	77	62.0	5.0	0.51	-16.66	N.A.
7.5	20	68	52.4	5.0	0.555	-20.49	N.A.
5	30	64	45.0	5.0	0.555	-20.23	N.A.

Table 4.6 Comparison of undrained predictions: Chandanaish clay (considering E = E_{50} for Mohr-Coulomb model)

Cell pressure (kPa)	OCR	Deviator Stress at failure (kPa)		Strain at failure (%)		Pore pressure at failure (kPa)	
		MCC	MC (Secant)	MCC	MC (Secant)	MCC	MC (Secant)
150	1	114	130.0	2.5	0.48	98.84	N.A.
75	2	98	108.6	0.625	0.495	32.17	N.A.
30	5	80	91.0	5.0	0.51	-4.33	N.A.
15	10	69	76.8	5.0	0.525	-13.67	N.A.
7.5	20	59	65.0	7.5	0.54	-17.69	N.A.
5	30	54	59.8	5.0	0.555	-0.09	N.A.

The Mohr-Coulomb model predicts only the total stress path of the coastal clays during undrained shear. It cannot predict excess pore pressures that may develop during shearing. Thus effective stress paths that develop during undrained shearing of clays cannot be predicted by the Mohr-Coulomb model. The Modified Cam Clay model can predict both the excess pore pressures and consequently the effective stress paths that develop during undrained shearing of clays. The Modified Cam Clay model gives a qualitatively correct approximation of the effective stress path that develops during undrained shearing of coastal clays, particularly for normally consolidated or highly overconsolidated clays.

The Modified Cam Clay model is capable of predicting the softening response of coastal clays at high overconsolidation ratios as observed experimentally for such clays. The Mohr-Coulomb model is unable to predict any kind of softening behaviour.

The same set of Modified Cam Clay model parameters may be used for predicting the drained and undrained triaxial shear response of coastal clays. Two different set of parameters are required for predicting the drained and undrained stress-strain response of coastal clays using the Mohr-Coulomb model.

The Mohr-Coulomb model is simple and requires 2 plastic and 2 elastic model parameters. These model parameters may be easily obtained by conventional laboratory tests. The Modified Cam Clay model is relatively more complex and requires 6 model parameters for its use.

Finite element predictions of geotechnical problems using the Mohr-Coulomb model may be easily compared with theoretical and analytical limit state solutions that are generally available for many such problems. Rigorous theoretical and analytical solutions using the Modified Cam Clay model are almost non-existent for most geotechnical engineering problems. Solutions of geotechnical problems using the Modified Cam Clay model may only be obtained by elasto-plastic numerical analysis of such problems. Thus the Mohr-Coulomb model is a widely used tool for Geotechnical engineers. The Modified Cam Clay model is still unfamiliar and complicated to use for most Geotechnical engineers for practical problems.

4.10 Strength and Weaknesses of the Modified Cam Clay Model

The Modified Cam Clay model is a good predictor of the stress-strain, excess pore pressure and effective stress path of coastal clays at various OCR's during undrained shear. The model has only 6 model parameters, all of which may be obtained relatively easily from conventional laboratory tests. Modified Cam Clay model parameters have clear physical meaning and interpretation. However, pressure dependent elasticity of the Modified Cam Clay model is not a realistic representation of the initially observed stress-strain response of overconsolidated coastal clays. The stress-strain response of all coastal clays including those at high OCR values appear to be clearly elasto-plastic from the very onset of loading. As the initial stress-strain response of the soil is important in many geotechnical problems, this may be identified as a shortcoming of the Modified Cam Clay model. The relative complexity of the Modified Cam clay model is also one of its weaknesses as it precludes its use in developing analytical and theoretical solutions of common geotechnical problems using this model.

4.11 Summary and Conclusions

The Modified Cam Clay model was incorporated in a finite element program. Finite element analysis was carried out using the Modified Cam Clay model to predict the stress-strain, excess pore pressure and effective stress path of coastal clays during undrained shearing under triaxial conditions. It was observed that the MCC model was a good qualitative predictor of the undrained shear response of coastal clays. It predicts the elasto-plastic strain hardening behaviour of coastal clays as observed experimentally. Softening, as observed experimentally, is also predicted by this model. The Modified Cam Clay model predicts elastic response of highly overconsolidated clays before the onset of yield. However, an observation of the effective stress path and stress-strain response of coastal clays indicates elasto-plastic behaviour of highly overconsolidated coastal clays from the onset of load application. The inability to predict elasto-plastic response before the onset of yield is a limitation of the Modified Cam Clay model. However, as a whole, the Modified Cam Clay model appears to be quite suitable to predict qualitatively the observed response of coastal clays during undrained shear in triaxial condition.

CHAPTER 5

DRAINED PREDICTIONS OF COASTAL CLAYS: THE MOHR-COULOMB MODEL

5.1 Introduction

Bashar (2002) conducted triaxial shearing of coastal clays in the laboratory. However Bashar did not carry out any drained triaxial shearing of such clays. In this chapter, the Mohr-Coulomb model is used to make drained predictions. The approach necessary to use the Mohr-Coulomb model for drained predictions is discussed. The method of obtaining drained Mohr-Coulomb model parameters for costal clays is then described. Two different approaches are used in making drained MC predictions. These methods are discussed, compared and evaluated. Finally drained stress-strain responses predicted by the Mohr-Coulomb model are compared with undrained predictions.

5.2 Drained Analysis

It is well known that for very slow or drained shearing of normally consolidated or low OCR saturated clays, the cohesion intercept c at the shear axis is generally close to zero. Thus for making drained predictions of normally consolidated or low OCR clays, a value of $c = 0$ is assumed. The effective drained friction angle ϕ' may be either assumed to be the effective peak or ultimate friction angle of the soil. For high OCR clays, ϕ' is generally taken to be the peak friction angle. In that case, peak failure stresses are predicted by the Mohr-Coulomb model. For normally consolidated or low OCR clays, ϕ' is taken to be the ultimate friction angle (friction angle at constant volume). In that case, ultimate failure stresses will be predicted. The Mohr-Coulomb model for drained analysis is given in Figure 5.1.

In the Mohr-Coulomb model, the dilation angle (ψ') is defined to be the angle of the incremental plastic strain with the J_2 axis. Generally, a value of the dilation angle equal to the friction angle or $\psi' = \phi'$ will predict large expansive volume strains.

This is generally correct for drained shearing of high OCR clays. A value of the dilation angle significantly lower than the friction angle of the soil i.e. $\psi' << \phi'$ will still predict expansive volume strain. However, in this case the magnitude of the expansive volume strains are much lower. For $\psi' = 0$ i.e. dilation angle equals to zero, incompressibility or zero volume change is predicted. A value of negative dilation angle i.e. $\psi' < 0$ will theoretically predict compressive volume change. However, negative values of dilation angle are generally not assumed in the Mohr-Coulomb model as this may result in numerical instability. Generally, drained triaxial shearing of normally consolidated or low OCR clays result in compressive volume strain of the soil samples. The Mohr-Coulomb model with zero or positive dilation angle is unable to predict such compressive volume changes. In drained analysis, all stresses are assumed to be effective stresses. The effective stress paths in drained analysis in $p' - q$ space is a straight line with slope 3:1. (Fig. 5.2)

5.3 Drained Mohr – Coulomb Model Parameters

For drained predictions, drained values of Mohr Coulomb parameters need to be obtained. For a fully drained analysis, the cohesion "c" of the clay is assumed to be zero. In this analysis, the value of the ultimate effective friction angle is used. This is the friction angle computed at constant ultimate effective stress, when the soil deforms at constant volume. Although Bashar (2002) conducted undrained tests, effective stresses were used to compute the ultimate friction angle. The effective stresses were computed by subtracting the excess pore pressure from total stress during shear. The drained Poisson's ratio of coastal clays was not computed by Bashar (2002). Generally, the drained Poisson's ratio for clays varies between 0.1-0.4. In the absence of any experimentally available value for coastal clays, an average value of 0.2 was used for the drained Poisson's ratio. It can be shown theoretically that the drained elastic stiffness $\overline{E}$ is equal to $E/1.15$, where E is the undrained elastic modulus. Actual experimental data of clays in the laboratory show that the drained elastic modulus $\overline{E}$ for clays varies between E/3.0 to $E/4.0$. For the current analysis, drained elastic modulus $\overline{E}$ for coastal clays of Anwara, Banshkhali and Chandanaish was taken equal to $E/3.5$, where E was the value of undrained elastic modulus obtained by Bashar (2002).

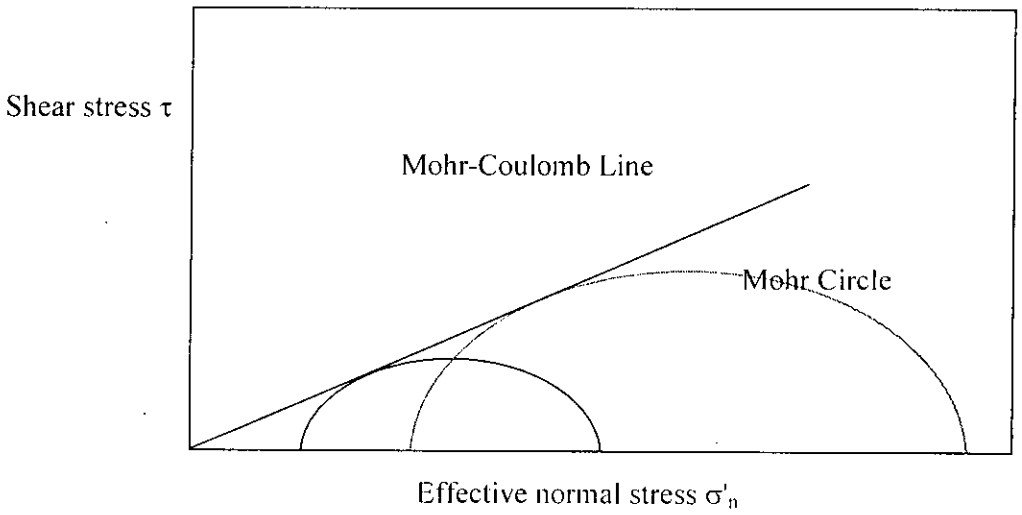

Figure 5.1 Mohr-Coulomb model under drained condition (Peck et al., 1974)

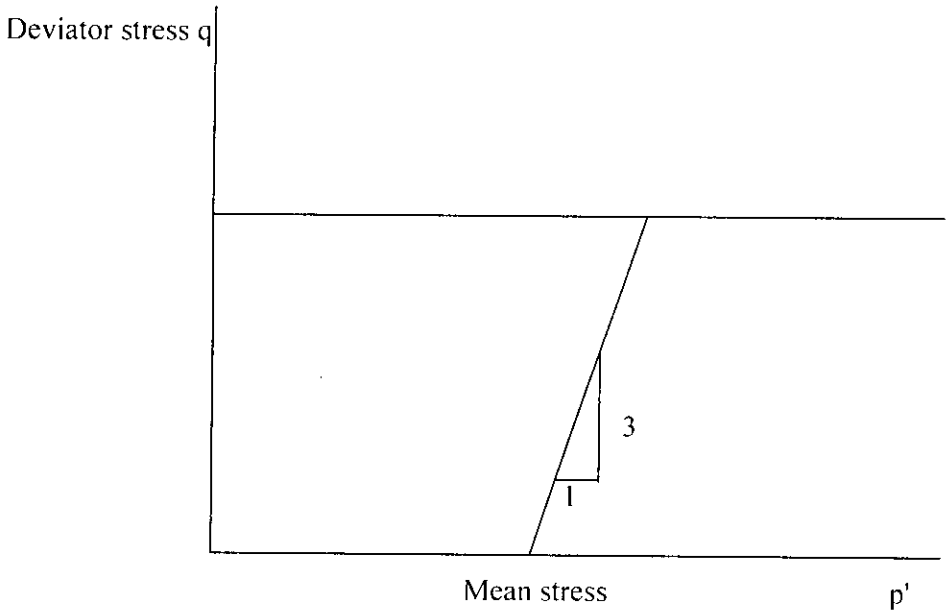

Figure 5.2 Effective stress path followed during drained triaxial shear (Atkinson and Bransby, 1978)

In the Janbu method of analysis using the Mohr-Coulomb method, the elastic stiffness is assumed to vary with the mean effective pressure as follows:

$$E = K(p')^n$$

For simplicity and in the absence of drained data for coastal clays, an average constant value of K is extrapolated from undrained elastic modulus of coastal clays and exponent n is assumed to the equal to 1.0. Mohr-Coulomb prediction using the Janbu approach was not carried out in this research study. The Mohr-Coulomb parameters used for making predictions of drained shearing of laboratory samples of coastal clays of Bangladesh under triaxial states of stress are shown in Appendix II. Two different sets of parameter values were used using two approaches in making drained predictions using the Mohr-Coulomb model.

5.3 Predictions of Consolidated Drained Test

The consolidated drained test of laboratory samples under triaxial states of stress were simulated using the Mohr-Coulomb model. Two different approaches were used when assuming the value of the constant elastic modulus. In the first instance, a constant value for the drained initial elastic modulus is assumed. In the second instance, a constant value for the drained secant elastic modulus is assumed.

5.4.1 Stress- Strain

Figure 5.3, 5.4, 5.5, 5.6, 5.7 and 5.8 show the stress-strain prediction of coastal clays (Anwara, Banshkhali, Chandanaish respectively) during triaxial shear under drained conditions using the Mohr-Coulomb model. In these cases, elastic modulus in the Mohr-Coulomb model has been assumed to be equal to the initial elastic stiffness of the clay samples as extrapolated from undrained values. Figure 5.9, 5.10, 5.11, 5.12, 5.13 and 5.14 show the stress-strain prediction of coastal clays (Anwara, Banshkhali, Chandanaish respectively) during triaxial shear under drained conditions using the elastic secant stiffness of the soil as the constant elastic modulus in the Mohr-Coulomb model. All the figures show an initial linear elastic behaviour, followed by perfectly plastic response when the soil deforms continuously at constant stress.

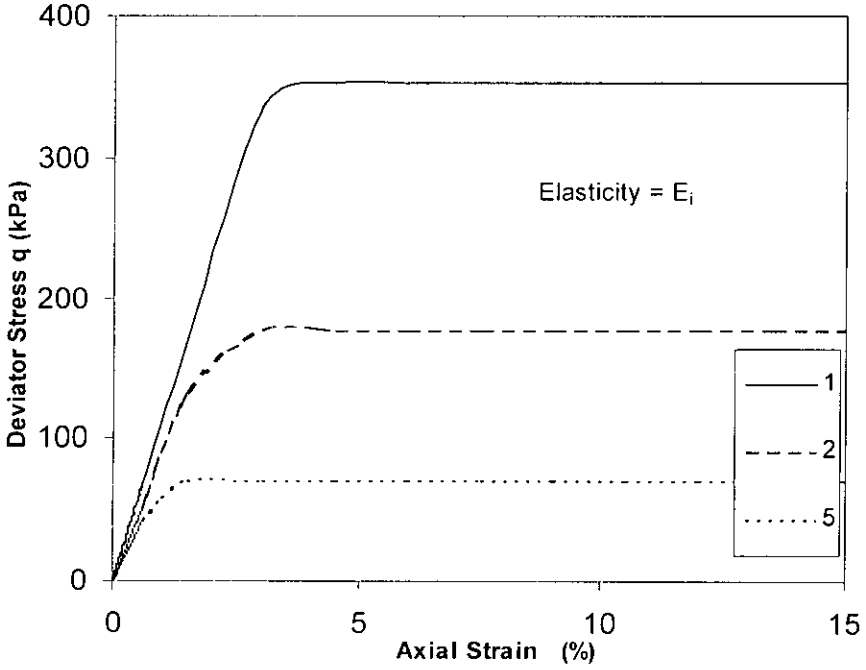

Figure 5.3 Mohr-Coulomb prediction of drained triaxial stress-strain response of Anwara clay with initial elastic modulus (OCR=1, 2, 5)

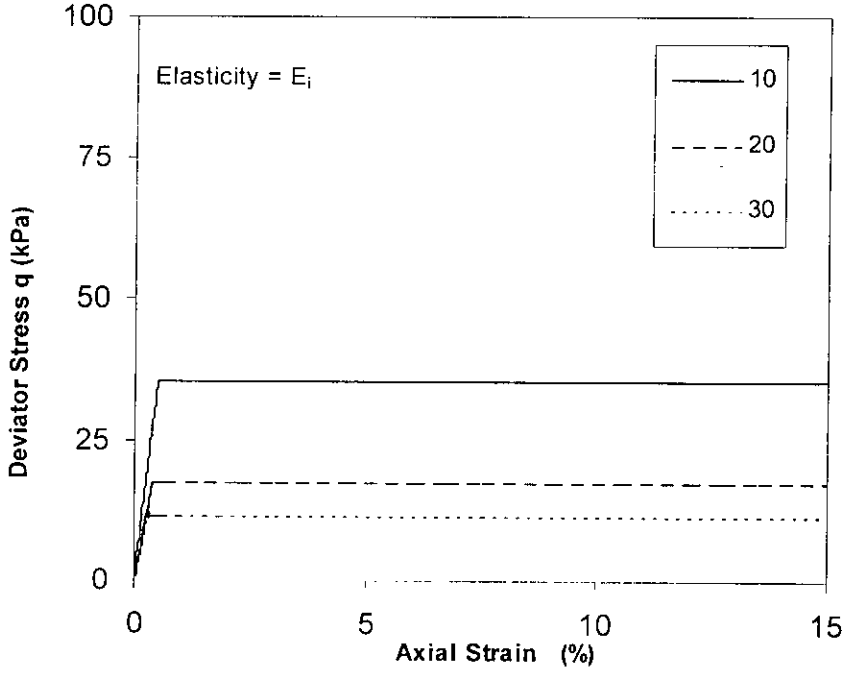

Figure 5.4 Mohr-Coulomb prediction of drained triaxial stress-strain response of Anwara clay with initial elastic modulus (OCR=10, 20, 30)

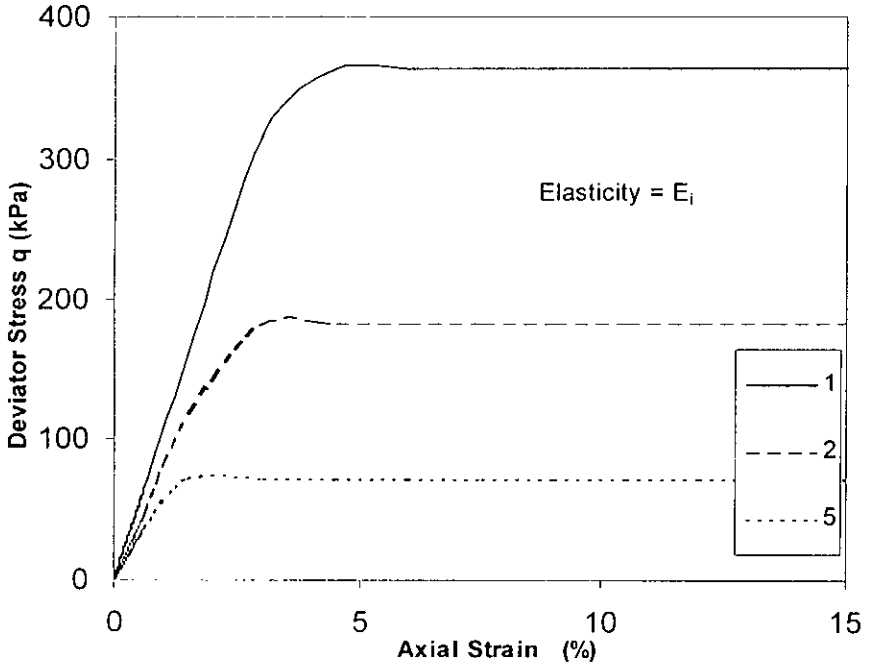

Figure 5.5 Mohr-Coulomb prediction of drained triaxial stress-strain response of Banshkhali clay with initial elastic modulus (OCR=1, 2, 5)

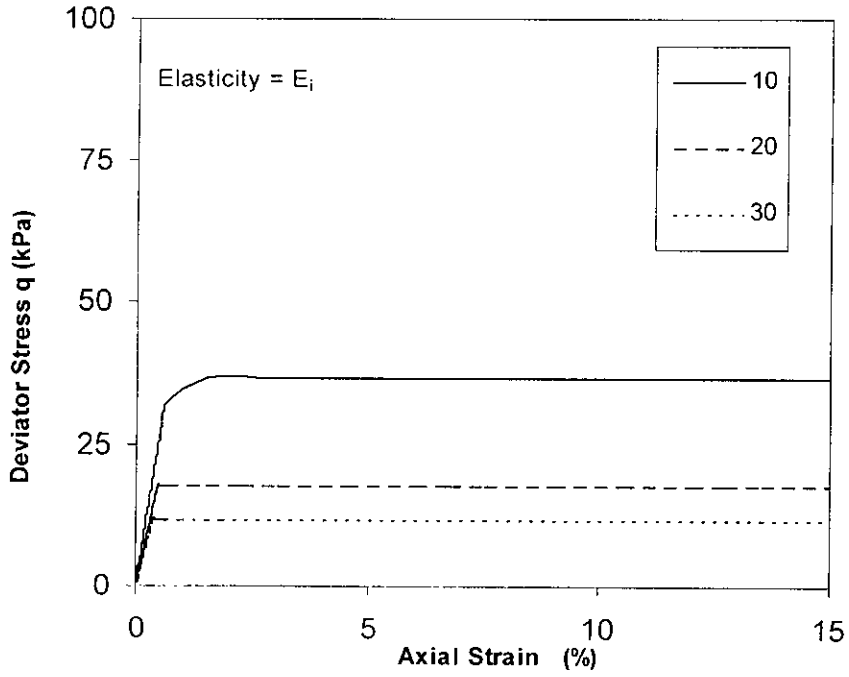

Figure 5.6 Mohr-Coulomb prediction of drained triaxial stress-strain response of Banshkhali clay with initial elastic modulus (OCR=10, 20, 30)

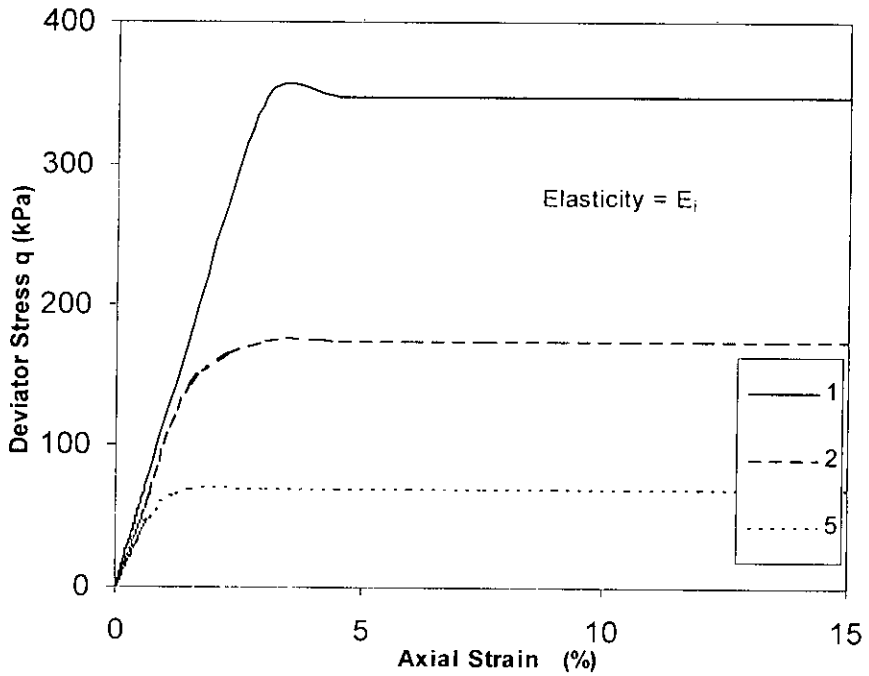

Figure 5.7 Mohr-Coulomb prediction of drained triaxial stress-strain response of Chandanaish clay with initial elastic modulus (OCR=1, 2, 5)

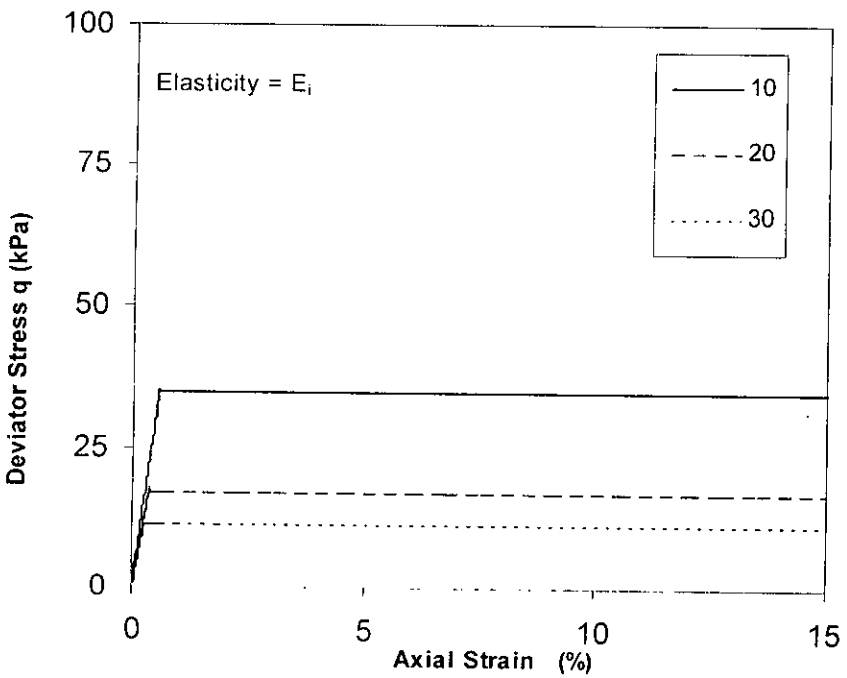

Figure 5.8 Mohr-Coulomb prediction of drained triaxial stress-strain response of Chandanaish clay with initial elastic modulus (OCR=10, 20, 30)

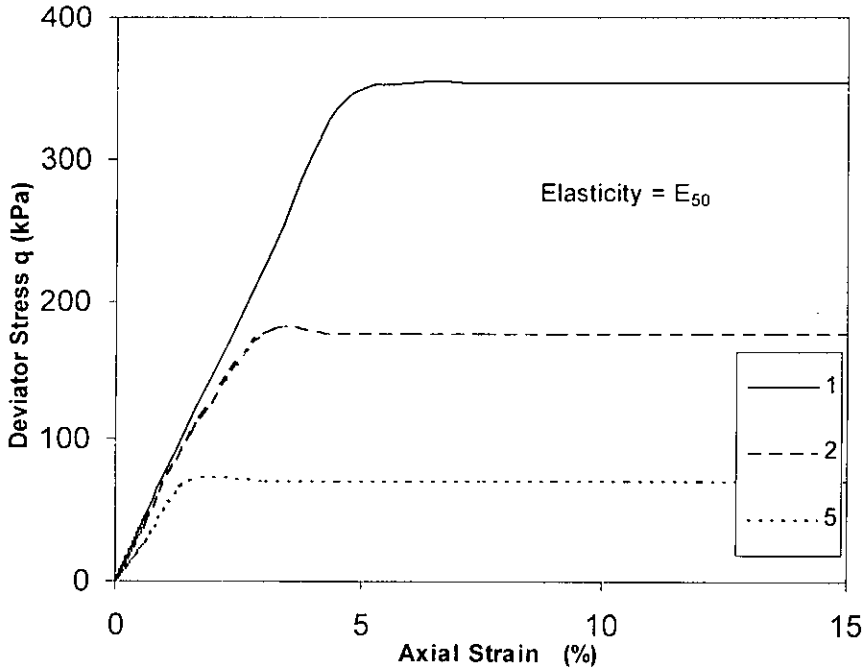

Figure 5.9 Mohr-Coulomb prediction of drained triaxial stress-strain response of Anwara clay with elastic secant modulus (OCR=1, 2, 5)

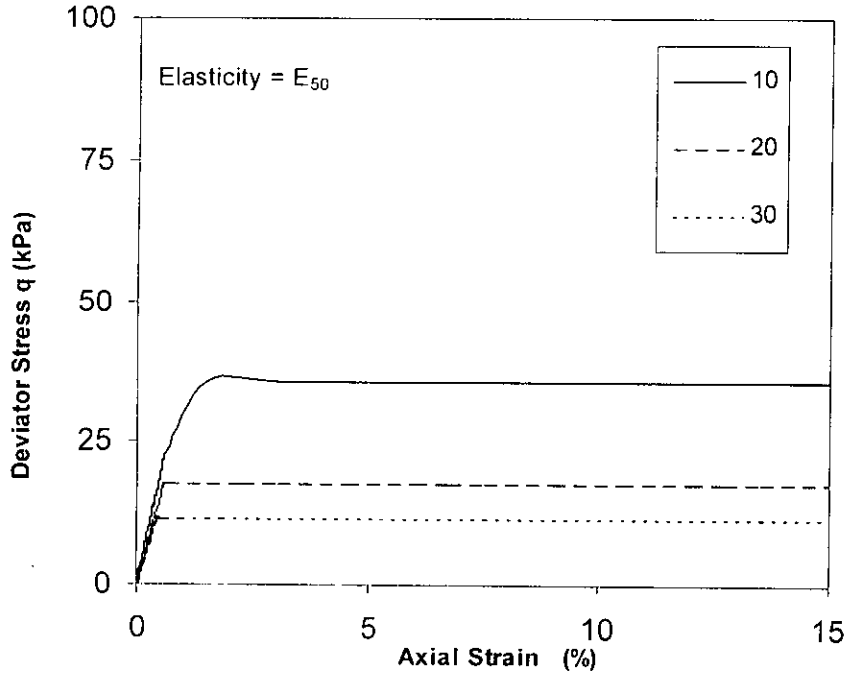

Figure 5.10 Mohr-Coulomb prediction of drained triaxial stress-strain response of Anwara clay with elastic secant modulus (OCR=10, 20, 30)

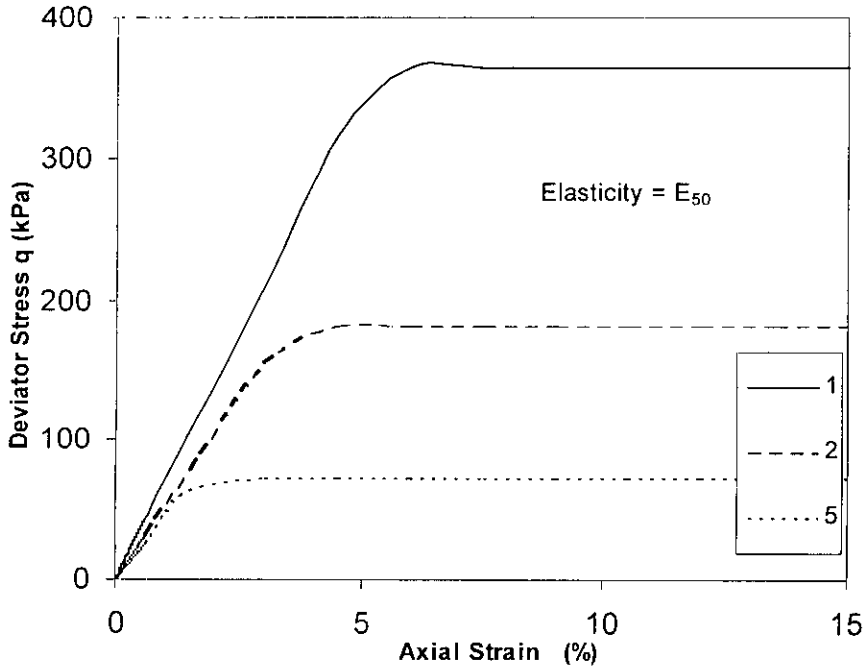

Figure 5.11 Mohr-Coulomb prediction of drained triaxial stress-strain response of Banshkhali clay with elastic secant modulus (OCR=1, 2, 5)

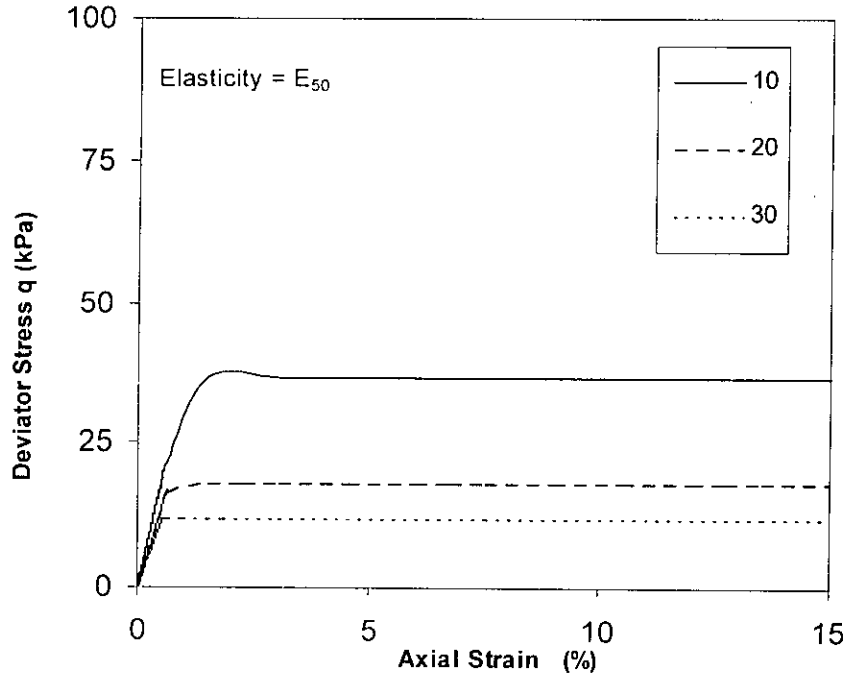

Figure 5.12 Mohr-Coulomb prediction of drained triaxial stress-strain response of Banshkhali clay with elastic secant modulus (OCR=10, 20, 30)

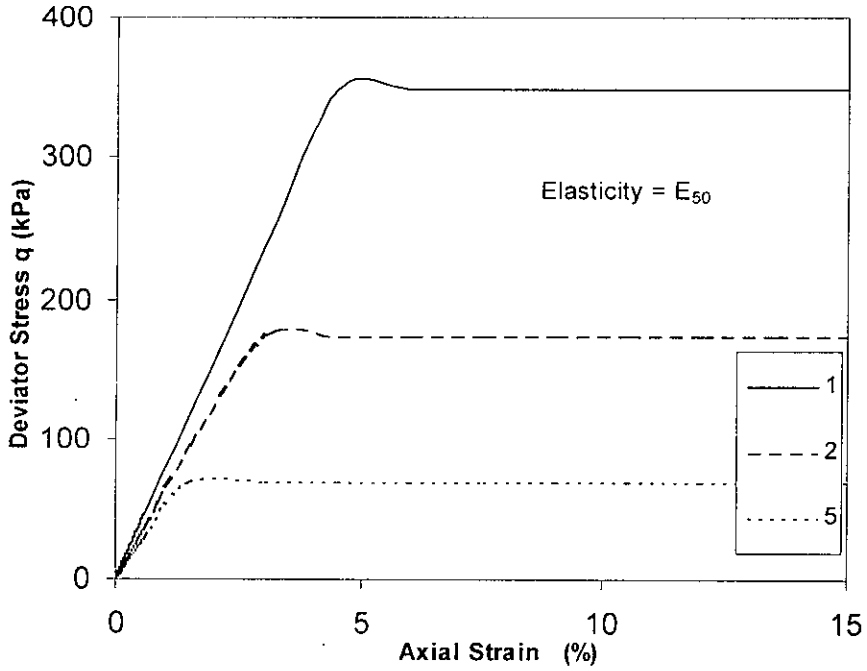

Figure 5.13 Mohr-Coulomb prediction of drained triaxial stress-strain response of Chandanaish clay with elastic secant modulus (OCR=1, 2, 5)

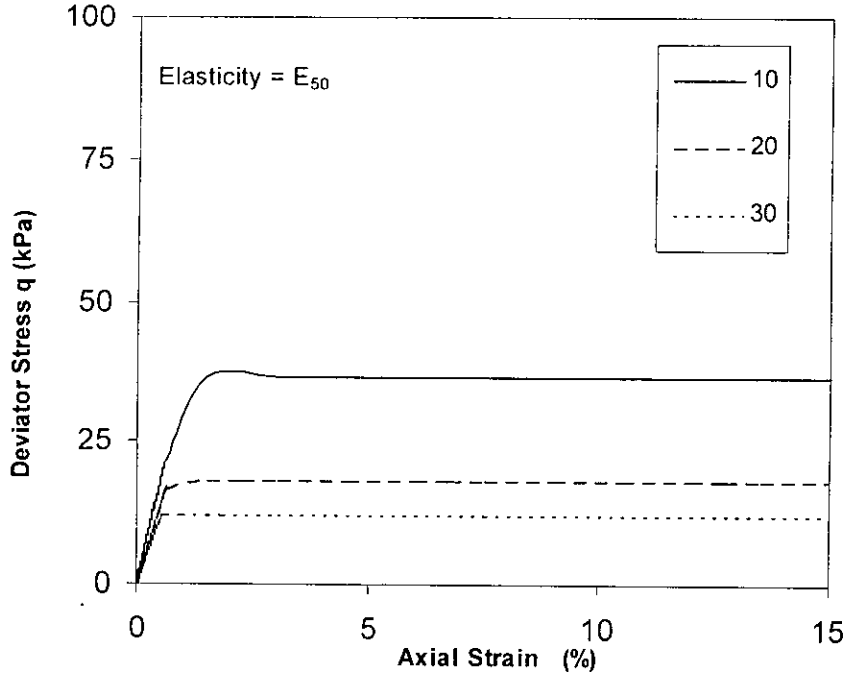

Figure 5.14 Mohr-Coulomb prediction of drained triaxial stress-strain response of Chandanaish clay with elastic secant modulus (OCR=10, 20, 30)

The drained response show the soil to deform significantly more elastically than in the undrained case before reaching the perfectly plastic condition. This is expected, as the drained elastic modulii of the soil are significantly lower than undrained values.

5.4.2 Stress Path

The stress paths for drained prediction of laboratory soil samples under triaxial states using the Mohr-Coulomb model are effective stress paths only. The stress paths show a slope increment of $\frac{\Delta q}{\Delta p'} = 3$ in $p' - q$ effective stress space. This is equivalent to keeping the cell pressure constant and then increasing the axial or deviatoric stress. Figure 5.15, 5.16, 5.17, 5.18, 5.19 and 5.20 show the effective stress path $p' - q$ in space for cell pressures of 150, 75, 30, 15, 7.5 and 5 kPa respectively.

5.4.3 Volume Change

Figures 5.21 and 5.22, Figures 5.23 and 5.24 and Figures 5.25 and 5.26 show the volume strain response of coastal clays (Anwara, Banshkhali, Chandanaish respectively) during triaxial shear under drained conditions using the Mohr-Coulomb model. In these cases the elastic modulus in the Mohr-Coulomb model has been assumed to be equal to the initial elastic stiffness of the clay as extrapolated from undrained values. Figures 5.27 and 5.28, Figures 5.29 and 5.30 and Figures 5.31 and 5.32 also show predictions of volume strain response for the coastal clays. In these cases the elastic modulus in the Mohr-Coulomb model has been assumed to be equal to the secant elastic stiffness of the clay as extrapolated from undrained values. In all of the above simulations of drained triaxial shearing using the Mohr-Coulomb model the associated flow rule has been used. This means that the dilation angle ψ' has been assumed to be equal to the drained friction angle ϕ' of the soil i.e. $\psi' = \phi'$. For all OCR's, expansive volume strains are predicted by the Mohr-Coulomb model with associated flow rule during triaxial shear under drained conditions. This prediction is qualitatively correct for drained triaxial shearing of high OCR clays. Thus the assumption of associated flow rule in the Mohr-Coulomb model is reasonable for high OCR clays.

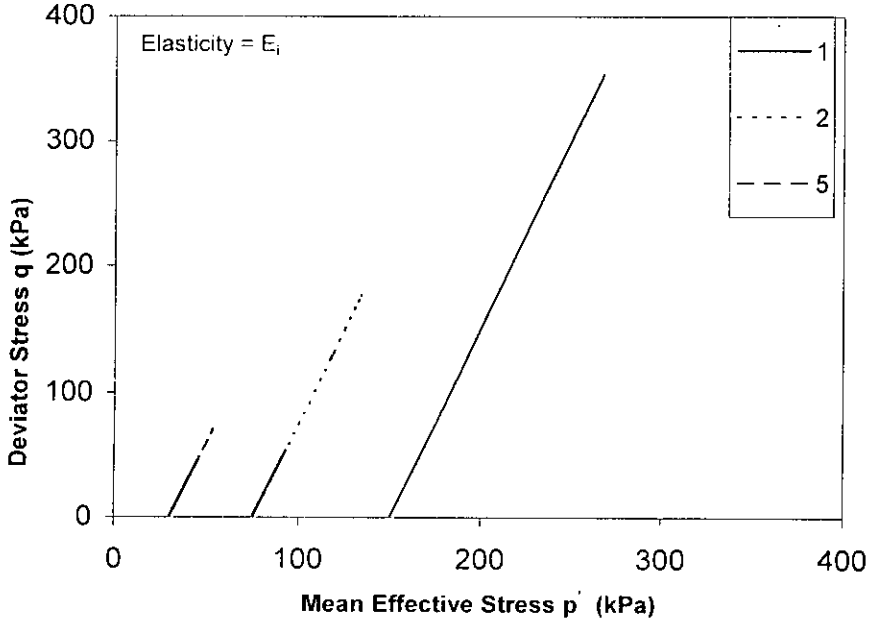

Figure 5.15 Mohr-Coulomb drained triaxial effective stress path of Anwara clay for initial elastic modulus (OCR=1, 2, 5)

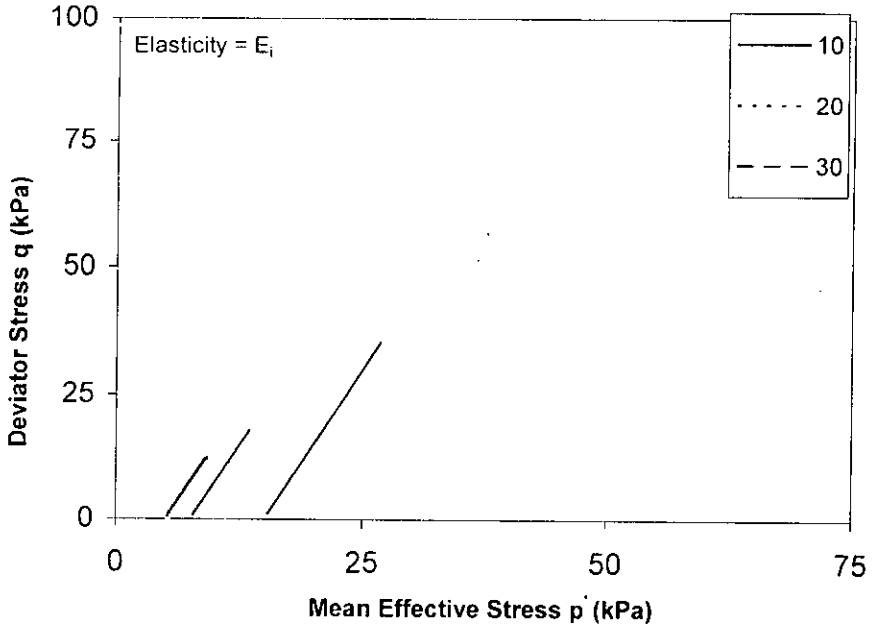

Figure 5.16 Mohr-Coulomb drained triaxial effective stress path of Anwara clay for initial elastic modulus (OCR=10, 20, 30)

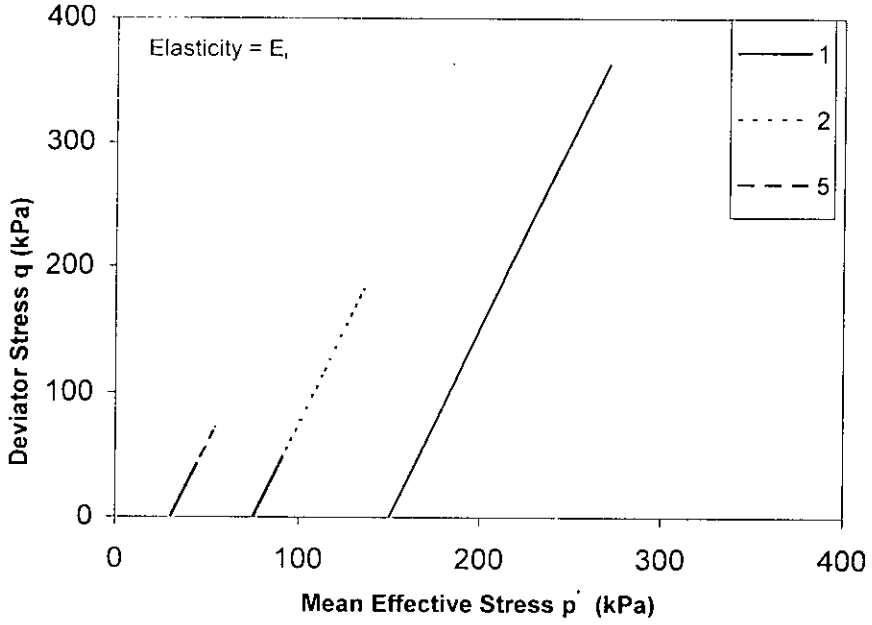

Figure 5.17 Mohr-Coulomb drained triaxial effective stress path of Banshkhali clay for initial elastic modulus (OCR=1, 2, 5)

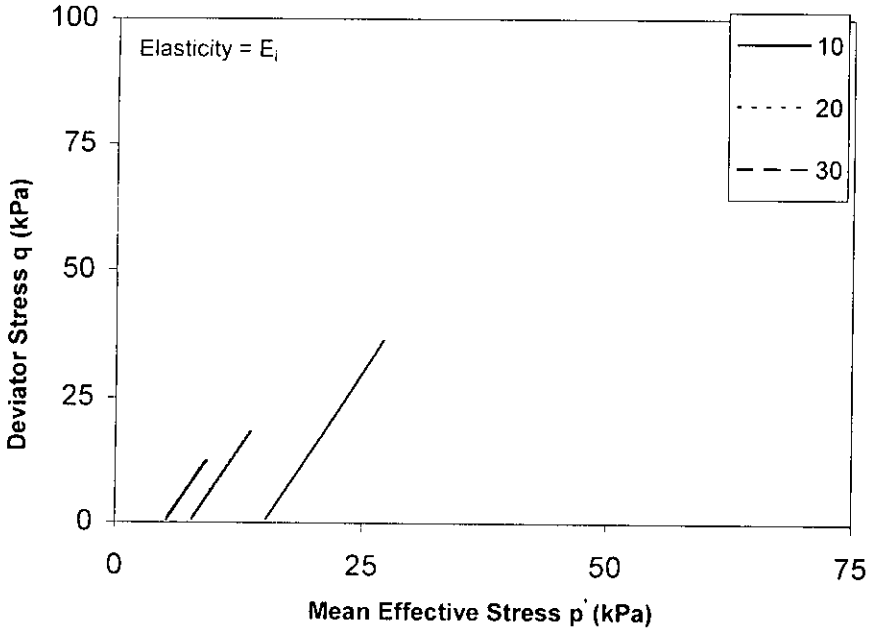

Figure 5.18 Mohr-Coulomb drained triaxial effective stress path of Banshkhali clay for initial elastic modulus (OCR=10, 20, 30)

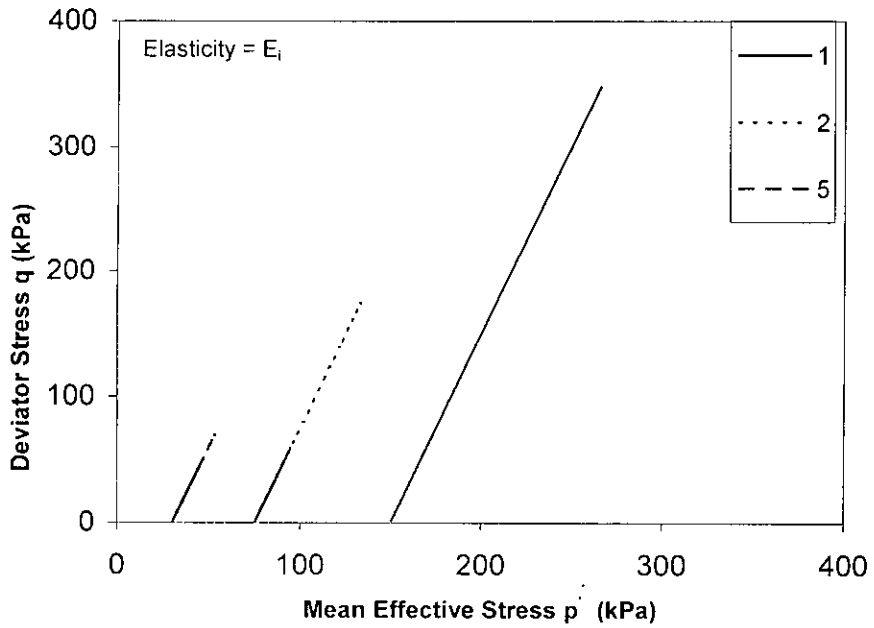

Figure 5.19 Mohr-Coulomb drained triaxial effective stress path of Chandanaish clay for initial elastic modulus (OCR=1, 2, 5)

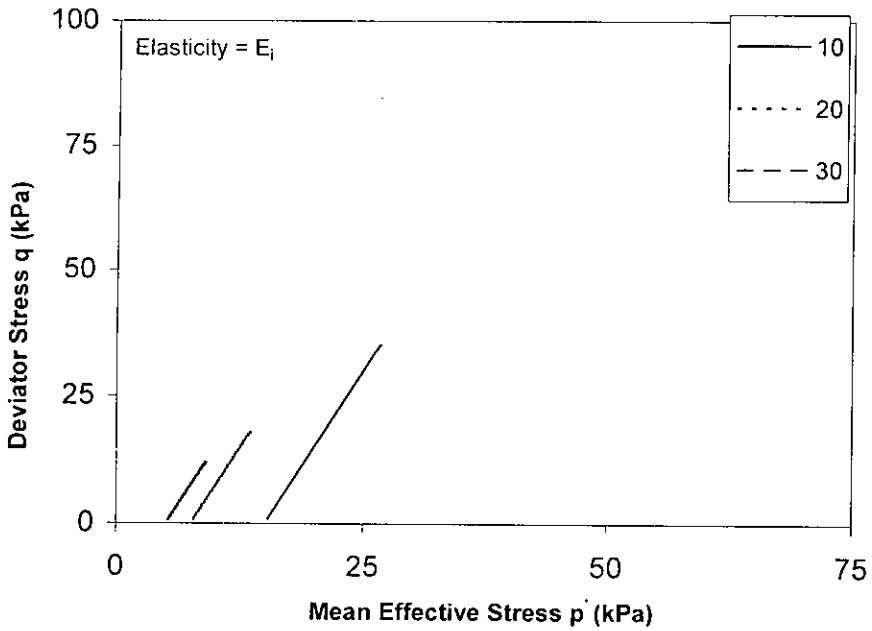

Figure 5.20 Mohr-Coulomb drained triaxial effective stress path of Chandanaish clay for initial elastic modulus (OCR=10, 20, 30)

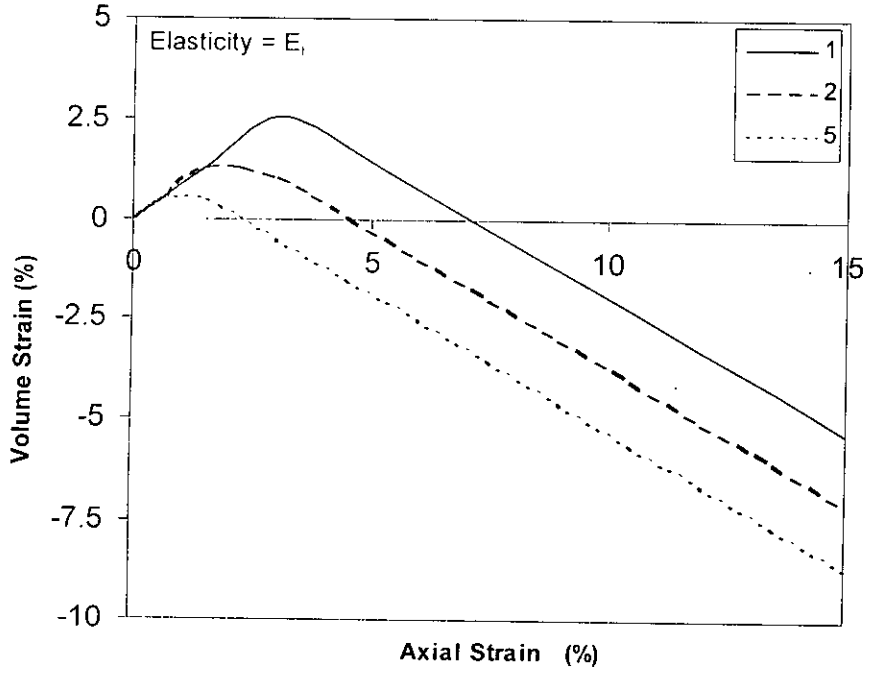

Figure 5.21 Mohr-Coulomb prediction of volume strain for drained triaxial test of Anwara clay for initial elastic modulus (OCR=1, 2, 5)

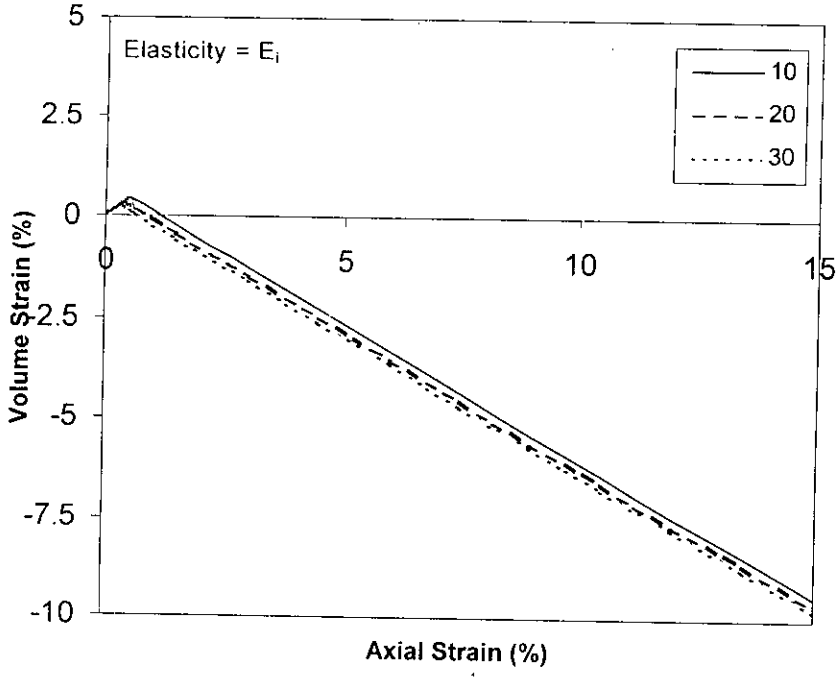

Figure 5.22 Mohr-Coulomb prediction of volume strain for drained triaxial test of Anwara clay for initial elastic modulus (OCR=10, 20, 30)

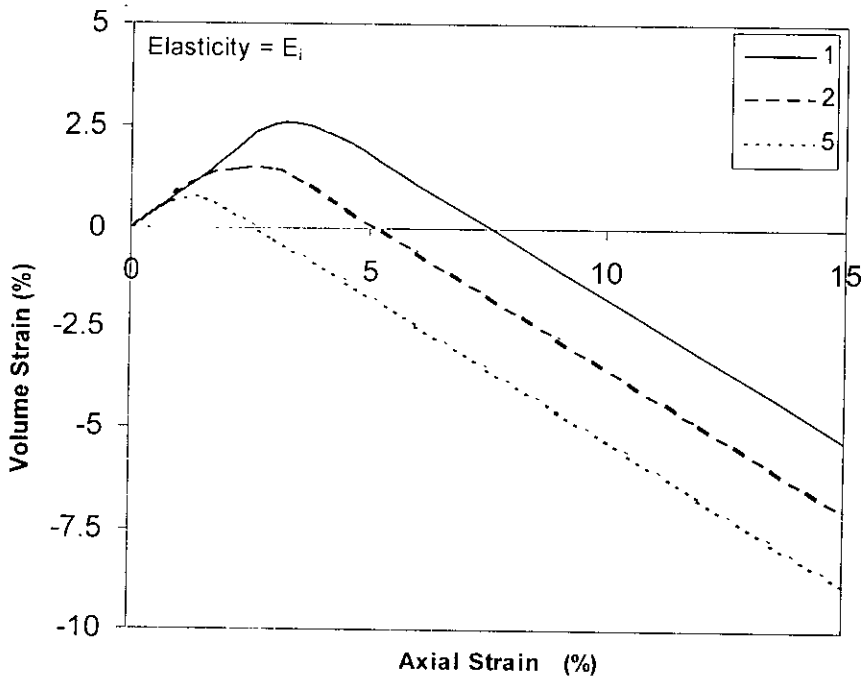

Figure 5.23 Mohr-Coulomb prediction of volume strain for drained triaxial test of Banshkhali clay for initial elastic modulus (OCR=1, 2, 5)

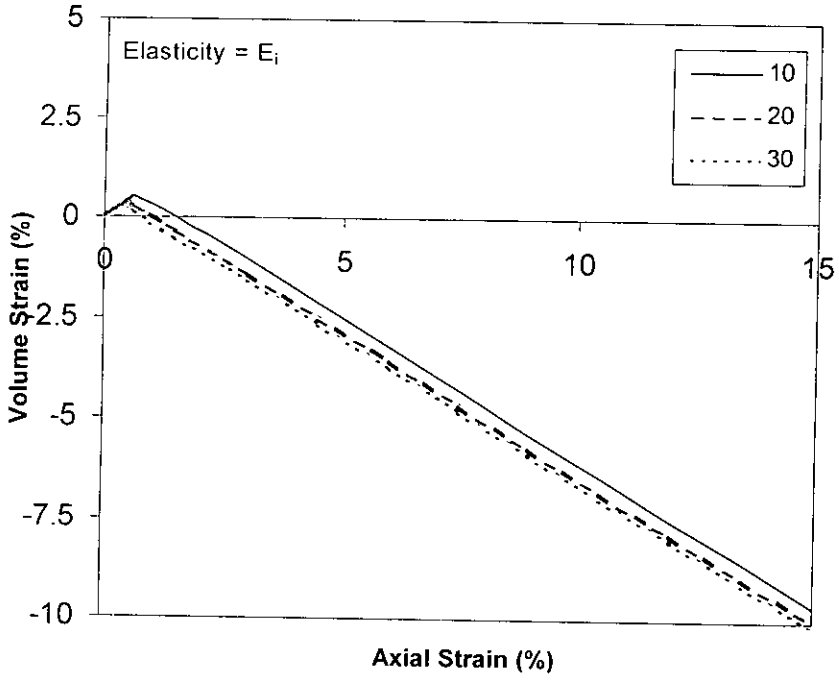

Figure 5.24 Mohr-Coulomb prediction of volume strain for drained triaxial test of Banshkhali clay for initial elastic modulus (OCR=10, 20, 30)

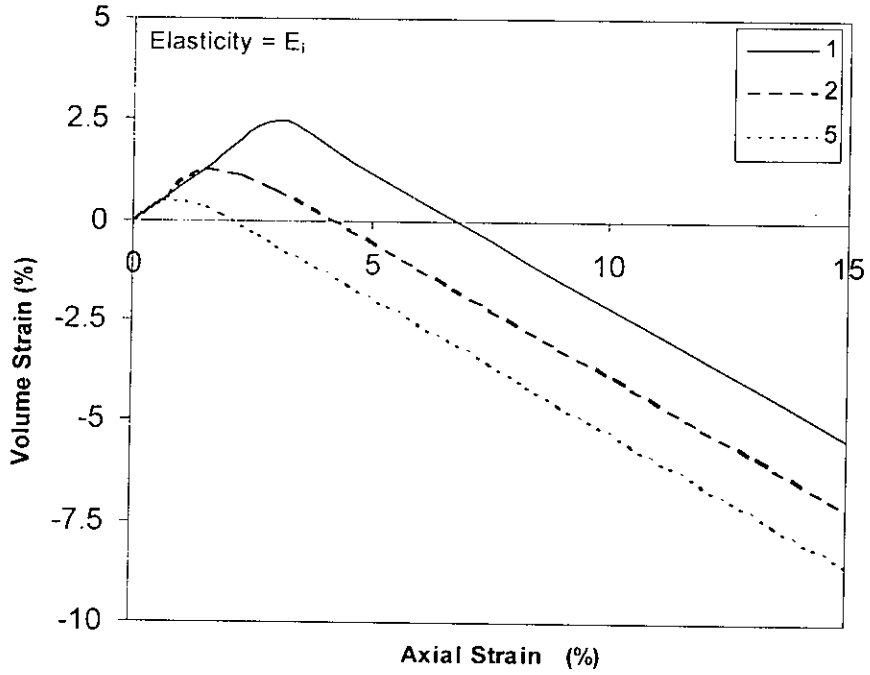

Figure 5.25 Mohr-Coulomb prediction of volume strain for drained triaxial test of Chandanaish clay for initial elastic modulus (OCR=1, 2, 5)

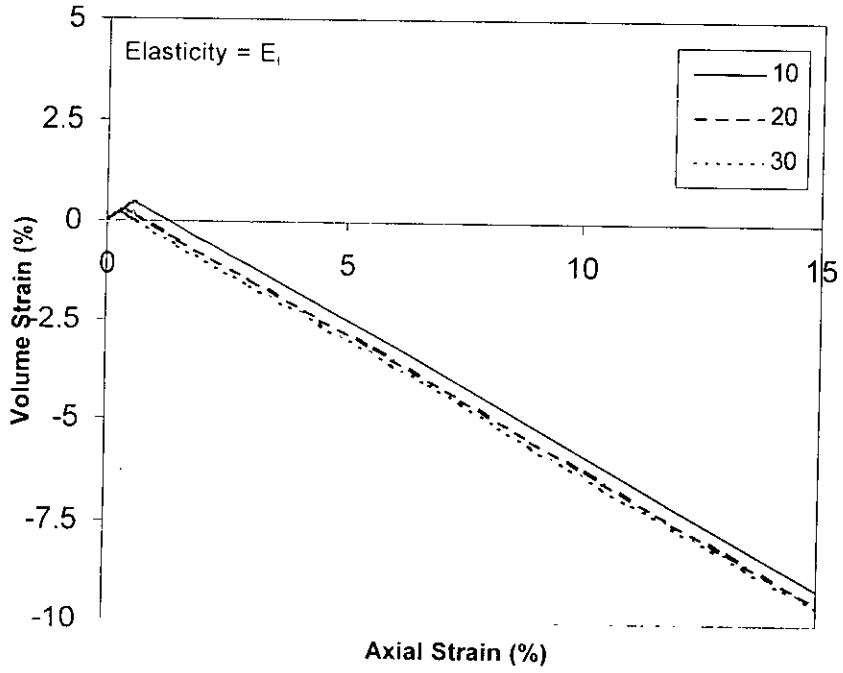

Figure 5.26 Mohr-Coulomb prediction of volume strain for drained triaxial test of Chandanaish clay for initial elastic modulus (OCR=10, 20, 30)

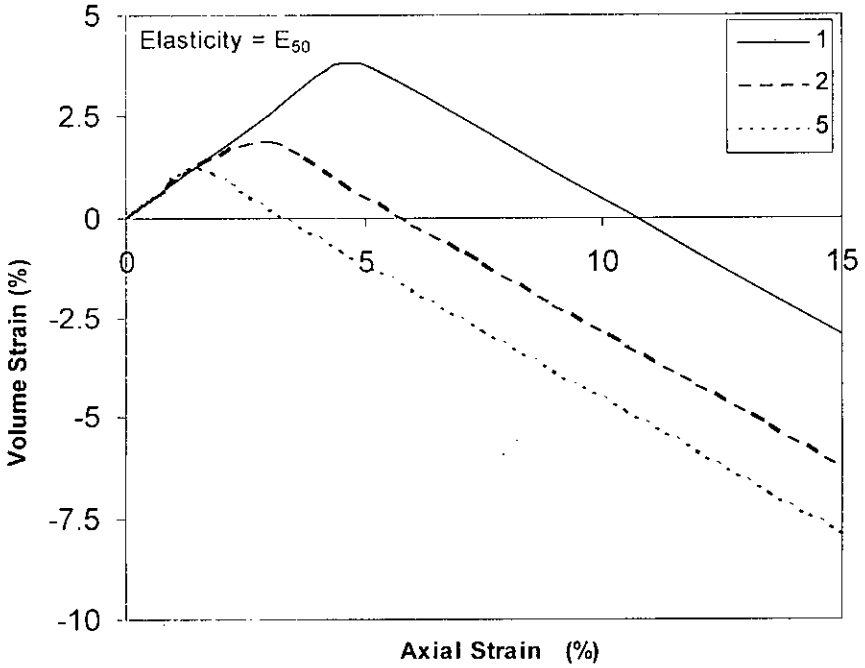

Figure 5.27 Mohr-Coulomb prediction of volume strain for drained triaxial test of Anwara clay for secant elastic modulus (OCR=1, 2, 5)

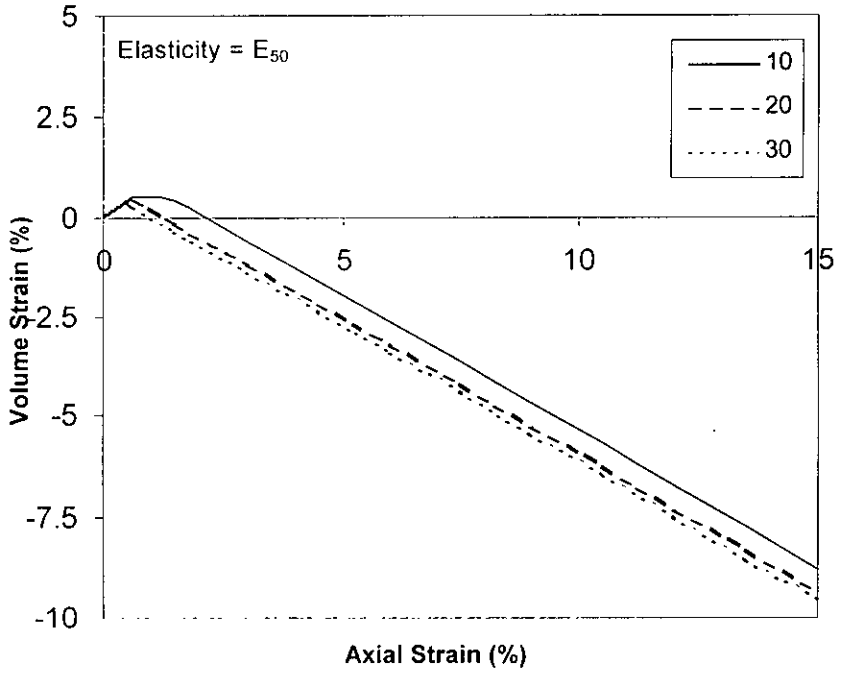

Figure 5.28 Mohr-Coulomb prediction of volume strain for drained triaxial test of Anwara clay for secant elastic modulus (OCR=10, 20, 30)

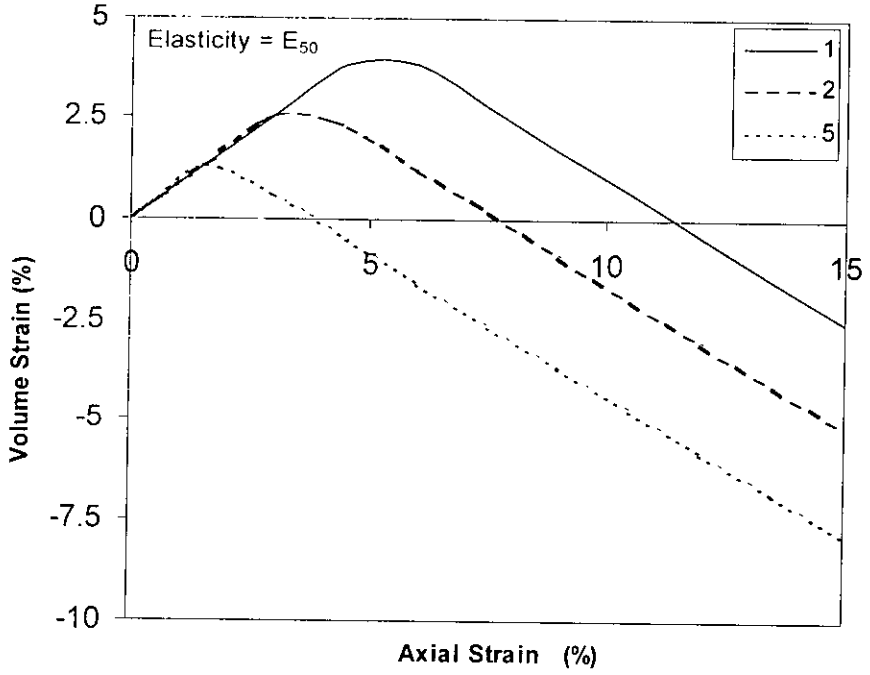

Figure 5.29 Mohr-Coulomb prediction of volume strain for drained triaxial test of Banshkhali clay for secant elastic modulus (OCR=1, 2, 5)

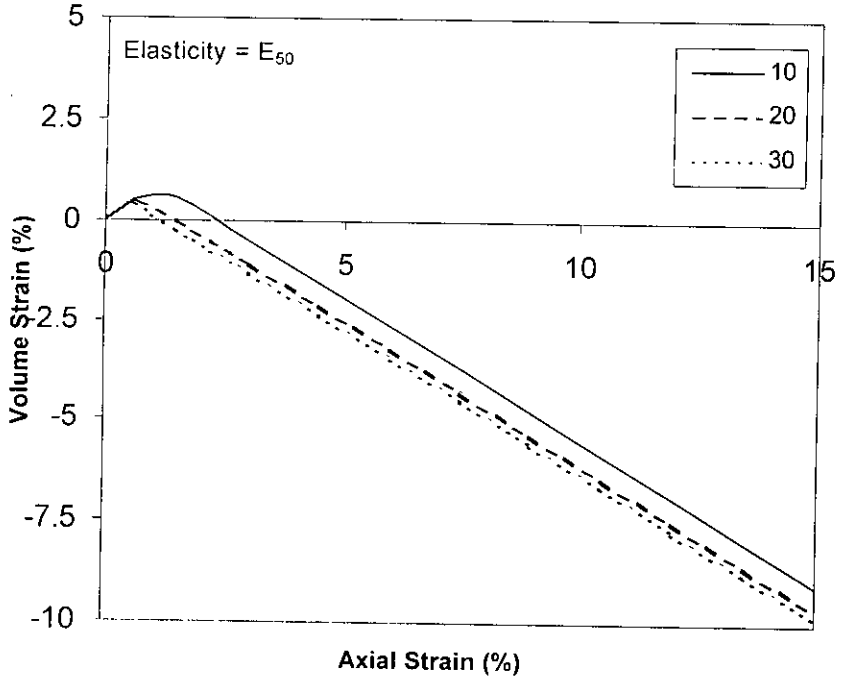

Figure 5.30 Mohr-Coulomb prediction of volume strain for drained triaxial test of Banshkhali clay for secant elastic modulus (OCR=10, 20, 30)

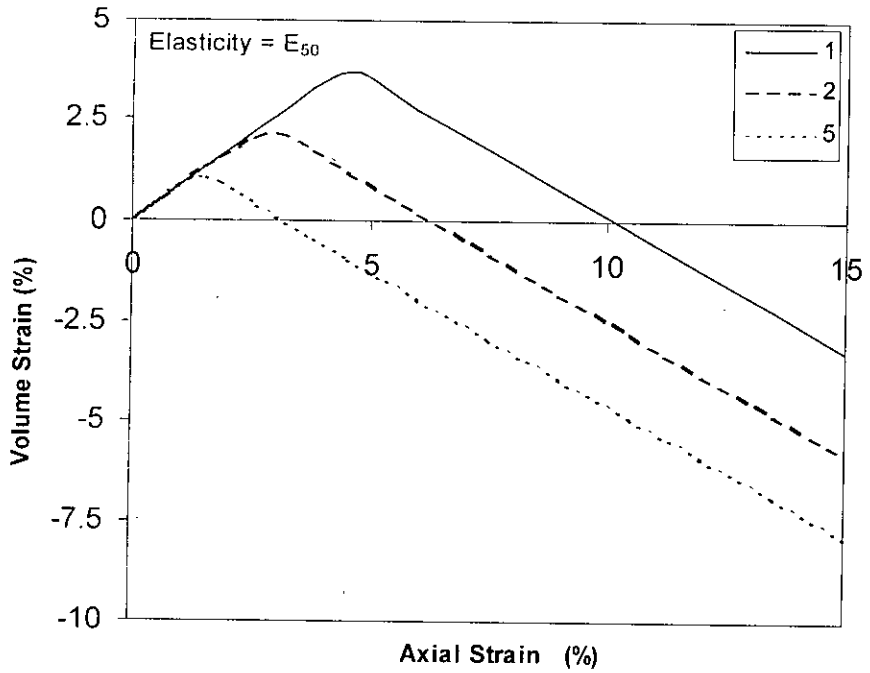

Figure 5.31 Mohr-Coulomb prediction of volume strain for drained triaxial test of Chandanaish clay for secant elastic modulus (OCR=1, 2, 5)

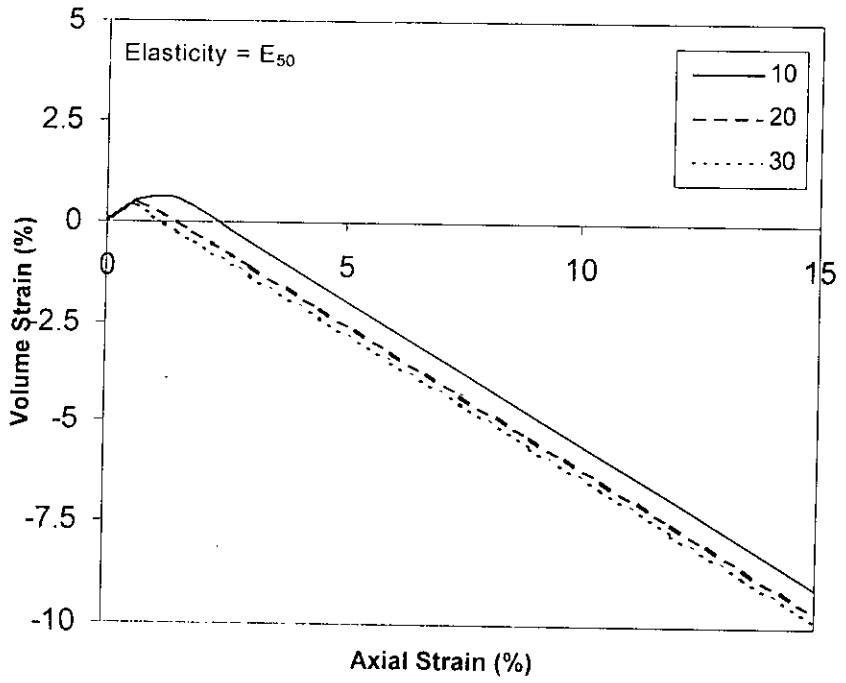

Figure 5.32 Mohr-Coulomb prediction of volume strain for drained triaxial test of Chandanaish clay for secant elastic modulus (OCR=10, 20, 30)

Low OCR and normally consolidated clays generally exhibit compressive volume changes during triaxial shear under drained conditions. Thus if the value of the dilation angle ψ' is assumed to be equal to the drained friction angle ϕ', unreasonable volume change predictions (expansive rather than compressive) will be obtained. Thus for low OCR and normally consolidated clays, it is probably more reasonable to assume a low value of the dilation angle ψ' in the Mohr-Coulomb model.

5.5 Comparison of Drained Predictions

Some salient features of drained Mohr-Coulomb model predictions using the various approaches namely, constant elastic initial stiffness and constant elastic secant stiffness are discussed in this section. The discussion is as follows.

5.5.1 Stress at Failure

The stresses at failure during drained triaxial shear of coastal clays (Anwara, Banshkhali or Chandanaish) using the Mohr-Coulomb model are identical whether the initial elastic stiffness, secant elastic stiffness or the Janbu approach is employed. This is reasonable as the stress at failure is determined by stress path followed during drained triaxial shear and the position of the Mohr-Coulomb line. This position is in turn determined by value of the drained ultimate friction angle ϕ' of the soil. The modulus of elasticity or the Poisson's ratio has no influence on stress at failure.

5.5.2 Strain at Failure

The predicted strain at failure during drained triaxial shear using the Mohr-Coulomb model is strongly influenced by the value of the elastic modulus used and also by the value of the elastic Poisson's ratio. The values of the initial elastic stiffness of coastal clays are significantly higher than the values of the secant elastic stiffness. Consequently the predicted strain at failure is significantly smaller when initial elastic stiffness is used compared to secant elastic stiffness in the Mohr-Coulomb model. The secant elastic stiffness is an approximate or average linear

representation of the stiffness of clay. Thus the secant elastic stiffness is generally significantly smaller in value than the initial elastic stiffness of the soil. The secant elastic stiffness approach, which represents the average stiffness of the clay during drained shear, is more likely to give a more realistic representation of the strain at failure. The strain at failure predicted using the Janbu approach will depend upon the value of K and n. K and n may be obtained by considering the experimental stiffness of laboratory triaxial samples at various cell pressures. In that case, a more realistic representation of the stress-strain curve of coastal clays as well as the strain at failure may be expected.

5.5.3 Volume Change at Failure

The elastic part of the volume change, which is the small initial compressive volume change, is relatively smaller when initial elastic stiffness is used as compared to the secant elastic stiffness. However, the final expansive volume change, which represents the significant part of volume change predicted by Mohr-Coulomb model during drained triaxial shearing, appears to be unaffected by the approach employed when assuming elastic stiffness of the soil. This is because the plastic volume change predicted by the Mohr-Coulomb model is dependent of the value of the dilation angle assumed for the soil and not dependent of the value of elastic stiffness.

5.5.4 Comparison of Drained and Undrained Mohr-Coulomb Prediction

When the Mohr-Coulomb model is used for drained predictions, the stresses obtained by the model are interpreted as effective stresses. On the other hand, when the Mohr-Coulomb model is used to make undrained predictions, the predicted stresses are interpreted as total stresses. At higher cell pressures, the drained Mohr-Coulomb model will predict higher strength, as both the deviator and mean effective stresses are predicted to increase during shearing. However, during undrained shearing, the Mohr-Coulomb model will predict significantly lower strength of the soil. The Possion's ratio is assumed to be close to 0.5 during undrained shear to simulate the incompressibility condition. This in turn implies that mean pressures remain constant.

At constant mean pressure significantly smaller deviator stresses are predicted on the Mohr-Coulomb line, on which lies the stress at failure. The drained elastic modulus and drained Poisson's ratio for clays are generally smaller than the undrained modulus and undrained elastic Poisson's ratio. Thus linear elastic part of the stress-strain curve predicted by the Mohr-Coulomb model during drained shearing has significantly flatter or lower slope than the corresponding part of the stress-strain curves for undrained shear. This results in significantly larger strains at failure being predicted during drained triaxial shearing using the Mohr-Coulomb model compared to undrained predictions.

During drained shearing the Mohr-Coulomb model will predict initially a small elastic compressive volume change followed by expansive plastic volume changes. This is because the associated flow rule is used in the Mohr-Coulomb to simulate drained shear of clays. In associated flow, the dilation angle ψ' is assumed to be equal to the ultimate mean friction angle ϕ' of the soil for drained predictions. For undrained predictions using the Mohr-Coulomb model, the model parameters are so selected that both elastic and plastic volume changes are forced to be zero. This is simulated in the Mohr-Coulomb model by assuming the elastic Poisson's ratio to be close to 0.5 and the dilation angle ψ' as zero.

Tables 5.1, 5.2 and 5.3 compare drained predictions for coastal clays using the Mohr-Coulomb model with two different approaches. Tables 5.4, 5.5 and 5.6 and Tables 5.7, 5.8 and 5.9 compare drained predictions for coastal clays using the Mohr-Coulomb model with two different approaches. One approach uses initial tangent modulus and the other uses the secant modulus as the modulus of elasticity.

Table 5.1 Comparison of drained Mohr-Coulomb model predictions: Anwara clay

Cell pressure kPa	OCR	Stress at failure (kPa)		Strain at failure (%)		Volume strain at failure (%)	
		Initial	Secant	Initial	Secant	Initial	Secant
150	1	353.56	336.15	4.5	6.0	1.75	3.83
75	2	176.78	176.78	3.0	3.2	1.05	1.90
30	5	70.71	70.71	1.5	1.7	0.49	1.25
15	10	35.36	35.36	0.51	1.5	0.41	0.41
7.5	20	17.68	17.88	0.39	0.57	0.30	0.48
5	30	11.79	11.79	0.315	0.45	0.23	0.35

Table 5.2 Comparison of drained Mohr-Coulomb model predictions: Banshkhali clay

Cell pressure (kPa)	OCR	Stress at failure (kPa)		Strain at failure (%)		Volume strain at failure (%)	
		Initial	Secant	Initial	Secant	Initial	Secant
150	1	363.29	363.29	4.5	6.0	2.15	3.83
75	2	181.65	181.65	3.0	4.5	1.50	2.28
30	5	72.66	72.66	1.5	3.0	0.75	1.28
15	10	36.33	36.33	1.5	1.5	0.38	0.53
7.5	20	18.16	18.16	0.465	1.5	0.37	0.43
5	30	12.11	12.11	0.375	0.54	0.28	0.40

Table 5.3 Comparison of drained Mohr-Coulomb model predictions: Chandanaish clay

Cell pressure (kPa)	OCR	Stress at failure (kPa)		Strain at failure (%)		Volume strain at failure (%)	
		Initial	Secant	Initial	Secant	Initial	Secant
150	1	348.37	348.37	3.0	4.5	2.47	3.71
75	2	174.18	174.18	3.0	3.0	0.77	2.16
30	5	69.67	69.67	1.5	1.5	0.37	1.05
15	10	34.84	36.33	0.57	1.5	0.45	0.53
7.5	20	17.12	18.16	0.33	1.5	0.28	0.43
5	30	11.61	12.11	0.27	0.54	0.20	0.40

Table 5.4 Comparison of drained and undrained Mohr-Coulomb model predictions: Anwara clay (considering $E = E_i$)

Cell pressure kPa	OCR	Stress at failure (kPa)		Strain at failure (%)		Volume strain (%)/ pore pressure at failure (kPa)	
		Drained	Undrained	Drained	Undrained	Drained	Undrained
150	1	353.56	125.4	4.5	0.33	1.75	N.A.
75	2	176.78	100.5	3.0	0.33	1.05	N.A.
30	5	70.71	85.5	1.5	0.345	0.49	N.A.
15	10	35.36	71.1	0.51	0.36	0.41	N.A.
7.5	20	17.79	60.0	0.39	0.375	0.30	N.A.
5	30	11.79	53.2	0.315	0.375	0.23	N.A.

Table 5.5 Comparison of drained and undrained Mohr-Coulomb model predictions: Banshkhali clay (considering $E = E_i$)

Cell pressure kPa	OCR	Stress at failure (kPa)		Strain at failure (%)		Volume strain (%)/ pore pressure at failure (kPa)	
		Drained	Undrained	Drained	Undrained	Drained	Undrained
150	1	363.29	119.2	4.5	0.33	2.15	N.A.
75	2	181.65	90.0	3.0	0.33	1.50	N.A.
30	5	72.66	75.6	1.5	0.36	0.75	N.A.
15	10	36.33	62.0	1.5	0.33	0.38	N.A.
7.5	20	18.16	52.4	0.465	0.375	0.37	N.A.
5	30	12.11	45.0	0.375	0.375	0.28	N.A.

Table 5.6 Comparison of drained and undrained Mohr-Coulomb model predictions: Chandanaish clay (considering $E = E_i$)

Cell pressure kPa	OCR	Stress at failure (kPa)		Strain at failure (%)		Volume strain (%)/ pore pressure at failure (kPa)	
		Drained	Undrained	Drained	Undrained	Drained	Undrained
150	1	348.37	130.0	3.0	0.315	2.47	N.A.
75	2	174.18	108.6	3.0	0.33	0.77	N.A.
30	5	69.67	91.0	1.5	0.345	0.37	N.A.
15	10	34.84	76.8	0.57	0.36	0.45	N.A.
7.5	20	17.12	65.0	0.33	0.36	0.28	N.A.
5	30	11.61	59.8	0.27	0.375	0.20	N.A.

Table 5.7 Comparison of drained and undrained Mohr-Coulomb model predictions: Anwara clay (considering $E = E_{50}$)

Cell pressure kPa	OCR	Stress at failure (kPa)		Strain at failure (%)		Volume strain (%)/ pore pressure (kPa) at failure	
		Drained	Undrained	Drained	Undrained	Drained	Undrained
150	1	336.15	125.4	6.0	0.48	3.83	N.A.
75	2	176.78	100.5	3.2	0.42	1.90	N.A.
30	5	70.71	85.5	1.7	0.525	1.25	N.A.
15	10	35.36	71.1	1.5	0.54	0.41	N.A.
7.5	20	17.88	60.0	0.57	0.555	0.48	N.A.
5	30	11.79	53.2	0.45	0.555	0.35	N.A.

Table 5.8 Comparison of drained and undrained Mohr-Coulomb model predictions: Banshkhali clay (considering $E = E_{50}$)

Cell pressure kPa	OCR	Stress at failure (kPa)		Strain at failure (%)		Volume strain (%)/ pore pressure at failure (kPa)	
		Drained	Undrained	Drained	Undrained	Drained	Undrained
150	1	363.29	119.2	6.0	0.495	3.83	N.A.
75	2	181.65	90.0	4.5	0.51	2.28	N.A.
30	5	72.66	75.6	3.0	0.525	1.28	N.A.
15	10	36.33	62.0	1.5	0.51	0.53	N.A.
7.5	20	18.16	52.4	1.5	0.555	0.43	N.A.
5	30	12.11	45.0	0.54	0.555	0.40	N.A.

Table 5.9 Comparison of drained and undrained Mohr-Coulomb model predictions: Chandanaish clay (considering $E = E_{50}$)

Cell pressure kPa	OCR	Stress at failure (kPa)		Strain at failure (%)		Volume strain (%)/ pore pressure at failure (kPa)	
		Drained	Undrained	Drained	Undrained	Drained	Undrained
150	1	348.37	130.0	4.5	0.48	3.71	N.A.
75	2	174.18	108.6	3.0	0.495	2.16	N.A.
30	5	69.67	91.0	1.5	0.51	1.05	N.A.
15	10	36.33	76.8	1.5	0.525	0.53	N.A.
7.5	20	18.16	65.0	1.5	0.54	0.43	N.A.
5	30	12.11	59.8	0.54	0.555	0.40	N.A.

5.6 Summaries and Conclusion

The Mohr-Coulomb model is a relatively simple elastic- plastic constitutive model. The model may be used to obtain realistic approximation of the stress-strain response behavior of coastal clays both during drained and undrained shearing of clays. Several approaches may be used when computing the elastic modulus and dilation angle parameters of the Mohr-Coulomb model. The particular approach chosen for a given problem depends on stresses and strains experienced by the soil domain under service loads and degree of overconsolidation of the soil. Limitations of the model include assumption of constant linear elasticity (other than Janbu approach), non- hardening perfect plasticity and prediction of expansive volume strain for dilation angle not equal to zero. These assumptions are not realistic representations of the true stress-strain response of coastal clays both during drained and undrained shear. Even then, the stresses and strains predicted by the Mohr-Coulomb model gives a realistic approximation of the behaviour of the soil in many geotechnical problems, both in drained and undrained conditions. Thus the Mohr-Coulomb model may serve as a powerful tool for both numerical and analytical prediction of boundary value problems in geotechnical engineering. This chapter is an attempt to reinvestigate the different aspects of this traditional model as applied to the triaxial shear response of coastal clays of Bangladesh.

CHAPTER 6

DRAINED PREDICTIONS: MODIFIED CAM CLAY MODEL

6.1 Introduction

The Modified Cam Clay model was developed in Cambridge to describe the stress-strain and volume change response of normally consolidated and low OCR clays, under drained condition. In this chapter, the Modified Cam Clay model is used to predict the stress- strain and volume change behaviour of coastal clays during drained triaxial shear. The drained Modified Cam Clay model parameters are computed and indirectly derived from the Modified Cam Clay model parameters obtained from effective stress paths of undrained tests. The Modified Cam Clay model is then used to make drained prediction of the triaxial response of coastal clays. In the absence of experimental data, the drained Modified Cam Clay predictions are compared with those of the Mohr-Coulomb model. Finally the strengths and limitations of the Modified Cam Clay model for predicting the drained response are discussed.

6.2 Approach in Drained Analysis

The fundamental difference between drained and undrained analysis is that excess pore water pressure is zero under drained condition and the sample changes in volume. In undrained condition, there is no volume change and consequently excess pore pressure develops within the soil sample. Fully saturated conditions are assumed in both the analyses.

The Modified Cam Clay model is more representative of the fundamental mechanical behaviour of clays. No separate approach is required for drained and undrained MCC analysis. However, in the undrained analysis the bulk modulus of water is input in the soil model (generally given a very high value relative to the bulk modulus of soil). This result in the incompressibility condition and the development of excess pore pressure. Bulk modulus of water is assumed to be equal to zero for drained condition. In that case, volume change occurs and no excess pore water pressures are predicted. For drained condition, the value of Poisson's ratio for clays varies generally 0.1 to

0.3. Figures 6.1 and 6.2 show the evolution of yield locus of the Modified Cam Clay model during triaxial shear under drained condition.

6.3 Drained Modified Cam Clay Model Parameters

All the model parameters for drained analysis are identical to that of undrained analysis as given in Appendix II. In the absence of experimental data, the drained Poisson's ratio for all of the different coastal clays has been assumed to be 0.2. For drained analysis, the bulk modulus of water is assumed to be zero.

6.4 Drained Modified Cam Clay Predictions

6.4.1 Stress-Strain

The stress- strain response of coastal clays of Anwara, Banshkhali and Chandanaish for cell pressure of 150, 75, 30, 15, 7.5 and 5 kPa i.e. for OCR of 1, 2, 5, 10, 20 and 30 are given in Figures 6.3 and 6.4, Figures 6.5 and 6.6 and Figures 6.7 and 6.8 respectively. It is observed that the stress-strain response is non-linear from the beginning of load application. There appears to be a yield stress, beyond which the clay behaves elasto-plastically until it reaches failure at ultimate stress state or the critical state condition.

6.4.2 Stress Path

The effective stress path in a drained triaxial test is equal to the total stress path as no excess pore pressure develops within the soil sample during shear. The drained stress path is constant in a triaxial test and it is independent of the soil model used. For triaxial test conditions, the ratio of the increment of deviator stress to the increment of mean effective pressure is 3. Thus for drained tests under triaxial conditions of stress

$$\frac{\Delta q}{\Delta p'} = \frac{\Delta q}{\Delta p} = 3$$

where $\Delta q, \Delta p', \Delta p$ are respectively the increment of deviator stress, increment of mean effective pressure and increment of total effective pressure in the soil sample.

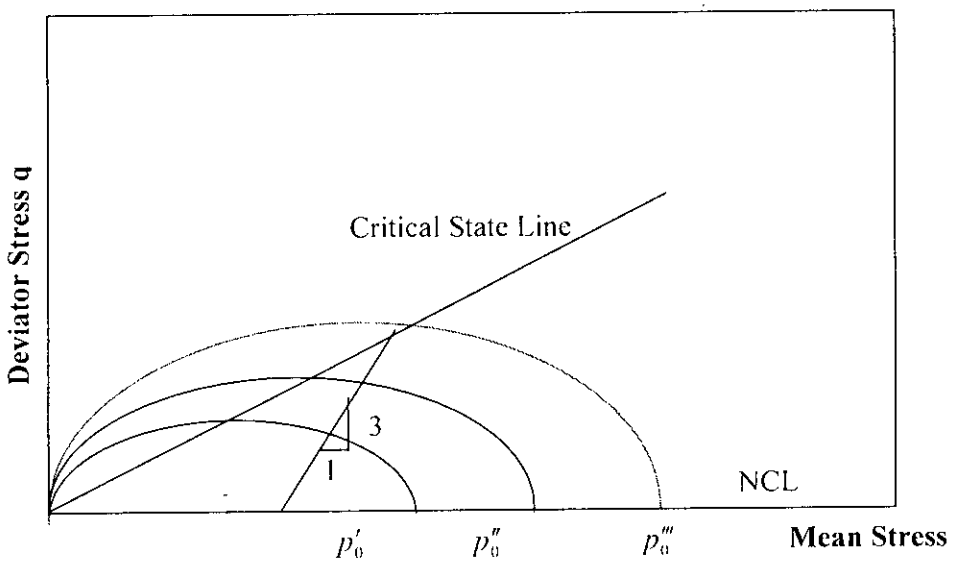

Figure 6.1 Modified Cam Clay (MCC) model elliptical yield surfaces (Schofield and Wroth, 1968)

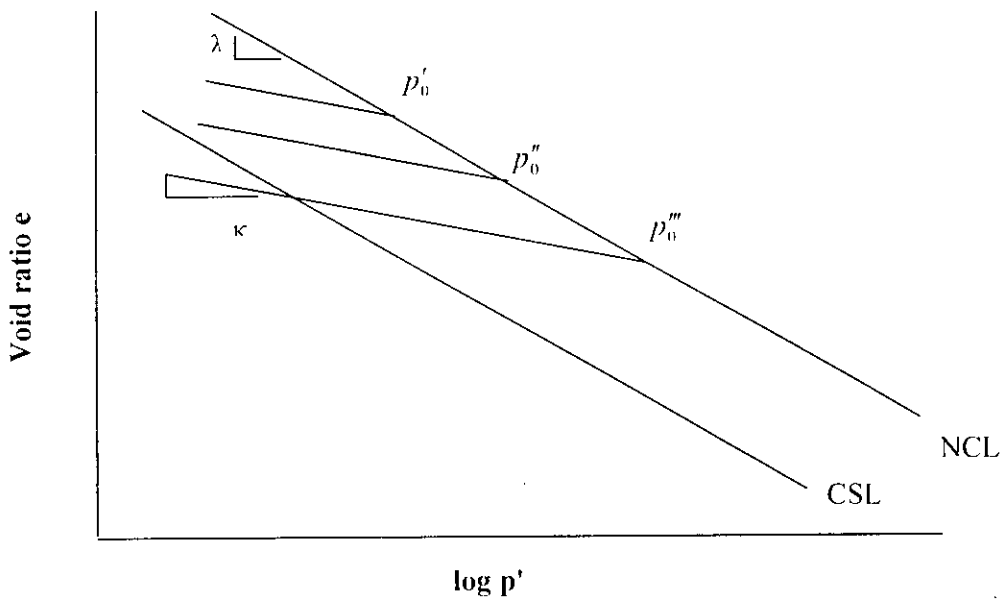

Figure 6.2 Modified Cam Clay (MCC) model Critical State Line (CSL) and Normal Consolidation Line (NCL) in e-ln p' space (Schofield and Wroth, 1968)

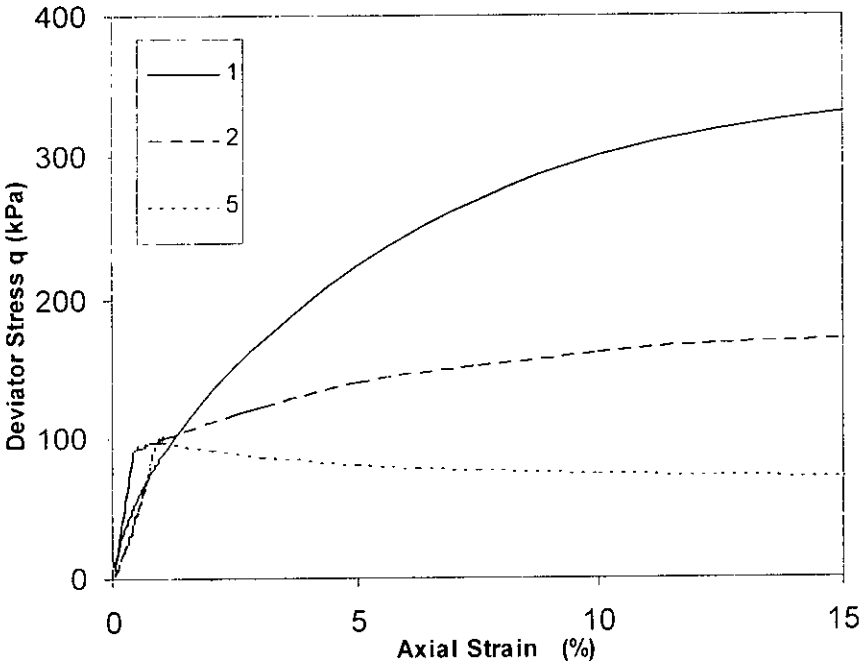

Figure 6.3 MCC prediction of drained triaxial stress-strain response of Anwara clay (OCR=1, 2, 5)

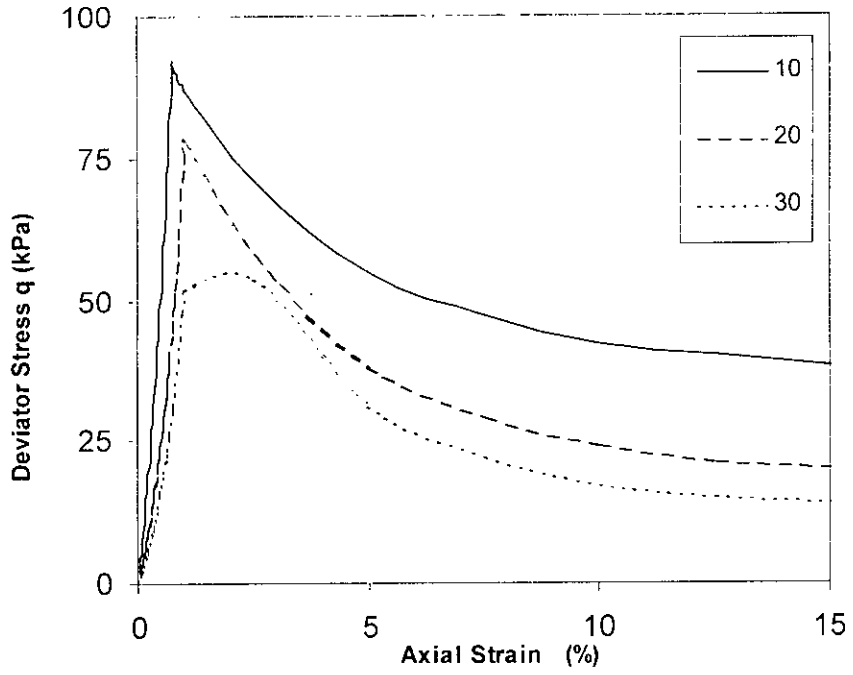

Figure 6.4 MCC prediction of drained triaxial stress-strain response of Anwara clay (OCR=10, 20, 30)

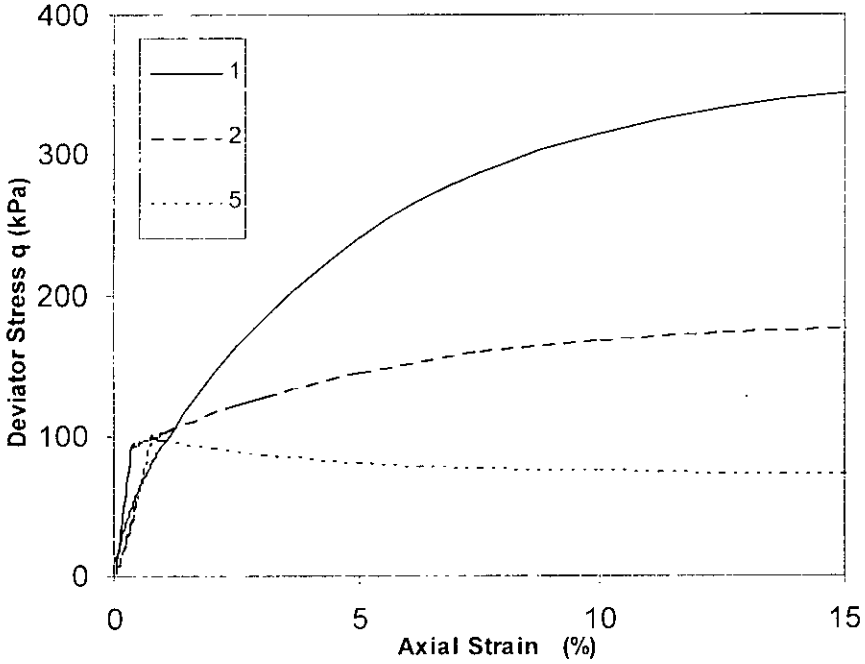

Figure 6.5 MCC prediction of drained triaxial stress-strain response of Banshkhali clay (OCR=1, 2, 5)

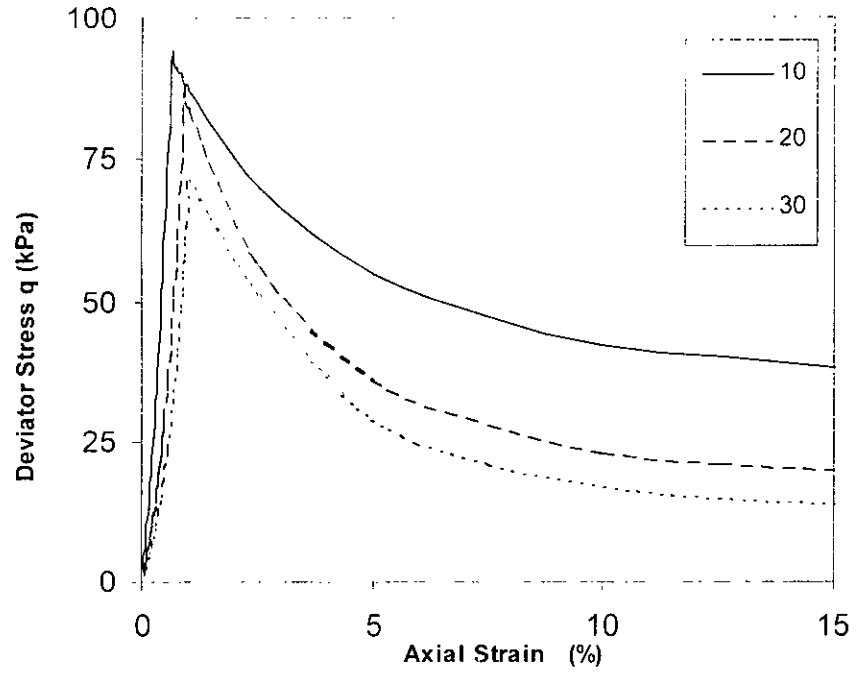

Figure 6.6 MCC prediction of drained triaxial stress-strain response of Banshkhali clay (OCR=10, 20, 30)

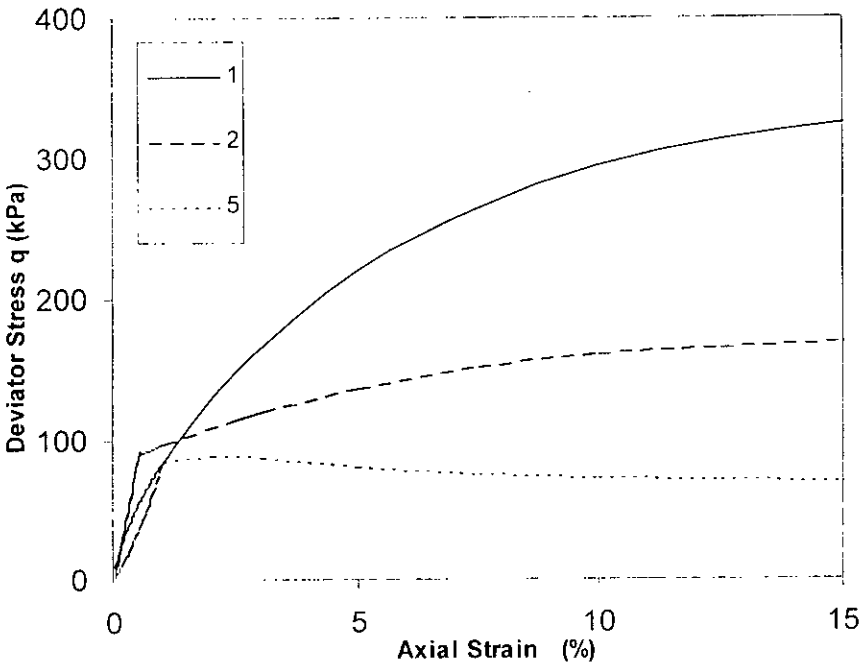

Figure 6.7 MCC prediction of drained triaxial stress-strain response of Chandanaish clay (OCR=1, 2, 5)

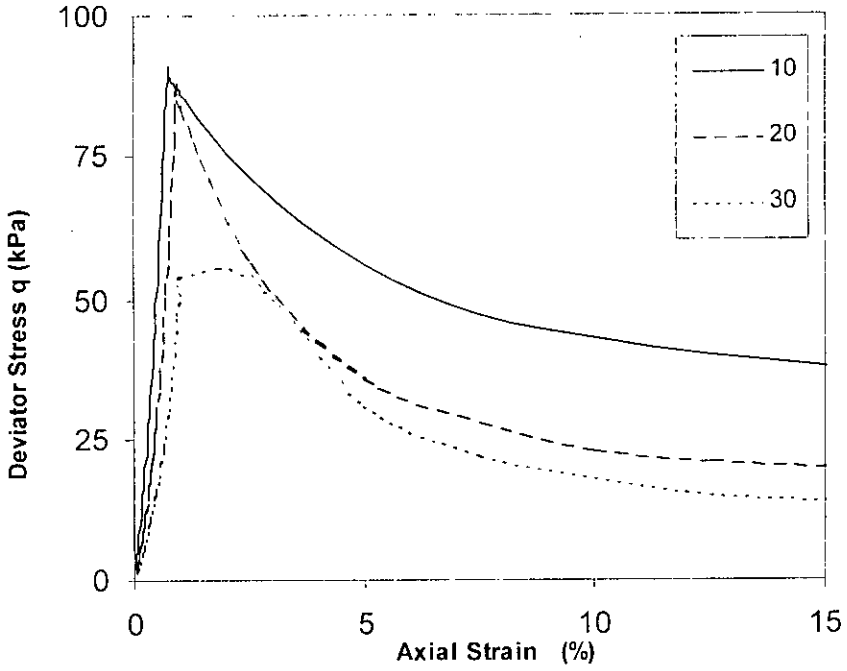

Figure 6.8 MCC prediction of drained triaxial stress-strain response of Chandanaish clay (OCR=10, 20, 30)

Figures 6.9 and 6.10, Figures 6.11 and 6.12 and Figures 6.13 and 6.14 give drained effective stress paths as predicted by the Modified Cam Clay model for triaxial shearing of coastal clays of Anwara, Banshkhali and Chandanaish.

6.4.1 Volume Change

Figures 6.15 and 6.16, Figures 6.17 and 6.18 and Figures 6.19 and 6.20 give the volume change response of the coastal clays of Anwara, Banshkhali and Chandanaish respectively during drained shearing for various values of the overconsolidation ratio or OCR. It is observed that at all overconsolidation ratios stresses, initially there is some small compressive volume change. This is the volume change during the elastic part of the stress-strain behaviour. Beyond elasticity and with the onset of yield most of the elasto-plastic response of the clay begins. At this stage, there is significant compressive volume change for normally consolidated and low OCR clays. On the other hand, for high OCR clays, volume expansion takes place as shown in Figures 6.16, 6.18 and 6.20. Standard literature on the drained shearing of clays under triaxial states of stress indicates that such volume change response is a realistic representation of the drained shearing of clays under triaxial conditions.

6.5 Comparison of Drained Predictions: Mohr-Coulomb and Modified Cam Clay Models

Both the drained Mohr-Coulomb and Modified Cam Clay analysis predict the same effective stress paths, which really represent test conditions and are independent of the constitutive properties of the soil. The drained Mohr-Coulomb model in general predicts constant elastic behaviour until the ultimate stress state is reached. The Modified Cam Clay model however predicts nonlinear pressure dependent elasticity initially for clay soils. When yield is reached, elastio-plastic strain-hardening behavior is predicted. In the Modified Cam Clay model, as strain-hardening plastic response is initiated at much lower stresses compared to the Mohr-Coulomb model. Thus the strain at which the soil is predicted to reach the ultimate stress state is much larger compared to the strain predicted by the Mohr-Coulomb model.

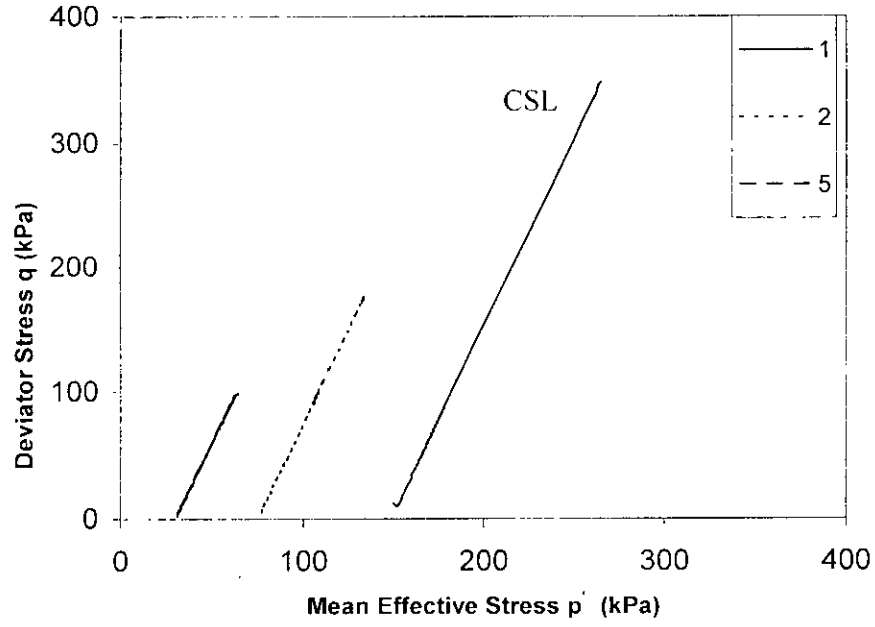

Figure 6.9 MCC drained triaxial stress path of Anwara clay (OCR=1, 2, 5)

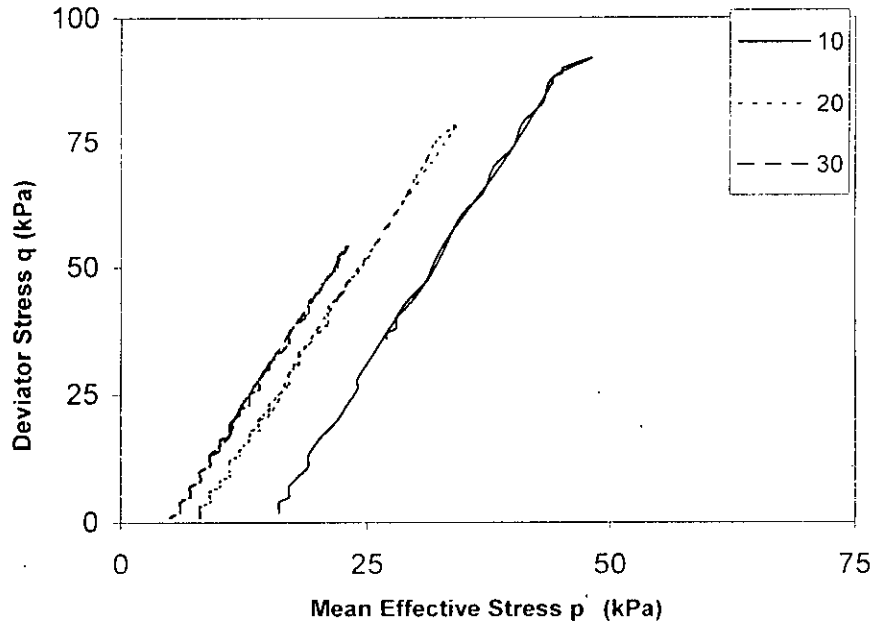

Figure 6.10 MCC drained triaxial stress path of Anwara clay (OCR=10, 20, 30)

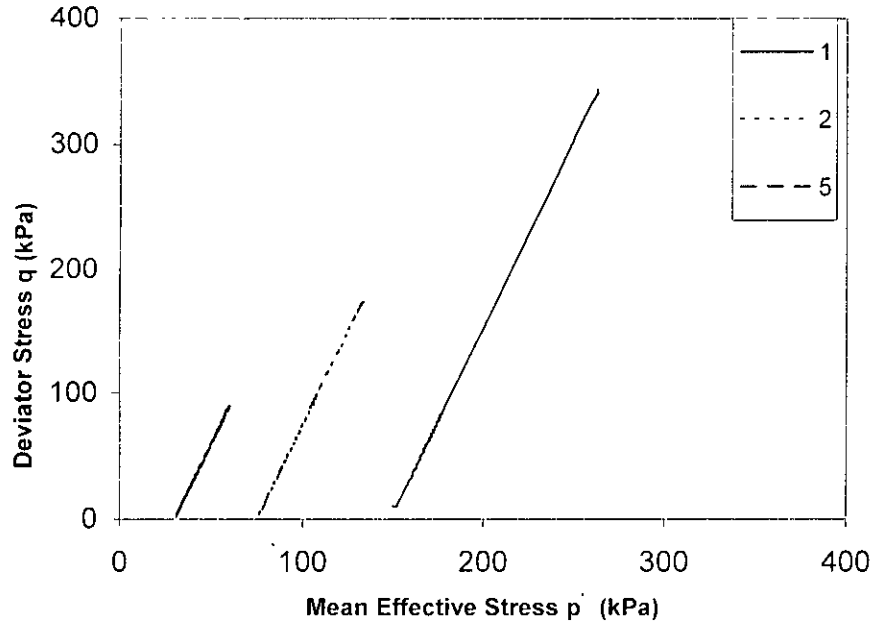

Figure 6.11 MCC drained triaxial stress path of Banshkhali clay (OCR=1, 2, 5)

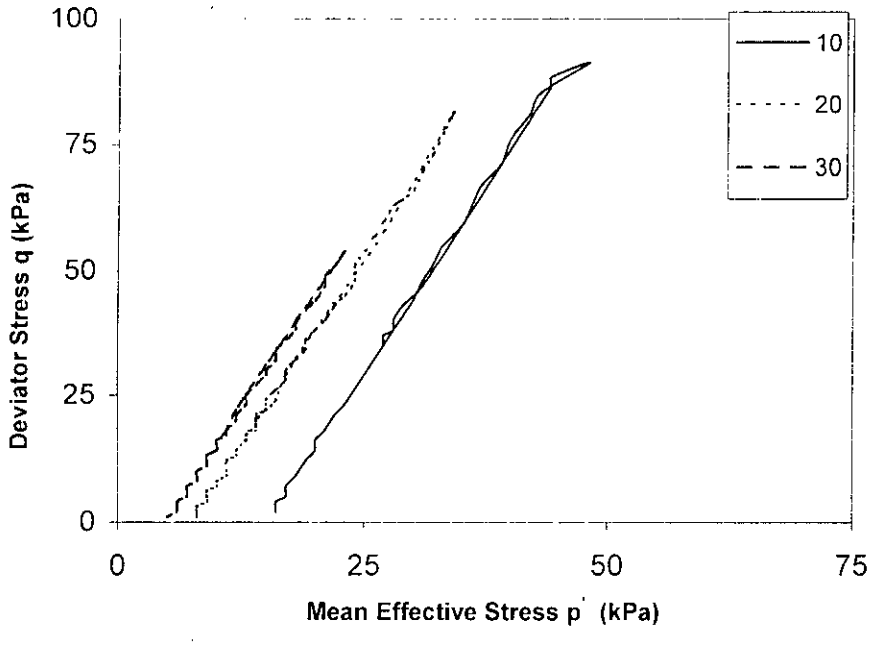

Figure 6.12 MCC drained triaxial stress path of Banshkhali clay (OCR=10, 20, 30)

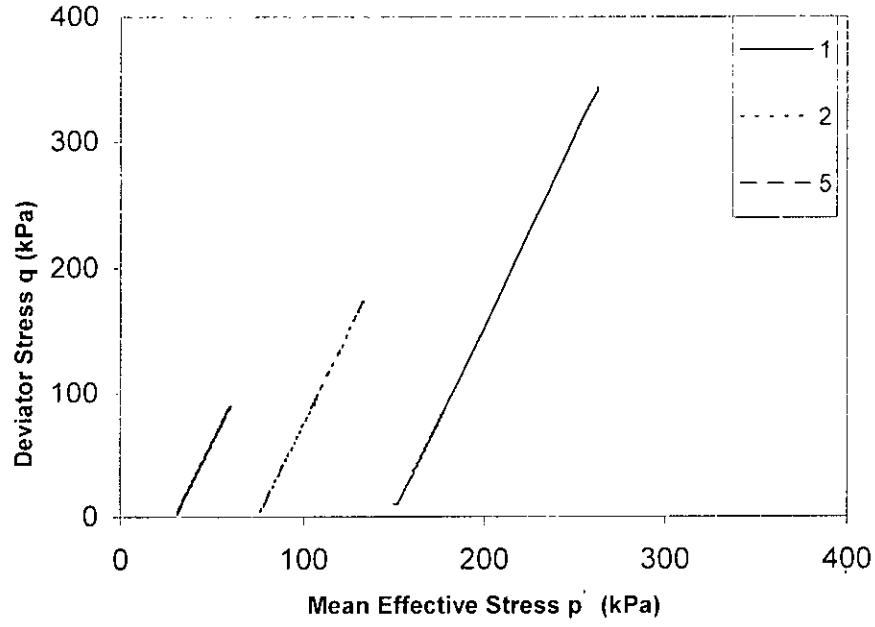

Figure 6.13 MCC drained triaxial stress path of Chandanaish clay (OCR=1, 2, 5)

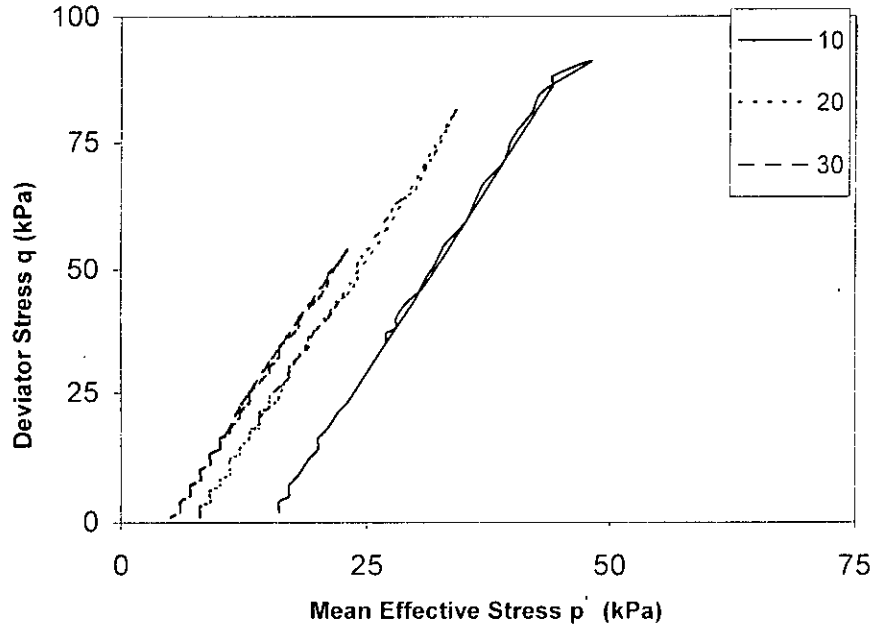

Figure 6.14 MCC drained triaxial stress path of Chandanaish clay (OCR=10, 20, 30)

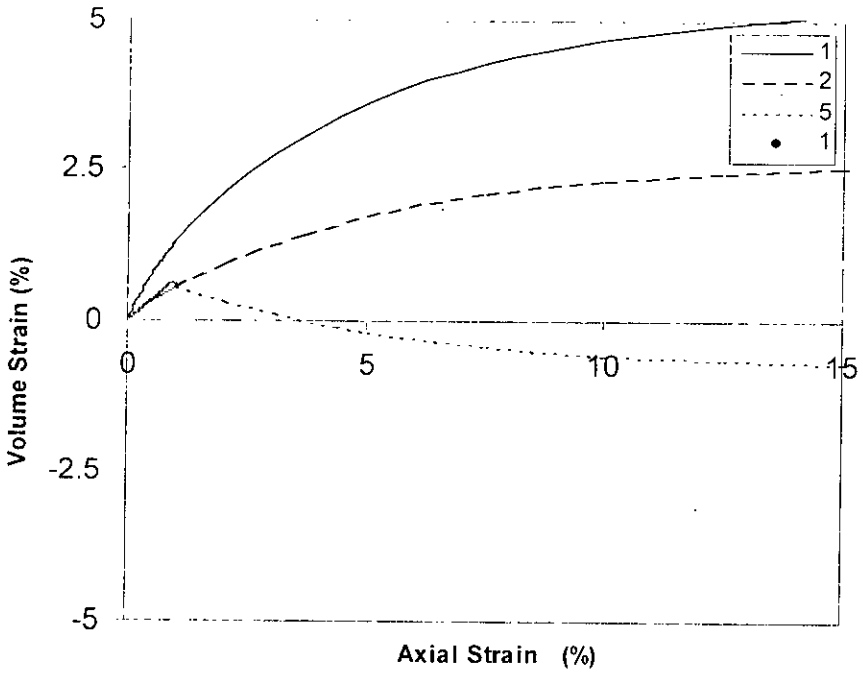

Figure 6.15 MCC drained test prediction of volume strain response of Anwara clay (OCR=1, 2, 5)

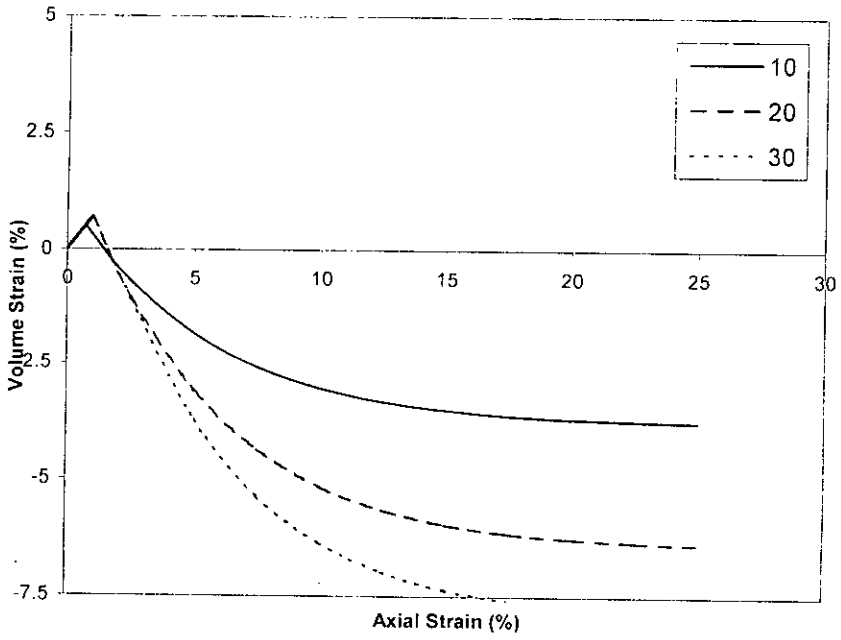

Figure 6.16 MCC drained test prediction of volume strain response of Anwara clay (OCR=10, 20, 30)

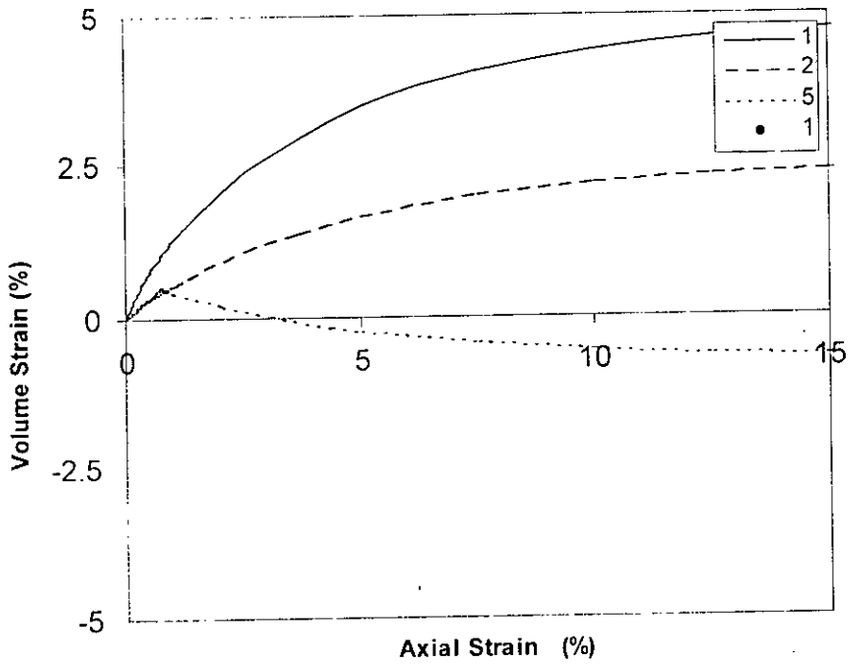

Figure 6.17 MCC drained prediction of volume strain response of Banshkhali clay (OCR=1, 2, 5)

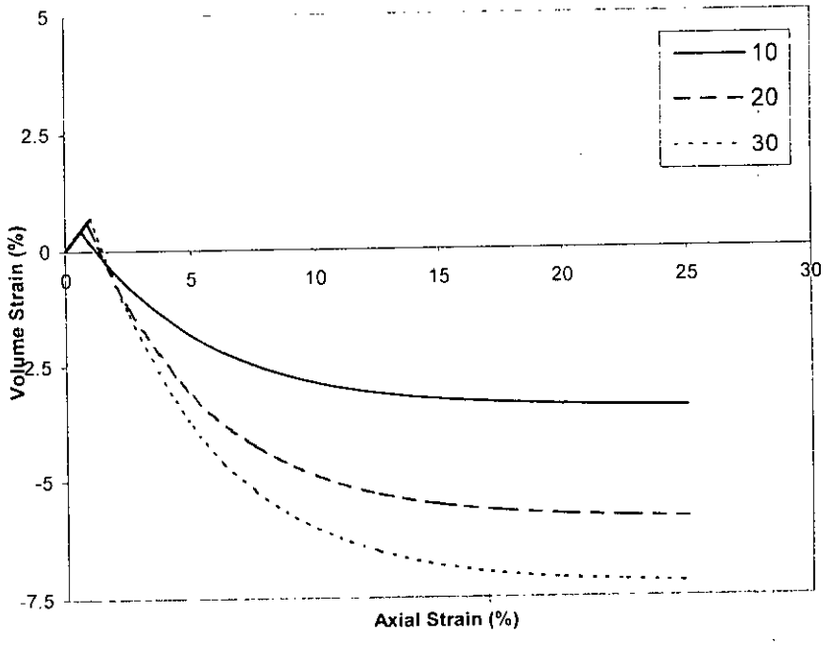

Figure 6.18 MCC drained prediction of volume strain response of Banshkhali clay (OCR=10, 20, 30)

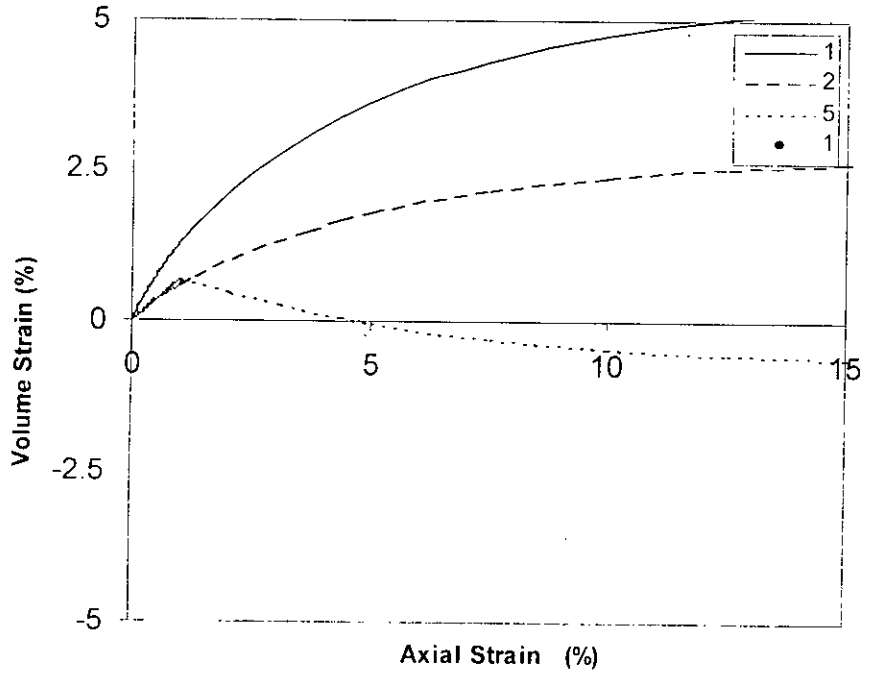

Figure 6.19 MCC drained prediction of volume strain response of Chandanaish clay (OCR=1, 2, 5)

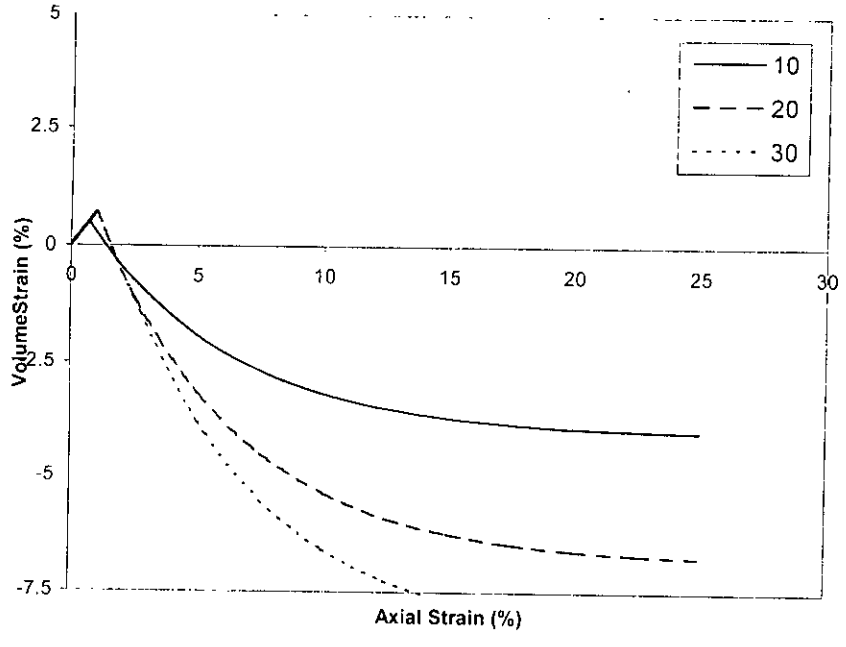

Figure 6.20 MCC drained prediction of volume strain response of Chandanaish clay (OCR=10, 20, 30)

The Mohr-Coulomb model fails to realistically predict the volume change response of coastal clays during drained shear at triaxial state of stress. The Modified Cam Clay model on the other hand is a good qualitative predictor of the volume change response of coastal clays at various OCR values during drained shear under triaxial conditions. The comparison of selected features of predictions of the Mohr-Coulomb and Modified Cam Clay model during drained shear under triaxial states of stress are tabulated in Tables 6.1, 6.2 and 6.3 ($E=E_i$ in Mohr-Coulomb model) and Tables 6.4, 6.5 and 6.6 ($E=E_{50}$ in Mohr-Coulomb model).

6.6 Comparison of Drained and Undrained Predictions: Modified Cam Clay Model

The effective stress path predicted by the Modified Cam Clay is based on the condition of the test (in this case a triaxial state of stress). It is independent of constitutive properties of the soil and is a constant for all soils and constitutive models used. On the other hand, the effective stress path actually followed by coastal clays during undrained shearing under triaxial stress conditions is dependent on the constitutive property of the clay. The predicted stress path is thus model dependent. The effective stress paths predicted by the Modified Cam Clay during undrained triaxial shear of coastal clays is qualitatively correct for various OCR's. For overconsolidated clays, the predicted initial effective stress paths in $p'-q$ space are vertical. The actual effective stress paths are slightly inclined.

An advantage of use of the Modified Cam Clay model is that identical model parameters may be used for both analyses. Positive excess pore pressures are predicted to occur during undrained shearing of normally consolidated and low OCR coastal clays. This implies that for these clays the effective mean pressure decreases during undrained shearing. As such, the predicted deviator stress at failure during undrained shearing of clays is significantly lower than that during drained shear. This is because, during drained shear the mean effective pressure is predicted to increase which in turn predicts a higher deviator stress at failure. At the same time, compressive volume change is predicted to occur in the soil sample by the Modified Cam Clay model during drained shear of normally consolidated and low OCR coastal clays.

Table 6.1 Comparison of drained predictions: Anwara clay (considering $E = E_i$ for Mohr-Coulomb model)

Cell pressure kPa	OCR	Deviator Stress at failure (kPa)		Strain at failure (%)		Volume Strain (%) at failure	
		MCC	MC (Initial)	MCC	MC (Initial)	MCC	MC (Initial)
150	1	348	353.56	25	4.5	5.33	1.75
75	2	176	176.78	25	3.0	2.64	1.05
30	5	71	70.71	20	1.5	-0.74	0.49
15	10	36	35.36	20	0.51	-3.71	0.41
7.5	20	18	17.68	20	0.39	-6.34	0.30
5	30	12	11.79	15	0.315	-7.73	0.23

Table 6.2 Comparison of drained predictions: Banshkhali clay (considering $E = E_i$ for Mohr-Coulomb model)

Cell pressure kPa	OCR	Deviator Stress at failure (kPa)		Strain at failure (%)		Volume Strain (%) at failure	
		MCC	MC (Initial)	MCC	MC (Initial)	MCC	MC (Initial)
150	1	359	363.29	25	4.5	4.92	2.15
75	2	181	181.65	22.5	3.0	2.44	1.50
30	5	73	72.66	17.5	1.5	-0.67	0.75
15	10	37	36.33	20	1.5	-0.39	0.38
7.5	20	19	18.16	17.5	0.465	-5.69	0.37
5	30	12	12.11	22.5	0.375	-7.18	0.28

Table 6.3 Comparison of drained predictions: Chandanaish clay (considering E = E_i for Mohr-Coulomb model)

Cell pressure kPa	OCR	Deviator Stress at failure (kPa)		Strain at failure (%)		Volume Strain (%) at failure	
		MCC	MC (Initial)	MCC	MC (Initial)	MCC	MC (Initial)
150	1	343	348.37	25	3.0	5.42	2.47
75	2	174	174.18	25	3.0	2.74	0.77
30	5	70	69.67	20	1.5	-0.64	0.37
15	10	35	34.84	25	0.57	-4.01	0.45
7.5	20	18	17.12	25	0.33	-6.74	0.28
5	30	12	11.61	20	0.27	-8.12	0.20

Table 6.4 Comparison of drained predictions: Anwara clay (considering E = E_{50} for Mohr-Coulomb model)

Cell pressure kPa	OCR	Deviator Stress at failure (kPa)		Strain at failure (%)		Volume Strain (%) at failure	
		MCC	MC (Secant)	MCC	MC (Secant)	MCC	MC (Secant)
150	1	348	336.15	25	6.0	5.33	3.83
75	2	176	176.78	25	3.2	2.64	1.90
30	5	97	70.71	20	1.5	-0.74	1.25
15	10	36	35.36	20	1.7	-3.71	0.41
7.5	20	18	17.88	20	0.57	-6.34	0.48
5	30	12	11.79	15	0.45	-7.73	0.35

Table 6.5 Comparison of drained predictions: Banshkhali clay (considering $E = E_{50}$ for Mohr-Coulomb model)

Cell pressure kPa	OCR	Deviator Stress at failure (kPa)		Strain at failure (%)		Volume Strain (%) at failure	
		MCC	MC (Secant)	MCC	MC (Secant)	MCC	MC (Secant)
150	1	359	363.29	25	6.0	4.92	3.83
75	2	181	181.65	22.5	4.5	2.44	2.28
30	5	73	72.66	17.5	3.0	-0.67	1.28
15	10	37	36.33	20	1.5	-0.39	0.53
7.5	20	19	18.16	17.5	1.5	-5.69	0.43
5	30	12	12.11	22.5	0.54	-7.18	0.40

Table 6.6 Comparison of drained predictions: Chandanaish clay (considering $E = E_{50}$ for Mohr-Coulomb model)

Cell pressure kPa	OCR	Deviator Stress at failure (kPa)		Strain at failure (%)		Volume Strain (%) at failure	
		MCC	MC (Secant)	MCC	MC (Secant)	MCC	MC (Secant)
150	1	343	348.37	25	4.5	5.42	3.71
75	2	174	174.18	25	3.0	2.74	2.16
30	5	70	69.67	20	1.5	-0.64	1.05
15	10	35	36.33	25	1.5	-4.01	0.53
7.5	20	18	18.16	25	1.5	-6.74	0.43
5	30	12	12.11	20	0.54	-8.12	0.40

Negative excess pore pressure is predicted to develop during undrained shearing of highly overconsolidated clays. This implies that for these clays the effective mean pressure increases during undrained shearing. As such, the predicted deviator stress at failure during undrained shearing of high OCR clays increases. During drained shearing of high OCR clays, expansive volume change and softening is predicted to occur. This results in a decrease in the predicted deviator stress at failure. Tables 6.7, 6.8 and 6.9 give a comparison of the drained and undrained prediction of the Modified Cam Clay model for coastal clays of Anwara, Banshkhali and Chandanaish.

6.7 Limitations of the Modified Cam Clay Model

Clays generally show some plastic response even at the onset of load application (as observed in the undrained shear response of coastal clays). The Modified Cam Clay model is unable to predict such plastic behaviour. Although qualitatively correct, good quantitative agreement of the stress-strain response predicted by the Modified Cam Clay model with experimentally observed behaviour is not obtained in many instances. The predictions of the Modified Cam Clay model for highly overconsolidated clays have generally not found to be very reliable.

6.8 Summary and Conclusion

The drained Modified Cam Clay predictions agree qualitatively with the experimental data of similar clays tested under similar conditions, as available in published literature. In the absence of experimental data on drained shearing of coastal clays of Bangladesh under triaxial conditions, actual comparisons of predictions with experimental data could not be made. However, the Modified Cam Clay predictions show the strength and usefulness of a model in obtaining realistic simulations when model parameters are available or can be derived. It was concluded that realistic predictions of the drained shear response of clays under triaxial conditions can be obtained using the Modified Cam Clay model compared to the Mohr-Coulomb model. The undrained Modified Cam Clay model predictions were compared with drained predictions. It was observed at a given cell pressure, the predicted drained shear strengths of clays are significantly higher than the predicted undrained shear strength. These predictions appear to agree with experimentally observed behaviour of clays.

Table 6.7 Comparison of MCC drained and undrained predictions: Anwara clay

Cell pressure kPa	OCR	Stress at failure (kPa)		Strain at failure (%)		Volume strain (%)/ pore pressure at failure (kPa)	
		Drained	Undrained	Drained	Undrained	Drained	Undrained
150	1	348	112	25	2.5	5.33	101.17
75	2	176	99	25	0.5	2.64	32.69
30	5	97	84	20	5.0	-0.74	-5.55
15	10	36	74	20	5.0	-3.71	-16.2
7.5	20	18	65	20	5.0	-6.34	-18.86
5	30	12	61	15	7.5	-7.73	-20.64

Table 6.8 Comparison of MCC drained and undrained predictions: Banshkhali clay

Cell pressure kPa	OCR	Stress at failure (kPa)		Strain at failure (%)		Volume strain (%)/ pore pressure at failure (kPa)	
		Drained	Undrained	Drained	Undrained	Drained	Undrained
150	1	359	112	25	2.5	4.92	102.45
75	2	181	101	22.5	0.425	2.44	33.05
30	5	73	86	17.5	5.0	-0.67	-5.61
15	10	37	77	20	5.0	-0.39	-16.66
7.5	20	19	68	17.5	5.0	-5.69	-20.49
5	30	12	64	22.5	5.0	-7.18	-20.23

Table 6.9 Comparison of MCC drained and undrained predictions: Chandanaish clay

Cell pressure kPa	OCR	Stress at failure (kPa)		Strain at failure (%)		Volume strain (%)/ pore pressure at failure (kPa)	
		Drained	Undrained	Drained	Undrained	Drained	Undrained
150	1	343	114	25	2.5	5.42	98.84
75	2	174	98	25	0.625	2.74	32.17
30	5	70	80	20	5.0	-0.64	-4.33
15	10	35	69	25	5.0	-4.01	-13.67
7.5	20	18	59	25	7.5	-6.74	-17.69
5	30	12	54	20	5.0	-8.12	-0.09

CHAPTER 7

EXPERIMENTAL AND NUMERICAL INVESTIGATIONS OF MODEL FOOTINGS AND PILES

7.1 Introduction

One of the most important studies in geotechnical engineering is the experimental and numerical investigation of the pressure-displacement response of model scale and prototype footings and piles. An experimental investigation of the pressure-displacement response of model scale footings and piles resting on Anwara clays was carried out as part of this research investigation. The details of the experimental setup is described in this chapter. A finite element analysis was then carried out to numerically simulate the pressure-displacement response of the model scale footings and piles in Anwara clay using elasto-plastic analysis and the Mohr-Coulomb and Modified Cam Clay models. The results of the numerical investigation and their comparison with the experimental results is also presented in this chapter.

7.2 Sample Preparation

Clay slurry was prepared using the Anwara clay samples with initial water content well beyond the liquid limit of the soil. The sample was dried in air and then pulverised using a grinding machine. The pulverised sample was sieved through sieve size 40. The sieved sample was thoroughly mixed with water. The water content used was a little higher than the liquid limit of the soil. The soil and water was first thoroughly and uniformly mixed by hand kneading. Subsequently it was further mixed in a Hobert rotary laboratory mixer for approximately 30 minutes.

The homogeneous soil slurry was K_0 consolidated in a cylindrical consolidation cell which was 210 mm in diameter and 180 mm in height. A 6 mm thick perforated steel disc with a filter paper on top was placed at the bottom of the cell. The sides of the cylidrical cell was coated with silicon grease to minimise side friction. The slurry was poured in the cylidrical cell and as it was poured it was stirred with a steel rod to remove entrapped air from the slurry material. The top of the soil surface was levelled

and two filter papers followed by two perforated steel discs were placed on top for easy drainage. The experimental set up for consolidation of the soil slurry is shown in Figure 7.1.

For the first 24 hours, the soil slurry consolidated to its self weight and weight of the perforated steel discs placed on top. Subsequently the required consolidation load of 50 kPa and 150 kPa was gradually applied on the slurry sample using a loading frame and proving ring in 10 equal increments applied for 24 hours each. The final pressure was maintained until the load displacement curve indicated the end of primary consolidation of the slurry sample. After the completion of consolidation, the soil sample in the cylindrical mold was used to conduct model scale footing and pile tests.

7.3 Experimental Setup

The experimental set up for the model scale footing and pile test was done using the same cylindrical mold used for consolidation of the soil slurry. A model scale circular steel footing 10 mm in thickness and 25 mm in diameter was made. The footing had a 10mm diameter and 50 mm long column at the centre. The top of the column was given a conical depression. The circular steel footing was placed at the centre of the consolidation mold on the surface of the consolidated clay. The column at the top of the circular footing was brought in contact with the centre of the proving ring. The footing was then axially loaded in ten assumed equal increments of load using the proving ring and the loading frame. The applied load was measured from the displacement of the proving ring as measured by a dial gauge placed inside it. This displacement was multiplied by the proving ring constant to compute the axial load applied to the footing at each increment. The loads were adjusted to a constant level. The displacement of the footing for each loading increment was measured by another dial gauge placed in contact with the surface of the circular steel footing.

Two model scale footing tests were carried out, one for a consolidation pressure of 50 kPa and another for consolidation pressure of 150 kPa of the consolidated soil slurry in the cylindrical mold. Figure 7.2 shows a model scale footing test being carried out in the cylindrical consolidation mold using the model scale steel footing, proving ring and the loading frame.

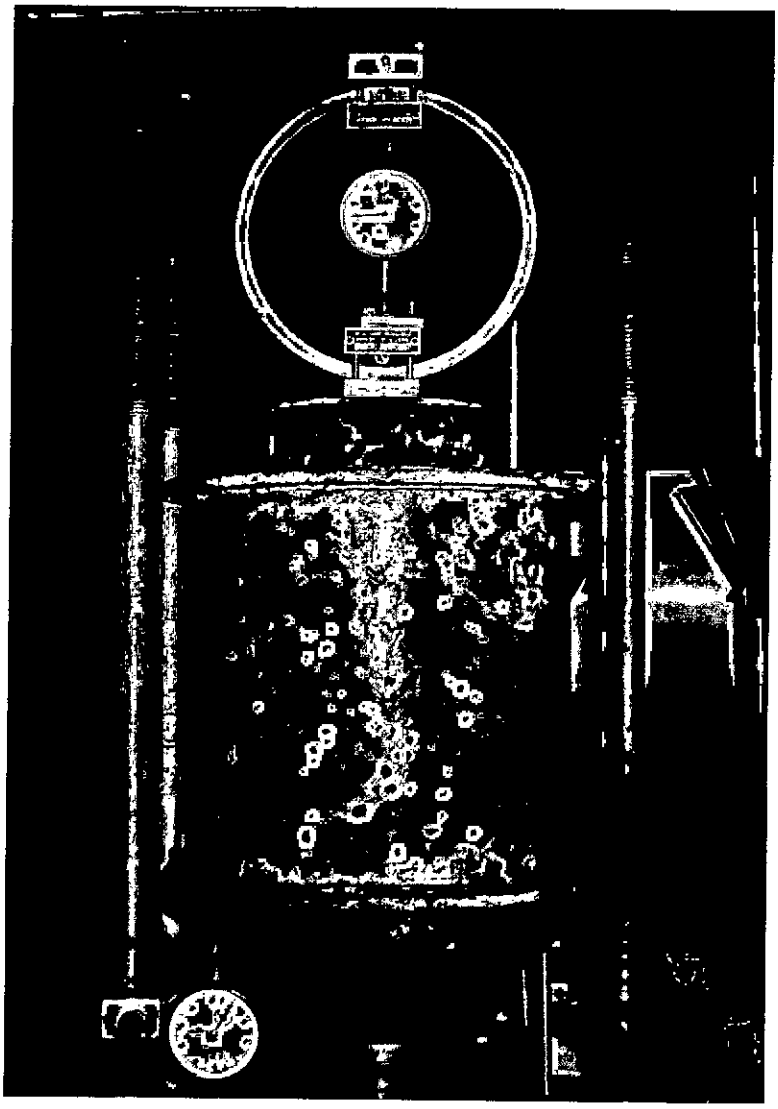

Fig. 7.1 Photograph of consolidation mold

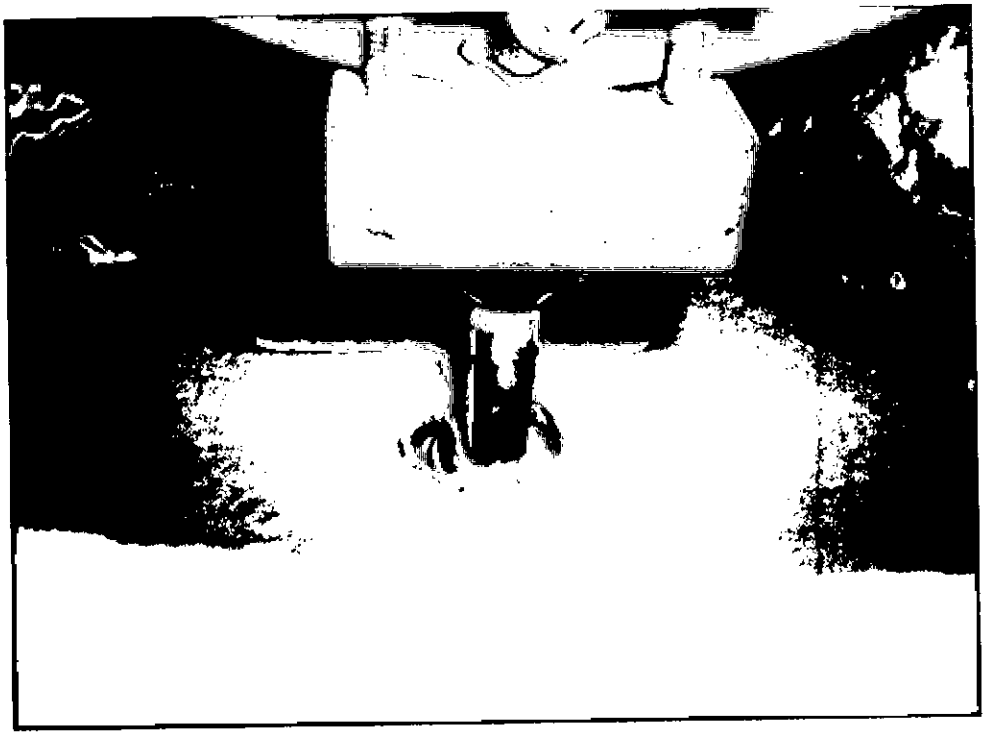

Fig. 7.2 Photograph of model scale footing on consolidation mold

For the pile test, a 100 mm long column (model pile) with 10 mm diameter was added to the bottom of the circular steel footing manufactured for the footing test. The 100 mm long column or pile was then pushed into the consolidated soil sample at the centre of the consolidation mold. This was construed as a single steel pile with a 25 mm diameter and 5 mm thick circular steel pile cap. The 50 mm long and 10 mm diameter column at the top of the pile cap was used to axially load the pile in ten equal assumed load increments using the proving ring and the loading frame. The displacement of the steel pile was measured as the axial vertical displacement of the steel pile cap using a separate dial gauge attached to the pile cap. A single model scale pile test was carried out for a consolidation pressure of 150 kPa of the consolidated clay slurry in the cylindrical mold.

7.1 Finite Element Modelling

The model scale footing and pile test was numerically simulated using the finite element method. The model scale footing test domain geometry was simulated using a total of 114, 8 noded quadrilateral elements with a total of 387 nodes. The steel footing was simulated using 4, 8 noded quadrilateral elements. For the model scale pile, 112, 8 noded quadrilateral elements with a total of 383 nodes and reduced integration was used. The 100 mm long and 10 mm diameter steel pile was geometrically modelled using 14, 8 noded quadrilateral elements at the centre of and embedded within the cylindindrical soil domain. Figure 7.3 shows a typical mesh geometry for finite element analysis of footing and pile problems using 8 noded quadrilateral elements. Figure 7.4 shows a typical isoparametric 8 noded quadrilateral element. The cylindrical domain boundary was at a distance of approximately 10 times the diameter of the circular footing from the centre of the footing. This generally is adequate to preclude any boundary effects on the problem at hand. The vertical boundary of the footing was restrained from movement in the horizontal direction but free to move in the vertically downward direction. The bottom boundary of the cylindrical domain was at a depth of approximately 10 times the footing diameter from the surface of load application, thus precluding any boundary effects of the bottom boundary on the given problem. The bottom boundary was restrained from moving both in the vertical and horizontal direction.

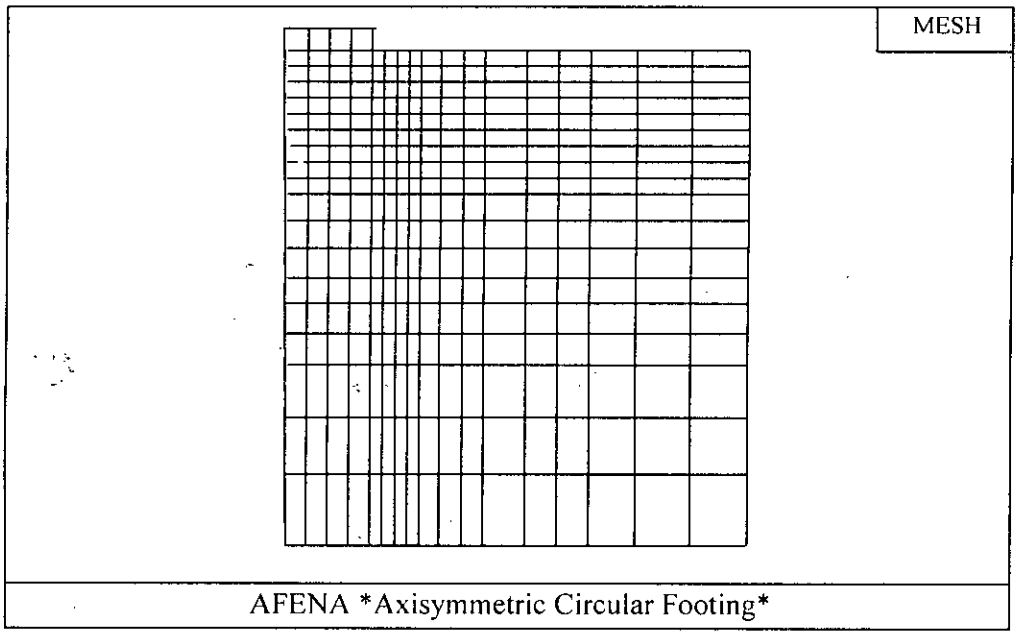

Figure 7.3 Finite element mesh for model footing using quadrilateral elements

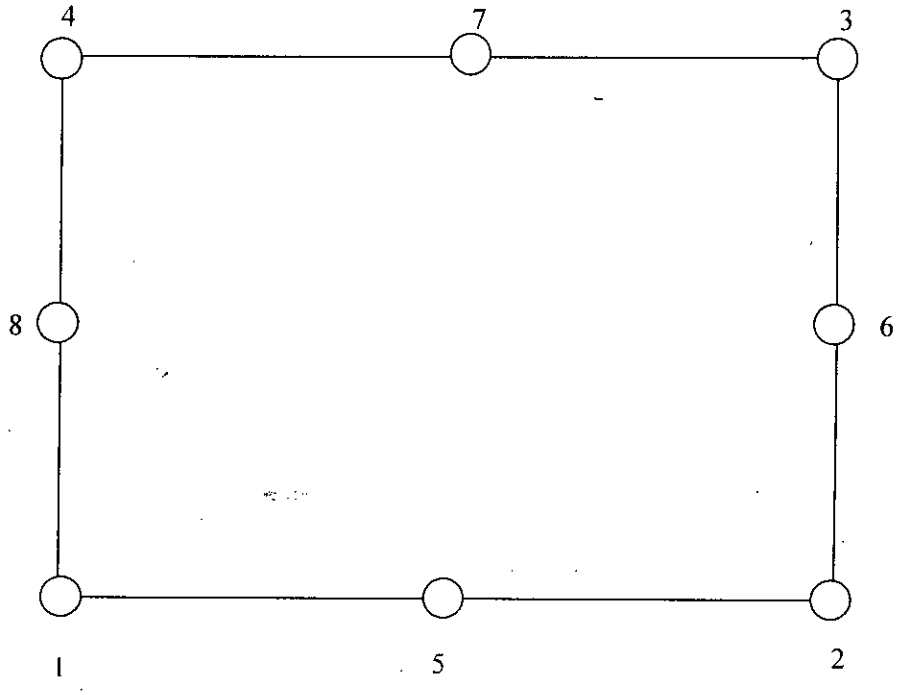

Figure 7.4 An 8 noded quadrilateral element

The soil was modelled using Mohr-Coulomb and Modified Cam Clay model with axisymmetric soil elements and appropriate soil parameters for each model. An incremental and iterative elasto-plastic finite element analysis using reduced integration was carried out to simulate the model scale footing and pile tests. The load-displacement data of the centre of the footing was plotted for each of the two model scale footing tests and the model scale pile test for both the Mohr-Coulomb and Modified Cam Clay model.

The soil parameter values used for the elasto-plastic finite element analysis are those given in Appendix B, which are the soil parameters for undrained loading of Anwara clays using the Mohr-Coulomb and Modified Cam Clay model respectively. The soil was assumed to be K_0 consolidated with overconsolidation ratio very close to 1 and a K_0 value of approximately 0.5.

7.2 Comparison of Pressure-Displacement Curves

The pressure-displacement curves under undrained conditions were obtained by numerical analysis. Results were obtained for the centre of the model scale footing and pile by elasto-plastic finite element analysis using the Modified Cam Clay as the soil constitutive model for Anwara clays. The plots show qualitatively reasonable results both for 50 kPa and 150 kPa consolidation pressure in model scale footing tests as well as for the test of model scale piles. The numerical predictions were compared with the experimental load-displacement data obtained for the two model scale footing tests and the model scale pile test. Figures 7.5, 7.6 and 7.7 show a reasonable agreement of the experimental data with the results of the numerical analysis. This shows that the Modified Cam Clay model is possibly a good predictor of the mechanical stress-strain response of coastal clays of Bangladesh under undrained conditions. However, this will only be true if reliable and accurate measurements are made of the soil parameters associated with the soil model.

The model scale footing and pile experimental data were compared with finite element predictions of the load-displacement response of the centre of the footing or pile using the Mohr-Coulomb model as the constitutive model for the soil domain. It may be observed in Figures 7.8, 7.9 and 7.10 show that the numerical predictions

obtained for the load-displacement response of the centre of the model scale footing and pile do not match quite well with the experimental data obtained in this research investigation.

7.3 Conclusions

The load-displacement response of model scale footings and piles in clays was investigated both experimentally as well as using elasto-plastic finite element analysis. It was observed that incremental elasto-plastic finite element analysis using the Modified Cam Clay model provides a reasonably good qualitative and quantitative approximation of the load-displacement response of model scale footings and piles in coastal clays of Bangladesh. More model scale and prototype footing and pile tests as well as more detailed numerical analysis needs to be conducted to validate the results of experimental and numerical investigations of the current research.

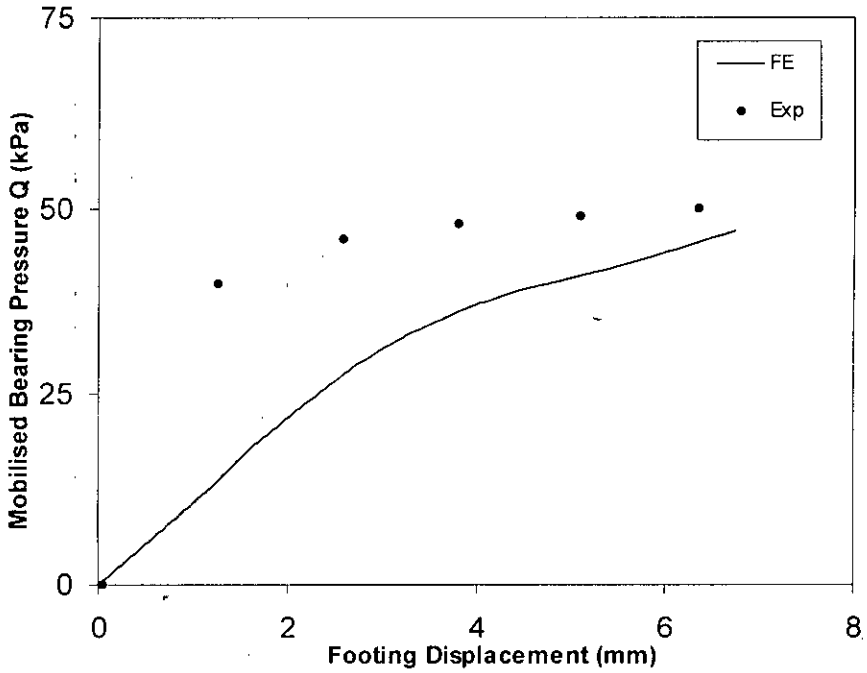

Figure 7.5 Comparison of experimental data of model scale footing test (σ'_v=50kPa) with numerical predictions using the Modified Cam Clay model

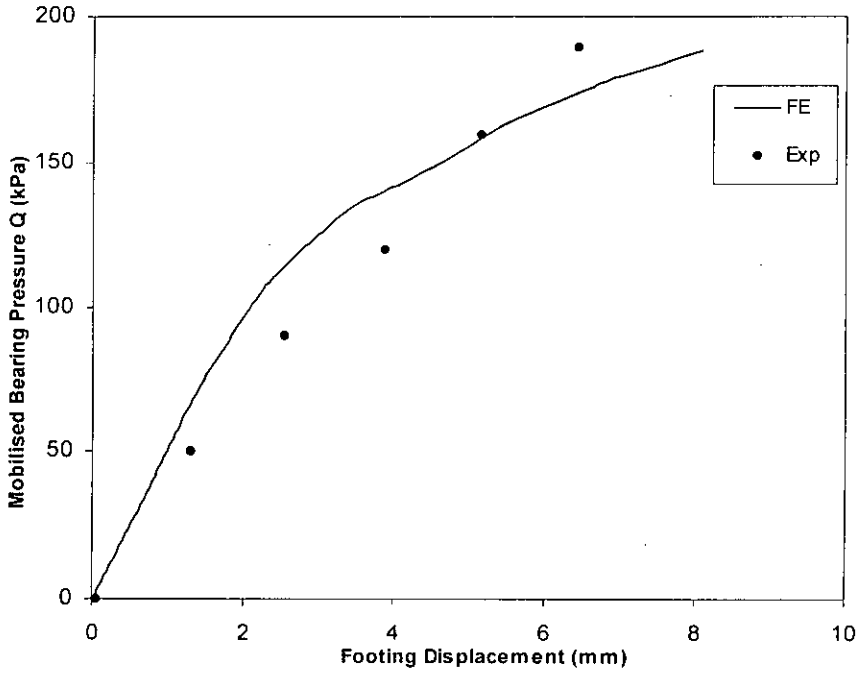

Figure 7.6 Comparison of experimental data of model scale footing test (σ'_v=150kPa) with numerical predictions using the Modified Cam Clay model

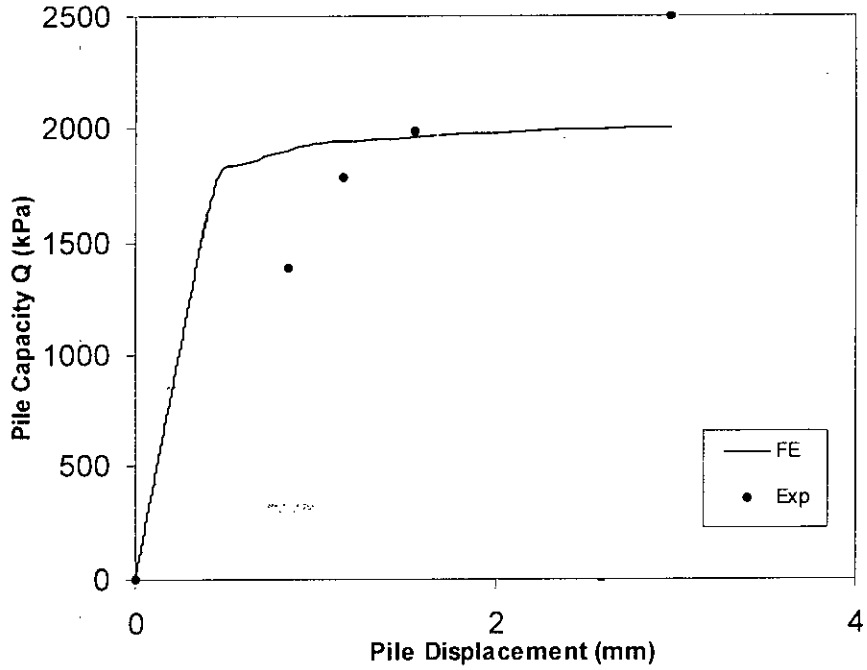

Figure 7.7 Comparison of experimental data of model scale pile test (σ'_v=150kPa) with numerical predictions using the Modified Cam Clay model

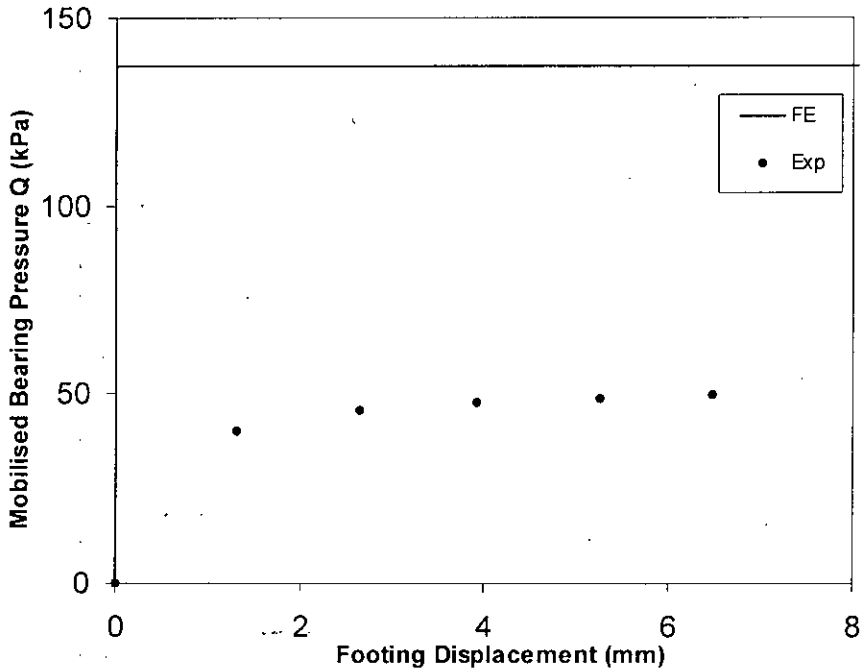

Figure 7.8 Comparison of experimental data of model scale footing test (σ'_v=50kPa) with numerical predictions using the Mohr-Coulomb model .

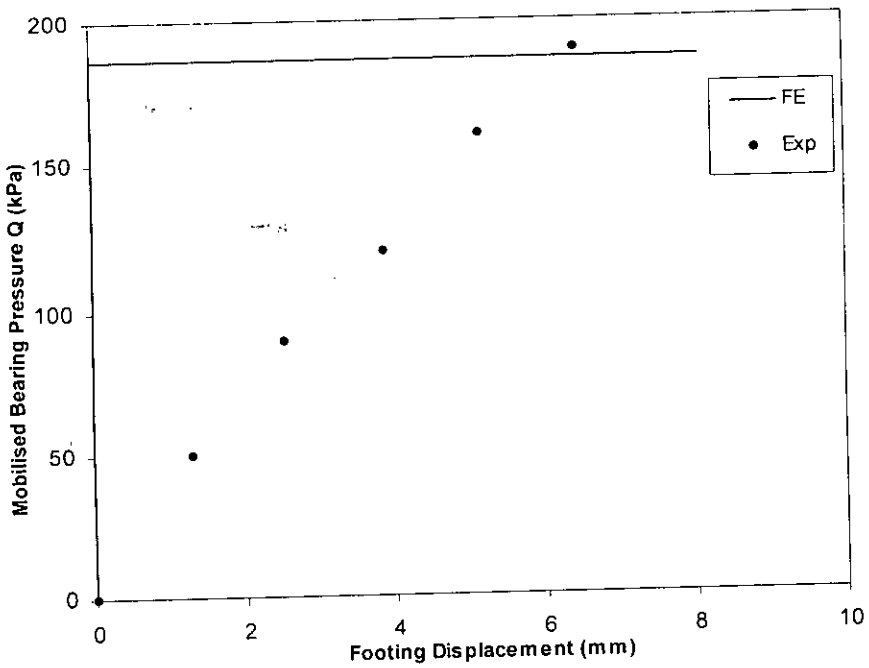

Figure 7.9 Comparison of experimental data of model scale footing test (σ'_v=150kPa) with numerical predictions using the Mohr-Coulomb model

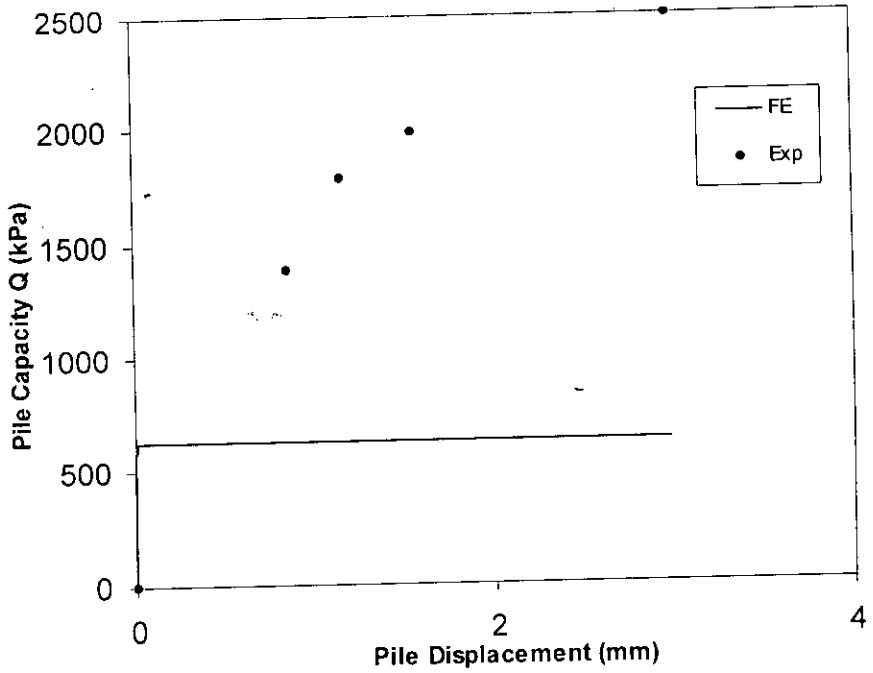

Figure 7.10 Comparison of experimental data of model scale pile test (σ'_v=150kPa) with numerical predictions using the Mohr-Coulomb model

CHAPTER 8

CONCLUSIONS AND RECOMMENDATIONS FOR FURTHER STUDY

8.1 Introduction

A numerical study of constitutive behaviour of coastal clays of Bangladesh was carried out. Experimental investigation of the load-displacement response of a model scale circular footing and pile resting on coastal clays of Bangladesh was also undertaken. Mohr-Coulomb model and Modified Cam Clay model was used to simulate the triaxial stress-strain response of coastal clays under drained and undrained conditions. These models were then used in a finite element procedure (using the software AFENA) to simulate the response of a model scale circular footing and pile resting on coastal clays subjected to axial load. The Mohr-Coulomb and Modified Cam Clay model was used as the constitutive models for the elasto-plastic finite element analysis. This is because these two models are widely used for analytical and numerical predictions of stress, strain, loads and displacement of various boundary value problems in geotechnical engineering.

In this chapter, the results obtained and observations made from the numerical study regarding the triaxial behaviour of coastal clays and the load-displacement response of a model scale circular footing and pile resting on coastal clays are summarized. Based on these observations, certain specific conclusions have been drawn and recommendations are put forward for further investigation of the stress-strain behaviour of coastal clays of Bangladesh and the load-displacement behaviour of model scale circular footings and piles resting on such clays.

8.2 Concluding Observations

Two existing constitutive models have been used in this thesis to simulate the shear stress by axial strain response of coastal clays of Bangladesh. The stress-strain response was simulated for triaxial stress states both for drained and undrained

conditions. One of the models was the Mohr-Coulomb model used for limit analysis assuming the soil to be an elastic-perfectly plastic frictional material. The other was the strain hardening Modified Cam Clay model based on critical state soil mechanics.

The findings of the present study are listed as follows:

i) With appropriate assumptions, the stress and strain at failure, during undrained triaxial shear are realistically approximated by the Mohr-Coulomb model. However, the Mohr-Coulomb model was unable to predict non-linearity and strain hardening prior to yield. The Mohr-Coulomb model was also unable to predict excess pore pressure and the undrained effective stress path of coastal clays.

ii) The stress and strain at failure, during drained triaxial shear, could be realistically approximated by this model. The volume strain predictions of the Mohr-Coulomb model for drained triaxial shearing of coastal clays do not appear to be qualitatively correct when compared to the volume change behaviour experimentally observed for many clays.

iii) The Modified Cam Clay model could predict reasonably well, both qualitatively and quantitatively, the stress-strain response of coastal clays of Bangladesh during triaxial shearing, under undrained conditions. The stress-strain response such as non-linearity and hardening for normally consolidated and lightly overconsolidated coastal clays, either under drained and undrained conditions, is well predicted by this model. Similarly, the Modified Cam Clay model correctly predicts a peak stress and subsequent non-linear softening behaviour for overconsolidated clays. The predictions of excess pore pressures and effective stress path for undrained shearing is correct both for normally consolidated and overconsolidated clays.

iv) The Modified Cam Clay model could predict both qualitatively and quantitatively, the stress-strain response of coastal clays of Bangladesh during triaxial shearing, under drained conditions. For drained shearing,

the Modified Cam Clay model makes correct qualitative predictions both for ultimate stress at failure and volume change response of the clay.

v) Realistic predictions could also be obtained of the ultimate load reached by a model scale footing and pile and the displacements undergone by the footing and pile to reach the ultimate load when using the Modified Cam Clay model and elasto-plastic finite element analysis.

However, coastal clays of Bangladesh were observed to exhibit non-linear and elasto-plastic stress-strain response from the onset of loading. The Modified Cam Clay model assumes non-linear elasticity prior to yield, Thus it is unable to predict non-linear elasto-plastic stress-strain response from the onset of loading except for normally consolidated clays.

8.3 Specific Conclusions

On the basis of the above observations, the following specific conclusions can be drawn:

i) When only stress and strain at failure is desired, then the Mohr-Coulomb model is appropriate. However, for service load conditions where settlements are important, then the Mohr-Coulomb model is not proper.

ii) The Mohr-Coulomb model is appropriate for predicting the ultimate load. The Mohr-Coulomb model should not be used for predicting settlements of structures on coastal clays under drained conditions.

iii) The Modified Cam Clay model is appropriate for predicting both the ultimate load as well as the load-displacement response of coastal clays under undrained condition. However, no analytical formulation of important geotechnical problems using Modified Cam Clay model are available. Thus the Modified Cam Clay model may be used only for numerical prediction using finite element, finite difference or other advanced numerical methods.

iv) The Modified Cam Clay model may be used for numerical prediction of consolidation problems in coastal clays in drained condition using numerical methods such as finite element, finite difference etc. However, analytical formulation for consolidation problems in geotechnical engineering using Modified Cam Clay model are not available.

v) The Modified Cam Clay model may be used for numerical predictions of load-displacement response of footings and piles resting on coastal clays.

8.4 Recommendations for Further Research

Several aspects of the work presented in this thesis require further investigation. Some of the important areas of possible further research may be listed below:

- The numerical analysis using the Mohr-Coulomb model and the Modified Cam Clay model was carried out using a single set of values for the model parameters. This research may be extended to study the effect of change of the values of the model parameters on the stress-strain response of coastal clays. Thus a sensitivity analysis of the model parameters of the Mohr-Coulomb model and the Modified Cam Clay model may be undertaken in future.

- Drained triaxial tests on Anwara, Banshkhali and Chandanaish clays may be carried out and compared with the numerical prediction in the study.

- Three coastal clays from Chittagong coastal belt have been used in this research to evaluate constitutive models. Further research on soils from different coastal belts of Bangladesh may be carried out to verify and validate these models.

- The scope of the experimental program has been limited to investigation of the load-displacement response of model-scale footings and piles resting on Anwara clay only. Further laboratory as well as field experiments may be

carried out to investigate response of footings and piles resting on other coastal clays.

REFERENCES

1. *Ameen, S.F. and Safiullah, A.M.M. (1986)* Undrained shear strength characteristics of Dhaka clay, Journal of the Institution of Engineers, Bangladesh, 14, 4, pp. 1-8.

2. *Amin, M.N., Kabir, M.H., Saha, G.P. and Ahmed, M. (1987).* Geotechnical behaviour of soils from coastal regions of Bangladesh, 9th SEAGC, Bangkok, pp5.1-5.12

3. *Ansary, M.A. (1993).* Evaluation of geotechnical properties of regional soils with particular emphasis on coastal region, M.Sc. Engg. Thesis, BUET, Dhaka

4. *Ansary, M.A., Siddique, A. and Safiullah, A.M.M. (1999),* Compressibiity and permeability characteristics of selected coastal soils of Bangladesh, Indian Geotechnical Journal, 29, 2, pp. 162-185

5. *Arora, K.R. (1992),* Soil Mechanics and Foundation Engineering, Standard Publishers, Delhi

6. *Atkinson, J.H. and Bransby, P.L. (1978).* The Mechanics of Soils – An Introduction to Critical State Soil Mechanics, McGraw-Hill, New York, NY, 375 pp.

7. *Balasubramaniam, A.S. and Chaudhary, A.R. (1978).* Deformation and strength characteristics of soft Bangkok clay, J. Geotech. Eng. Div, ASCE, 104, GT9, pp.1153-1167

8. *Balasubramaniam, A.S. and Hwang, Z.M.. (1980).* Yielding of weathered Bangkok clay, Soils and Foundations, 20, 2, pp. 1-15.

9. *Barden, L. (1969).* Time dependent consolidation of normally consolidated clays and peats, J. *Soil Mech. Found Div*, ASCE, 95(SM1), pp. 1-31

10. *Bashar, M.A. (2002).* Stress-deformation charcteristics of selected coastal soils of Bangladesh and their sampling effects, PhD. thesis, Department of Civil Engineering, Bangladesh University of Engineering and Technology, Dhaka, Bangladesh

11. *Berre, T. and Bjerrum, L. (1973).* Shear strength of normally consolidated clays, *Proc 8th Int Conf Soil Mech Found Eng*, Moscow,1,1,pp.39-50

12. Bishop, A.W. and Henkel, D.J. (1962). The Measurement of Soil Properties in the Triaxial Test. Edward Arnold, London, 2nd ed., 228 pp.

13. *Bjerrum, L. (1967).* Engineering geology of Norwegian normally consolidated marine clays as related to settlements of buildings, *Geotechnique*, 17, pp. 81-118

14. *Bjerrum, L. (1954).* Geotechnical properties of Norwegian marine clays, *Geotechnique*, 4, pp.49-69

15. *Bowles, F.A., Byrant, W.R. and Wallin, C. (1969).* Microstructure of unconsolidated and consolidated marine sediments, *J. Sediment Petrol*, 39, pp. 1546-1551

16. *Brand and Brenner (1981),* Soft Clay Engineering, Elsevier Scientific Publishing Co., Amsterdam, the Netherlands pp. 326-542

17. *Britto, A.M. and Gunn, M.J. (1987).* Critical state soil mechanics via finite elements, Ellis Horwood Series in Civil Engineering, Halsted Press, New York, USA

18. *Burland, J.B. (1990).* The Thirtieth Rankine Lecture: On the compressibility and shear strength of natural clays, Geotechnique, 40, 3, pp. 329-378

19. Carter, J.P. and Balaam, N.P. (1995). AFENA-A Finite Element Numerical Algorithm, Users' Manual, Centre for Geotechnical Research, University of Sydney

20. *Chen, W.F. and Mizuno, E. (1990).* Nonlinear analysis in soil mechanics, elsevier Science Publishers B.V., New York, USA.

21. *Crawford C.B. (1959)* The Influence of Rate of Strain on Effective Stresses in Sensitive Clay, ASTM Spec. Tech. Pub. no. 254, pp. 36-48.

22. *de Borst, R. and Vermeer, P.A. (1984).* Possibilities and limitations of finite elements for limit analysis, Geotechnique, 34, 2, pp. 199-210.

23. *Dimaggio, F.L. and Sandler, I.S. (1971).* Material model for granular soils, Journal of Engineering Mechanics Division, ASCE, 97(EM3), pp. 935-950.

24. *Drucker, D.C. (1959).* A description of stable inelastic material, Jour Appl. Mech, 26, pp. 101-126.

25. *Drucker, D.C. (1956).* On uniqueness in the theory of plasticity, Quart Appl. Math, 14, pp. 35-42.

26. *Drucker, D.C.and Prager, W. (1952).* Soil mechanics and plasticity analysis or limit design. Quart Appl Math, 10(2), pp. 157-175.

27. *Duncan, J.M. and Chang, C.Y. (1970).* Non-linear analysis of stress and strain in soils. J. Soil Mech. Found Div, ASCE, 96, SM5, pp. 1629-1653

28. *Gens, A. and Potts, D.M. (1988).* Critical state models in compuational geomechanics, Engineering Computations, 5, pp. 178-197.

29. *Hanzawa, H. (1979).* Undrained strength characteristics of an alluvial Marine clay in the Tokyo Bay, *Soils and Foundations*, 19, 4, pp.69-84

30. *Hill, R. (1950). The Mathematical Theory of Plasticity*, Clarendon Press, Oxford, 365 pp.

31. *Kamaluddin, M. (1990).* Compressibility and shear strength of remoulded Dhaka clay, MSc. Engg. Thesis, BUET, Dhaka

32. *Kamaluddin, M. (1999).* Intrinsic compressibility, strength properties ans some strength models for Dhaka clay, Journal of Civil Engg, IEB, Bangladesh, 27, 2, pp155-173

33. *Kenney, T.C, Moum, J. and Berre, T. (1967*). An experimental study of bonds in natural clay, *Proc Geotech Conf*, Oslo, 1, pp. 65-69

34. *Koutsoftas, D.C. (1981).* Undrained shear behaviour of a marine clay, Laboratory Shear Strength of Soils, ASTM, STP 740, pp. 254-276.

35. *Ladd, C.C (1964)* Stress-strain response of clay in undrained shear, *J. Soil Mech. Found. Div*, ASCE, 90, SM5, pp. 103-132

36. *Ladd, C.C., Foott, R., Ishihara, K., Schlosser, F. and Poulos, H.G.(1977).* Stress-deformation and strength characteristics, *Proc 9th Int Conf Soil Mech Found Eng.*, Tokyo, 2, pp. 421-494

37. *Lade, P.V. (1977).* Elastoplastic stress-strain theory for cohesionless soils with curved yield surfaces, Int. Jour. of Solids and Structures, 133, 11, pp. 1019-1035.

38. *Lade, P.V. and Duncan, J.M. (1975).* Elastoplastic stress-strain theory for cohesionless soil, J. Geotech. Engg. Div., ASCE, 101(GT10), pp. 1037-1053.

39. *Lagioia and Nova (1995),* An experimental and theoretical study of the behaviour of a Calcarenite in triaxial compression, Geotechnique, vol 45, No. 4, pp. 633-648

40. *Lambe and Whitman (1979)*, Soil Mechanics, John Wiley and Sons, pp 302-442.

41. *Leonards, G.A. and Altshaeff, A.G. (1964).* Compressibility of clay. *J. Soil Mech. Found. Div.*, ASCE, 90(SM5), pp. 133-155.

42. *Loiselle, A., Massiera, M. and Sianani, U.R. (1971).* A study of the cementation bonds of the sensitive clays of the Outardes River region, *Can. Geotech. J.*, 8, pp.479-498

43. *Mayne, P.W. (1980)* Cam Clay predictions of undrained strength, Journal of Geotech Engg Div, ASCE, Vol 116, Gt11, pp. 1216-1240

44. *Mesri, G. and Rokshar, A. (1974).* Theory of consolidation for clays. *J. Geotech. Engg. Div.*, ASCE, 100(GT8): pp. 889-904.

45. *Mesri, G., Rokhsar, A. and Bohor, B.F. (1975).* Composition and compressibility of typical samples of Mexico City clay, *Geotechnique*, 25, pp.527-554

46. *Mitchell, J.K. and Houston, W.N. (1969).* Causes of clay sensitivity, J. Soil Mech Found. Div., ASCE, 95, SM3, pp. 845-871

47. *Mitchell, J.K. (1960).* Fundamental aspects of thixotropy in soils, J. Soil Mech. Found. Div, ASCE, 86, SM3, pp19-52

48. *Mitchell, R.J. (1970).* On the yielding and mechanical strength of Leda clays, *Can. Geotech J.*, 7, pp. 297-312

49. *Morgernstern, N.R. and Tchalenko, J.S. (1967).* The optical determination of preferred orientation in clays and its application to the stufy of microstructure in consolidated kaolin II. *Proc. Royal Soc.*, A 300, pp. 235-250

50. *Nakase, A, Kamei, T and Kusakabe, O (1988).* Constitutive parameters estimated by plasticity index, Journal of Geotechnical Engineering, ASCE, 114, 7, paper No. 22635, pp. 844-858

51. *Olson, R.E. (1977).* Consolidation under time dependent loading. *J. Geotech Eng. Div.*, ASCE, 103(GT1), pp. 55-60.

52. *Parry, R.H.G. and Nadarajah, V. (1973).* A volumetric yield locus for lightly overconsolidated clay, *Geotechnique*, 23, pp. 450-453.

53. *Pastor, M., Zienkiewicz, O.C. and Chan, A.H.C. (1990).* Generalized plasticity and modelling of soil behaviour, International Journal for Numerical and Analytical Methods in geomechanics, 14, 151-190.

54. *Peck, R.B., Hansen W.B. and Thornburn T.H. (1974).* Foundation Engineering, John Wiley & Sons Inc., New York.

55. *Penner, E. (1964).* Studies of sensitivity and electro-kinetic potential in Leda clay, Nature, 204(4960), pp.808-809

56. *Penner, E.. and Burn, K.N. (1978).* Review of engineering behaviour of marine clays in eastern Canada. *Ca. Geotech. J*

57. *Potts, David M. (1999).* Finite element analysis in geotechnical engineering, Thomas Telford Publishing, London, pp. 34-35

58. *Poulos, H.G. and Davis, E.H. (1974).* Elastic solutions for soil and rock mechanics, New York, N.Y., John Wiley.

59. *Pusch, R. (1966)* Quick clay microstructure, *Engineering Geology*, 1, pp.433-443.

60. *Pusch, R. (1973a)* Influence of salinity and organic matter on the formation of clay microstructure. Proc Int Symp Soil Structure, Gothenburg, pp 161-174., 15, pp269-282

61. *Pusch, R. (1973b)* Physico-chemical processes which affect soil structure and vice versa. Proc Int Symp Soil Structure, Gothenburg, pp 27-35

62. *Rendulic, L. (1936).* Relation between void ratio and effective stress for a remoulded silty clay. *Proc. 1st Int Conf SMFE*, Harvard, 3, pp.48-51

63. *Roscoe, K.H., Burland, J.B. (1968).* On the generalized stress-strain behaviour of wet clay, Engg Plasticity, Eds heyman, J. & Leckie, F.A., Cambridge University Press, Cambridge, Mass, pp. 535-609.

64. *Roscoe, K.H., Schofield, A.N. and Thurairajah, A. (1963).* Yielding of clays in states wetter than critical. *Geotechnique*, 13, pp. 211-240.

65. *Roscoe, K.H., Schofield, A.N. and Wroth, C.P. (1958).* On the yielding of soils. *Geotechnique*, 8, pp. 22-53

66. *Rowe, P.W. (1962).* The stress-dilatancy relation for static equilibrium of an assembly of particles in contact. *Proceedings, Series A, Vol 269, Royal Society of London*, pp.500-527

67. *Sangrey, D.A.(1972a).* On the causes of natural cementation in sensitive soils. *Can. Geotech. J.*, 9, pp117-119

68. *Sangrey, D.A.(1972b).* Naturally cemented sensitive soils, *Geotechnique*, 22, pp. 139-152.

69. *Schofield, A.N. and Wroth, C.P. (1968). Critical State Soil Mechanics*, McGraw-Hill, London, 310 pp.

70. *Siddique, A. and Farooq, S.M. (1997).* Geotechnical characteristics of reconstituted soft soils from a coastal area of Bangladesh, The Indian Engineer Journal, India, 40, 10, pp. 1-14

71. *Smith, I.M. (1982)* Programming via the finite element method, New York: Wiley.

72. *Yong, R.N. and Sheeran, D.E.(1973)* Fabric unit interaction and soil behaviour, *Proc. Int Symp Soil Struc*ture, Gothenburg, pp. 176-183

73. Yudhbir and Vadarajan, A. (1975). Stress-path dependent deformation moduli of clay, J. Geotech. Eng. Div., ASCE, 101, GT3, pp. 315-327

74. *Zienkiewicz, D.C. and Naylor, D. J. (1971).* The adaptation of critical state soil mechanics theory for use in finite elements, *Proc Roscoe Memorial Symp. Stress-Strain Behaviour of Soils*, Cambridge, England, pp. 537-547.

APPENDIX I

CONSOLIDATION AND SHEAR PROPERTIES OF COASTAL CLAYS

Table A1.1 Consolidation properties of coastal clays (after Bashar, 2002)

	LL	PI (%)	K_o consolidation		isotropic consolidation	
			Cc	Cs	Cc	Cs
Anwara	40	16	0.288	0.048	0.295	0.053
Banshkhali	34	10	0.256	0.039	0.265	0.044
Chandanaish	45	20	0.309	0.060	0.313	0.063

Table A1.2 Undrained shear properties for reconstituted isotropic normally consolidated clays (after Bashar, 2002)

Location of soil	PI (%)	σ'_v	s_u kN/m^2	ε_p (%)	A	E_i kN/m^2	E_{50} kN/m^2
Anwara	16	150	62.7	11.8	0.79	39345	26145
Banshkhali	10	150	59.6	11.0	0.82	37095	24525
Chandanaish	20	150	65.0	13.5	0.74	41355	27555

Table A1.3 Undrained shear properties for reconstituted Anwara clay (after Bashar, 2002)

OCR	1	2	5	10	20	30
s_u	62.7	50.25	42.75	35.55	30.0	26.6
ε_p (%)	11.8	10.12	9.25	8.7	8.2	7.32
A	0.79	0.28	-0.11	-0.19	-0.33	-0.40
E_i/s_u	627.5	610.4	586.0	569.8	554.5	541.7
E_{50}/s_u	417.0	405.0	391.0	377.5	368.0	363.0

Table A1.4 Undrained shear properties for reconstituted Banshkhali clay (after Bashar, 2002)

OCR	1	2	5	10	20	30
s_u	59.6	45.0	37.8	31.0	26.2	22.5
ε_p (%)	11.0	9.35	8.72	8.14	7.5	7.24
A	0.82	0.33	-0.07	-0.13	-0.28	-0.34
E_i/s_u	622.3	607.5	578.0	559.0	543.0	537.0
E_{50}/s_u	411.5	402.0	386.4	371.8	365.0	361.2

Table A1.5 Undrained shear properties for reconstituted Chandanaish clay (after Bashar, 2002)

OCR	1	2	5	10	20	30
s_u	65.0	54.3	45.5	38.4	32.5	29.9
ε_p (%)	13.5	11.75	10.56	10.0	8.86	8.52
A	0.74	0.23	-0.14	-0.25	-0.37	-0.45
E_i/s_u	636	615	595	577	559	548
E_{50}/s_u	424	409	396	385	375	368

APPENDIX II

MODEL PARAMETERS OF COASTAL CLAYS

Table A2.1 Modified Cam Clay model parameters for Coastal Clays (after Bashar, 2002)

MCC Parameters	Anwara Clay	Banshkhali Clay	Chandanaish Clay
λ	0.128	0.115	0.136
κ	0.023	0.019	0.03
M	1.32	1.34	1.31
p'_o (kPa)	150	150	150
μ	0.3	0.3	0.3
N	2.37	2.29	2.45

Table A2.2 Undrained Mohr-Coulomb parameters: Anwara clay (after Bashar, 2002)

Cell Pressures (kPa)	OCR	Mohr-Coulomb parameters				
		ultimate c (kPa)	ϕ'	E_i (kPa)	E_{50} (kPa)	μ
150	1	62.7	0	39,345	26,145	0.5
75	2	50.25	0	30,675	24,038	0.5
30	5	42.75	0	25,062	16,710	0.5
15	10	35.55	0	25,026	13,420	0.5
7.5	20	30.0	0	16,635	11,040	0.5
5	30	26.6	0	14,410	14,410	0.5

Table A2.3 Undrained Mohr-Coulomb parameters: Banshkhali clay (after Bashar, 2002)

Cell Pressures (kPa)	OCR	Mohr-Coulomb parameters				
		Ultimate c (kPa)	ϕ'	E_i (kPa)	E_{50} (kPa)	μ
150	1	59.6	0	37,095	24,525	0.5
75	2	45.0	0	27,338	18,105	0.5
30	5	37.8	0	21,840	14,610	0.5
15	10	31.0	0	18,825	12,414	0.5
7.5	20	26.2	0	14,228	9589	0.5
5	30	22.5	0	12,083	8127	0.5

Table A2.4 Undrained Mohr-Coulomb parameters: Chandanaish clay (after Bashar, 2002)

Cell Pressures (kPa)	OCR	Mohr-Coulomb parameters				
		Ultimate c (kPa)	ϕ'	E_i (kPa)	E_{50} (kPa)	μ
150	1	65	0	41,355	27,555	0.5
75	2	54.3	0	33,420	22,223	0.5
30	5	45.5	0	27,072	18,018	0.5
15	10	38.4	0	22,170	14,760	0.5
7.5	20	32.5	0	18,162	12,188	0.5
5	30	29.9	0	16,385	11,005	0.5

Table A2.5 Drained Mohr-Coulomb model parameters: Anwara clay

Cell pressure kPa	OCR	Mohr-Coulomb Parameters				
		c	ϕ' degree	$\overline{E}_i$ kPa	$\overline{E}_{50}$ kPa	μ
150	1	0	32.75	11,241	7,470	0.2
75	2	0	32.75	8,764	6,868	0.2
30	5	0	32.75	7,161	4,774	0.2
15	10	0	32.75	7,150	3,834	0.2
7.5	20	0	32.75	4,752	3,154	0.2
5	30	0	32.75	4,117	2,759	0.2

Table A2.6 Drained Mohr-Coulomb model Parameters: Banshkhali clay

Cell pressure kPa	OCR	Mohr-Coulomb Parameters				
		c	ϕ' degree	$\overline{E}_i$ kPa	$\overline{E}_{50}$ kPa	μ
150	1	0	33.21	10,599	7,007	0.2
75	2	0	33.21	7,811	5,173	0.2
30	5	0	33.21	6,240	4,174	0.2
15	10	0	33.21	5,379	3,547	0.2
7.5	20	0	33.21	4,065	2,740	0.2
5	30	0	33.21	3,452	2,322	0.2

Table A2.7 Drained Mohr-Coulomb model parameters: Chandanaish clay

Cell pressure kPa	OCR	Mohr-Coulomb Parameters				
		c	ϕ' degree	$\bar{E}_i$ kPa	$\bar{E}_{50}$ kPa	μ
150	1	0	32. 5	11,816	7,873	0.2
75	2	0	32. 5	9,549	6,349	0.2
30	5	0	32. 5	7,735	5,148	0.2
15	10	0	32. 5	6,334	4,217	0.2
7.5	20	0	32. 5	5,789	3,482	0.2
5	30	0	32. 5	4,681	3,144	0.2